DESIGN OF MICELLE EMBEDDED CHITOSAN NANOCOMPOSITES FOR TARGETED DELIVERY OF HYDROPHOBIC DRUGS

A Thesis Submitted to
the Graduate School of Engineering and Sciences of
İzmir Institute of Technology
in Partial Fulfillment of the Requirements for the Degree of

MASTER OF SCIENCE

in Chemistry

by
Esra CİHAN

December 2016
İZMİR

We approve the thesis of **Esra CİHAN**

Examining Committee Members:

Prof. Dr. Hürriyet POLAT
Department of Chemistry, İzmir Institute of Technology

Prof. Dr. Nuran ELMACI
Department of Chemistry, İzmir Institute of Technology

Assist. Prof. Dr. Güler Narin
Department of Chemical Engineering, Uşak University

26 December 2016

Prof. Dr. Hürriyet POLAT
Supervisor, Department of Chemistry,
İzmir Institute of Technology

Prof. Dr. Ahmet Emin EROĞLU
Head of the Department of Chemistry

Prof. Dr. Bilge KARAÇALI
Dean of the Graduate School of
Engineering and Sciences

ACKNOWLEDGEMENTS

I would like to thank several people who really motivated and helped me.

Firstly, I would like to express my sincere and special thanks to my advisor Prof. Dr. Hürriyet POLAT for all of her support since beginning of my thesis study, for her motivation, sharing knowledge, friendship and endless devotion. Her guidance helped me in writing thesis and through my whole life. She always helps me in any case. I deeply appreciated.

Besides my advisor, I would like to thank the rest of my thesis committee: Prof. Dr. Nuran ELMACI IRMAK and Assist.Prof.Dr. Güler NARIN.

I also thank to Prof. Dr. Mehmet POLAT for his support during this research and his suggestions during my life in any case.

My sincere thanks also go to my friends, who helped me writing of this thesis, for their encouragement, friendship and support.

Finally, I would like to state my special thanks to my parents and my brother for supporting me mentally along writing this thesis and all of my life in all situations.

ABSTRACT

DESIGN OF MICELLE EMBEDDED CHITOSAN NANOCOMPOSITES FOR TARGETED DELIVERY OF HYDROPHOBIC DRUGS

When successed to synthesize in a nanoparticulate form, chitosan has found to be a very effective biomaterial for drug delivery purposes owing to its extremely attractive characteristics such as its positive charge and pH sensitivity in aqueous medium. However, its structure as it is, is not suitable for oil soluble drugs. Even a close control on the size and shape of chitosan particles alone becomes a state of art and the production of chitosan nanoparticles is very difficult. Therefore, in this study, several methods were designed and used for synthesis of chitosan nanoparticles (<100 nm) with a hydrophobic core that are suitable for oil soluble drugs.

Characterization of these nanoparticles were done by Fourier Transform Infrared Spectroscopy (FTIR), Scanning Electron Microscope (SEM), Scanning Transmission Microscope (STEM), Transmission Electron Microscope (TEM), surface tension and zeta potential measurements.

It was concluded that the best method was the coupling of drug loading with simple ionic gelation method among all the others. Hydrophobic drug loaded micelle embedded chitosan nano particles were able to manufactured successfully. The sizes of chitosan particles that embed Pluronic-123 micelles were larger (<100 nm) than the sizes of Pluronic-123 micelles (20 nm) alone. It was also possible to obtain smaller chitosan nanoparticles (<50 nm) that embed drug loaded Pluronic-123 micelles when their structure is modified by Sodiumdodecylsulfate.

ÖZET

HİDROFOBİK İLAÇLARIN HEDEFLENMİŞ İLAÇ TAŞINIMINDA KULLANIMI İÇİN MİSEL GÖMÜLÜ KİTOSAN NANO KOMPOZİTLERİN ÜRETİLMESİ

Nanopartikül olarak sentezlenebildiğinde kitosan, sulu ortamda pozitif yükü ve pH duyarlı olması gibi etkili karakteriktist özelliklerine bağlı olarak ilaç taşınımında etkili bir biyo malzeme olarak bulunmuştur. Bununla birlikte olduğu gibi yapısı yağda çözünür ilaçlar için uygun değildir. Kitosan parçacıklarının boyut ve şekilleri üzerinde yakın bir control bile bir sanat haline gelir ve kitosan nanopartiküllerinin üretimi çok zordur. Bu nedenle bu çalışmada, yağda çözülebilen ilaçlarl için uygun olan hidrofobik bir çekirdek ile kitosan nanopartiküllerinin (<100 nm) sentezi için çeşitli yöntemler tasarlanmış ve kullanılmıştır.

Bu nanopartiküllerin karakterizasyonu Fourier Dönüşümlü İnfrared Spektoskopi (FTIR), Taramalı Elektron Mikroskobu (SEM), Taramalı İletim Mikroslobu (STEM), İletim Elektron Mikroskobu (TEM), yüzey gerilimi ve zeta potansiyel ölçümleri ile yapıldı.

En iyi yöntemin, ilaç yüklemesinin basit iyonik jelleştirme yöntemi ile diğer tüm yöntemlerin birleştirilmesi olduğu sonucuna varıldı. Hidrofobik ilaç yüklü misel gömülü kitosan nanopartikülleri başarıyla üretildi. Pluronik-123 miselleri gömülü kitosan tanelerinin boyutu (<100 nm) tek başına Pluronik-123 misellerinin boyutundan (20 nm) daha büyüktü. Yapısı Sodyumdodesilsülfat ile modifiye edildiğinde ilaç yüklü Pluronic-123 miselini yerleştiren daha küçük kitosan nanopartiküllerinin (<50 nm) elde edilmesi de mümkün oldu.

TABLE OF CONTENTS

LIST OF FIGURES

Figure **Page**

Dedicated to my brother

CHAPTER 1

INTRODUCTION

1.1. Statement of the Problem

Drug delivery system can be defined as a formulation which provides the delivery of drugs to specific targets of the body at a controlled rate. Therefore, an ideal drug carrier should be inert, biocompatible, mechanically strong, capable of loading high amount of drug and releasing at a controlled rate and simple to administer and remove. Some of the commonly used carriers are polymeric micelles, vesicles, nanospheres, nanohydrogels liposomes, liquid crystals, nanocapsules, lipoproteins, microcapsules, and microparticles (Hu et al. 2016).

Delivering the therapeutic agents to target site has prominent importance in treatment of many diseases. Release of drug in the right time and right part of the body, minimizing undesirable side effects and protecting the tissues which are not required to treatment, are some of the advantages of controlled drug delivery. In other respects, using less amount of drug can be another advantage depending on drugs toxic properties (Wilczewska et al. 2012).

Nano carriers have superiority on drug loading and release efficiency due to their unique sizes (Singh and Lillard 2009), their stability and their surface properties which allow for modification. Targeting delivery provides great convenience to drugs to reach parts where they are required. However, carrying drugs can be a problem depending on the physical and chemical properties of drugs. In most cases because of the blood flow, drug loaded nanoparticles lost their drug before they reach the target organ and influence the treatment.

1.2. Chitosan as a Drug Carrier

Natural polymers such as cellulose, starch, chitosan, carrageenan, aliginates etc. are among the preferred materials for drug delivery due to their chemically inert, nontoxic, biocompatible, biodegradable structures and availability. Among them

chitosan-based nano particles received tremendous attention as one of the most promising delivery vehicles for controlled release and targeted delivery. Their characteristics were listed in the literature as below: 1) Cell membrane penetrability, 2) High drug-carrying capacities, 3) pH-dependent therapeutic unloading, 4) Ability to have a multi-functionality and 5) Prolonged circulating time (Fan et al. 2011, Gerweck 1998, Pilar Calvo 1997, Zhang, Yu, et al. 2016). Therefore there are so many studies in literature on the application of chitosan nanoparticles and methods to prepare these particles. The synthesis methods were summurized by Grenha, 2012 as follows. Emulsification and cross-linking method (Ouchi et al. 1994), emulsion droplet coalescence method (Hiryuki Tokumitsu 1999) emulsion solvent diffusion method (El-Shabouri 2002a), Reverse micellization method (S. Mitra 2001a), ionic gelation method (Fan et al. 2011, Pilar Calvo 1997), polyelectrolyte complexation method (Grenha 2012, Kaihara, Suzuki, and Fujimoto 2011, Severian Dumitriu 1998), modified ionic gelation with radical polymerization method (Hu Yong 2002) and desolvation method (Agnihotri and Aminabhavi 2007).

There are also so many studies on the drug carrying properties of chitosan (Wang et al. 2009, Duarte, Mano, and Reis 2009) have found chitosan to have anticancer effects besides its good carrier properties.

Chitosan is intrinsically pH sensitive which promote drug release in acidic environment. It is reported that many types of cancer cells exhibit different biological response in temperature and pH compare to the biological conditions of healty cells. pH values are lower in cancer cells rather than healty ones because of hypoxia (Tian and Bae 2012) (Zhang, Chen, et al. 2016). Hovewer, the range of pH values of cancer cells are matching with the value that chitosan stands soluble. Therefore there have been many studies on this feature of chitosan as drug carrier (Carson et al. 2009, Yu et al. 2009), (Salahuddin and Abdeen 2013, Deng et al. 2011), (Kamari and Ghiaci 2016), (Sionkowska, Kaczmarek, and Gadzala-Kopciuch 2016).

In addition, chitosan is known to pass the blood brain barrier (BBB) because of its positive surface charge. BBB is a system that protects brain from the harmfull compounds (pathogens, toxins, etc.). However, this barrier also does not allow some drugs which are needed for treatment of central nervous system diseases, to pass through the brain. Chitosan can directly transmit drugs to brain and there are also several studies on chitosan based brain targeted carriers (Xu et al. 2016, Ahmad et al.

2016, Hombach and Bernkop-Schnurch 2009, Saboktakin et al. 2011, Trapani et al. 2011).

1.3. Scope of the Study

Because of a need for a method to produce chitosan nano particles (~100nm) that embed hydrophobic drug. In general the chitosan based carriers are usually not suitable for uptaking and encapsulating hydrophobic drug active materials unless there is an additional modification of either drug or chitosan. This study aims to propose a method to manufacture chitosan nano particles that embed polymeric micelles (of PEO-PPO-PEO type three block copolymer, Pluronic P123) that enclose hydrophobic drug in its core.

Characterization of these nanoparticles were achieved by Fourier Transform Infrared Spectroscopy (FTIR), Scanning Electron Microscope (SEM), Scanning Transmission Microscope (STEM), Transmission Electron Microscope (TEM), surface tension and zeta potential measurements. UV-Vis spectrophotometer was used to determine the drug uptake and release.

CHAPTER 2

GENERAL INFORMATION

2.1. Drug Delivery

Drug delivery deals with transporting drugs to required spaces in body with systems which are designed for this purpose. It may include drug carrier designs or devices to provide long duration time and effective delivering.

There are several kind of drug delivery (Figure 2.1.). Depending on to required treatment and illness, proper drug delivery can be used. Transdermal, oral, mucosal, ocular drug deliveries are some of the examples of various kind of drug delivery. Oral delivery systems generally includes simple tablets or modified capsules with controlled release of drugs. Various polymer and hydrogel based formulations are commonly used in these capsules to provide effective treatment. Implanting drug to under the skin is the way of injection based drug delivery system executed. Mucosal type of drug delivery involve nasal, buccal and pulmonary part of the body. According to route of drug administration (nose or mouth) drugs are excreted by this route. In addition to this route alveolar epithelium presents good surface area especially for lipid soluble drugs. Transdermal drug delivery starts with applying drug loaded adhesive patches on the skin. Diffusion, is the reason that make drugs to cross skin surface to blood circulation.

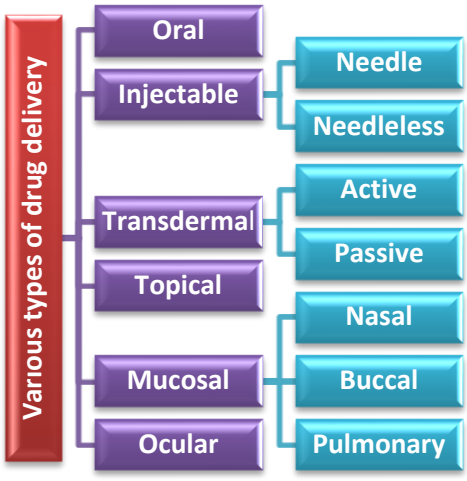

Figure 2.1.Various types of drug delivery.

Delivering drugs to required organs vitally important. Especially most of the cancer treatment techniques lead to side effects. Loss of weight, hair shedding and skin rash are some of the examples to undesirable side effects of either chemotherapy or cancer drugs. Since chemotherapy is the cure of cancer, it cause to damage of healty part of the body. Controlling and targeting drugs provide longer duration of action, increase bioavailibity and decrease adverse effects. Additively, it is possible to aim for the tumor and send the cure to predetermined side with targeting drugs like stand any other diseases. In other words, it is also enable to heal some forceful sicknesses. For example central nervous system (CNS) disorders one of the most challenging issue in medicine. Cure have to be sended directly to brain in large amount of CNS cases. Alzheimer's disease, Parkinson's disease, Huntington's disease and migraine are some of the examples for this type of CNS disorders (Duarte-Neves, Pereira de Almeida, and Cavadas 2016). The main challenges are blood brain barrier and the blood flow on delivering drugs to brain. Plenty amount of drug lost before they reach to brain because of the blood flow in body circulation. This leads to decrease on treatment effectivness. Blood brain barrier is the anaother reason to cause drugs lost. Blood brain barrier is the barrier that keeps exterior substance originating from its tight junctions (Warnken et al. 2016). It is possible to overcome these tight junctions and transport the cure to brain with drug delivery. This situation obviously show the requirement of drug delivery in treatments.

As we think for the cancer treatment and the central nervous system deseases, drug delivery can minimize these undesirable side effects and provide effective treatment for many diseases even in most compelling cases. Targeted delivery of drugs is more effective by comparison with natural treatment with drugs.

Briefly main idea in drug delivery, minimizing undesirable side effects, protecting healty tissues, providing constant release and increasing effectiveness of treatment. For this purpose drug carriers are highly benefical materials.

2.2. Drug Cariers

Drug carriers are the materials, devices or systems that include proper structures to host drugs and transport them where the cure is needed. Not only combining drug to the nanocarrier but also the way its targeting is crucial for targeted therapy. Drug

carriers are suitable for many therapeutic applications with their sizes shapes and various administration routes.

In drug delivery there are some parameters to be considered if dealing with nanoparticulate systems. As it seen from the Figure 2.2. this consideration must contain route of administration and even teeny tiny interactions between drug and the medium. The important situation in this case is hydrophilic and hydrophobic interactions between the drug and the system.

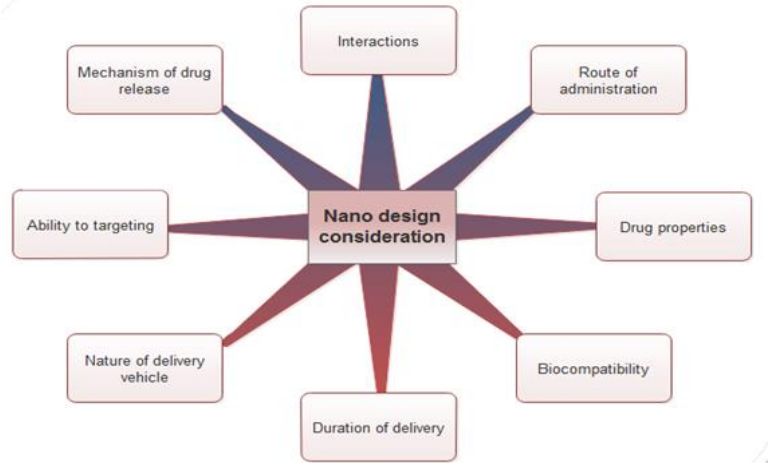

Figure 2.2.Consideration on nano design.

Drug adsorping or attaching covalently to nanocarriers surface is the one way to carrying drug. The other way is encapsulation. Nanotubes, micelles, nanospheres, emulsions, vesicles, dendrimers, lipozomes, liquid crystals can be used for this purpose.

As well as their usage in many fields according to their thermal and electrical properties carbon nanotubes are considerably important in drug delivery. They provide growth of bone cell as a scaffolding material in tissue engineering. Thermal properties of carbon nanotubes make them sufficient material to heal cancer cells based on adsorbing and converting electromagnetic radiation (Zhou et al. 2012). Relying on substracting undesirable systemitic effects of chemotherapeutic drugs carbon nanotubes accepted as a carriers for controlled and targeted delivery (Zhuang Liu 2007).

Nanospheres commonly used as a carrier because of their uniqe sizes. They have numerous advantageous on transporting drugs. Some of these materials are, gold nanoparticles, silica nanoparticles, quantum dots.

Nanocarriers which are aimed for medical applications have to be biocompatible and nontoxic. They are expected to associate with a biological system whitout any negative effect on immune response. Undesirable effects of nanoparticles highly depend on nanoparticles hydrodynamic size, shape, amount, surface chemistry, the route of administration, reaction of the immune system and residence time in the bloodstream.
Future opportunities of nanocarriers for drug delivery can be ordered like below,

- Nanocarriers provide massive advantages regarding drug targeting, delivery with additional potential to combine diagnosis and therapy.
- Usage on anti-tumor therapy, gene therapy, AIDS therapy, radiotherapy.
- Involved in delivery of virostatics, vaccines and as vesicles to pass blood brain barrier.

2.3. Chitin

Chitin (Figure 2.4.), poly (β-(1→4)-N-acetyl-D-glucosamine) is the second natural biopolymer substance in nature after cellulose (Figure 2.3.). It is obtained from a range of naturel resources i.e. insects, fungi and exoskeletons of crustaceans, lobsters (Hamed, Özogul, and Regenstein 2016). Extraction from crustacean shell is the way of production for commercial chitin (Elgadir et al. 2015). There are chemical and biological methods to produce chitin from crustacean shells.

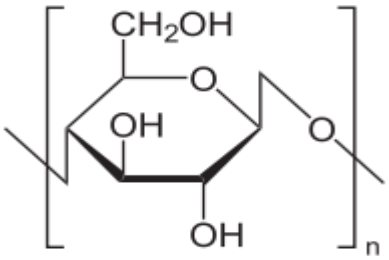

Figure 2.3. Structure of cellulose.

Chemical methods includes acidic treatment with hydrochloric acid after shells washed, dried and powdered. After that with alkali treatment demineralisation executes. By using acetone or organic mixtures pigments are removed. Finally with decolaration chitin observed. Correlatively in biological method, acidic treatment happens with lactic

acid to producing bacteria. Alkali treatment in chemical method yield to proteases in this method. For deproteisation acetone or organic mixtures can be used. After decolaration chitin can be produced.

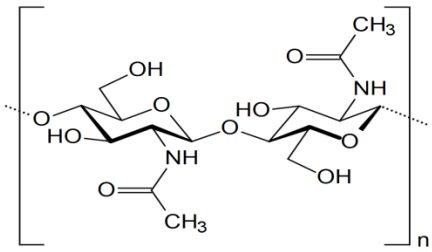

Figure 2.4. Structure of chitin.

Ordered crystalline microfibrils is the form of chitin in nature (Merzendorfer 2011). It is found that chitin exists in three forms ; α-chitin, β-chitin and γ-chitin. α-chitin is the must abunded and most stable form which presents anti-parallel strands. β is less stable and presents parallel chains. γ is the mixed form of α-chitin and β-chitin (Hamed, Özogul, and Regenstein 2016).

As a natural biopolymer, chitin and its derivatives have many biological properties. In addition to the polysaccaride structure they are biocompatable, non-toxic, biodegradable and favorable compounds to use in many applications such as biotechnology, pharmacy, agriculture, food engineering.

Various forms of chitin (hydrogels, nanogels, microparticles, sponges, scaffolds, membranes, nanofibers) used in various biomedical application like drug delivery and tissue engineering (De et al. 2013),(Sivashanmugam et al. 2015), (Smitha et al. 2013). Beside these excellent properties, drawback of chitin is its water insolubility. It is highly hydrophobic and insoluble in most organic solvents. To eliminate this problem chitin's water soluble derivatives has been using in proper situations. Chitosan is the most important derivative of chitin.

2.4. Chitosan

Chitosan is natural polysaccharide contains β-(1-4)-D-glucosamine and N-acetyl-β-(1-4)-D-glucosamine units. It is produced by deacetylation of chitin. Deacetylation process includes treatment of chitin with aqueous NaOH at 110-115℃ for

several hours without oxygen. When deacetylation degree is over 50% production called ‘chitosan’ (Chang 1997).

Chitosan is presented at fungi and yeast innately (L. Illum* 2001). Dissimilarly cellulose, chitosan contains hydroxyl groups, acetylamine or free amino groups that provide of many unique properties to chitosan (Figure 2.5.). Correspondingly these amino groups and also hydroxyl groups it is sufficient for modification. According the assigned field it can be modified. For example, modification with trimethyl and thiolate groups make it hydrophilic or to make it much more muchoadhesive etc. Chitosan has become an important material because of its benefical properties in various fields. Properties of chitosan will be explain in this chapter.

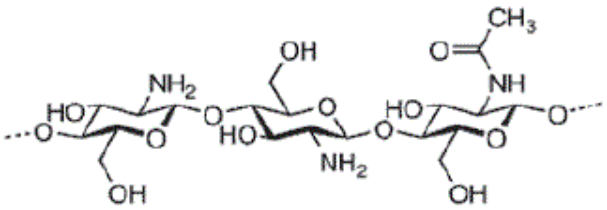

Figure 2.5. Structure of chitosan.

2.4.1 Deacetylation Degree of Chitosan

Deacetylation degree affects properties of chitosan including reactivity, solubility, viscosity, heavy metal ion gelation, proteinacous material coagulation, antimicrobial activity. It is found that deacetylation-depolymerisation sequence doesn’t affect the resultant chitosan molecular weight, deacetylation degree and repeating unit (Pankaj R. Rege 1999). From a different viewpoint it’s found that deacetylation degree affects antimicrobial activity less than the effects of molecular weight. (Mohammadi, Hashemi, and Hosseini 2016).

2.4.2 Molecular weight of Chitosan

Molecular weight of chitosan is another parameter which affects a lot of properties of chitosan based systems. Molecular weight and molecular fraction of glucosamine units in the chitosan structure influence the solubility, antimicrobial and biological activity. (Tikhonov et al. 2006).

2.4.3 Solubility of Chitosan

Chitosan, is soluble in aqueous acidic solutions depending on its amino groups but insoluble in water and alkaline solutions (Krajewska 2004). It is found that protonation of chitosan in different acidic environment depends on pH and pK value of the acid (M. Rinaudo 1999). Most of the polysaccharides has found neutral or negatively charged in acidic media. When chitosan dissolved in acidic environment the amino groups ($-NH_2$) of the glucosamine are protonated ($-NH_3^+$) and positively charge chitosan come into existence.

2.4.4 Muchoadhesive Property

Chitosan is widely used in oral delivery relying on its muchoadhesive property. Because of the negative charge of mucosal surface strong muchoadhesive force occurs between chitosan and mucosal surface. The nature of this polymer is sufficient for controlled release in oral delivery. It is found that muchoadhesion of chitosan inreases with an increasing deacetylation degree and decreases with an increase in the crosslinking (George and Abraham 2006). In addition that thiolation and trimethylation increases muchoadhesion of chitosan.

2.4.5 pH Dependence

Chitosan is soluble in weakly acidic solutions (formic acid, acetic acid, hydrochloric acid etc.) so it is suitable to use as a pH dependent material. Depending on the degree of deacetylation and the value of pKa it is insoluble in acidic environment

which is pH value is around 6.5. Because of this reason pH must be regarded if any system consist of chitosan.

Besides these properties chitosan exhibits good permeation enhancement, immunity activator and antimicrobial activity. It is also a efflux pump inhibitor and strongly heals wounds.

2.5. Chitosan as a Drug Carrier

Chitosan can be in film, hydrogel and mostly nanoparticulate form to use in general applications. For drug delivery purposes chitosan nanoparticles and hydrogels are commonly used depending on the conditions.

Because of its sufficient structure to modification it is possible to convert chitosans properties to proper chemical structures. In some cases chitosan can be modified to develop its properties like molecular weight, muchoadhesion and solubility. Conjugating materials and their effects on chitosan properties are given below (Figure 2.6.).

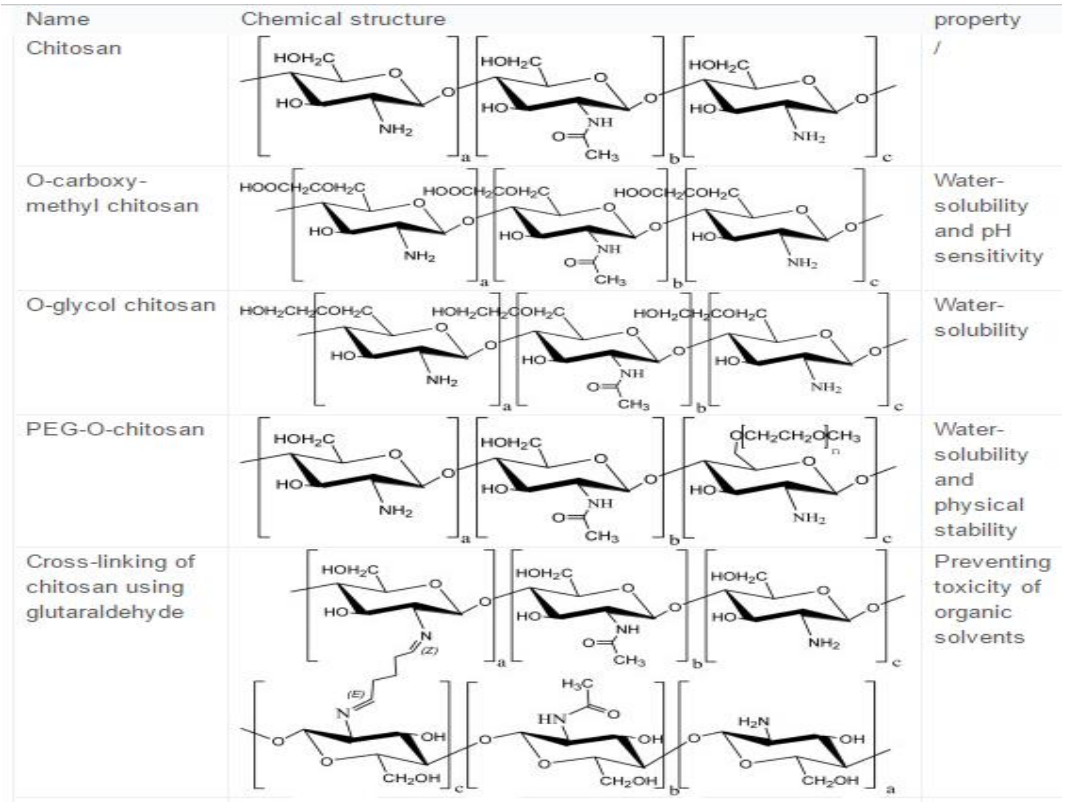

Figure 2.6. Conjugating effect on chitosan properties (Zhang, Yang, et al. 2016).

2.6. Synthesis of Chitosan Nanoparticles

Methods for synthesis of chitosan nanoparticles is a continual issue. Chitosan nanoparticles have been studying for drug delivery purposes since 1994. Production processes have been adapted according to usage field of chitosan nanoparticles. Extant production methods will be explained below.

In emulsification and crosslinking method is based on W/O emulsion which was created with Toluene and Span 80 as an oil phase and chitosan as water phase. This is the first method that chitosan nanoparticles investigated by Ohya et al. in 1994. After W/O emulsification, methods includes addition of cross-linking agent aimed for hardening droplets. This mechanism explained by covalent cross-linking amino groups of chitosan and aldehyde groups of gluteraldehyde as in Figure 2.7.

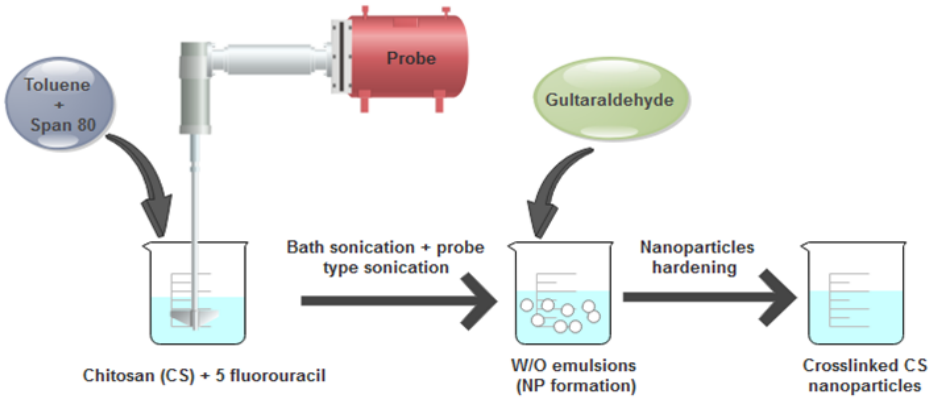

Figure 2.7. Emulsification and crosslinking method.

Emulsion droplet coalescence method which was used for the microparticle production first, is adjusted for nanoparticles production. Gadolinium loaded chitosan nanoparticles were produced with an aim for neutron-capture therapy for cancer (Tokumitsu H. 1999). Method based on mixing two type W/O emulsions which have difference on their water phases. One of the emulsions are gadolinium and chitosan, the other consist of NaOH solution (precipitating agent) as it shown in Figure 2.8. Paraffin and sorbitan sesquiolate (Span 83) were used as an oil phase. At the end of the process, mixing of these two emulsions with high-speed homogenizer leads to coalescence.

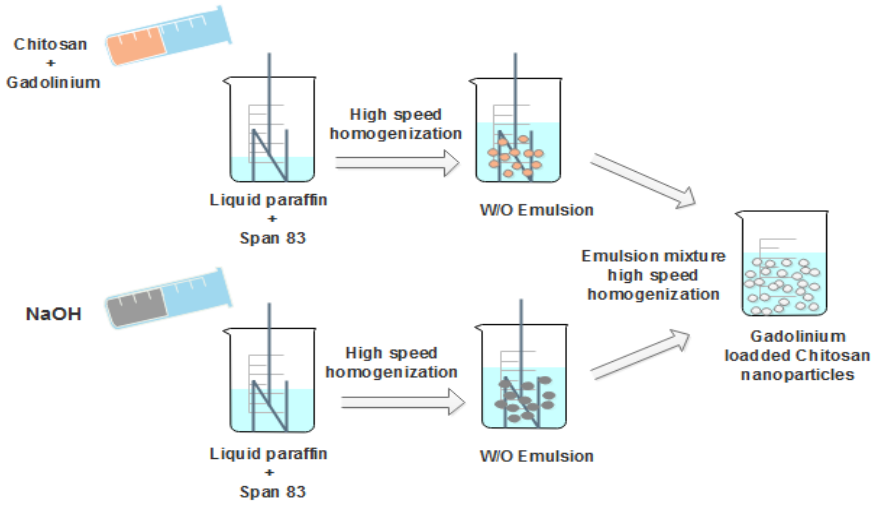

Figure 2.8. Emulsion droplet coalescence method.

Emulsion solvent diffusion method is not only sufficient as a harsh process but also a convenient method for producing carrier of hydrophobic drugs. In this method organic phase (methylene chloride and acetone) which contains hydrophobic drug is added to aqueous solution of chitosan and stabilizer as in Figure 2.9. After high speed homogenization methylene chloride is removed under reduced pressure at room temperature. Depending on the diffusion of acetone nanoparticles become on polymer precipitation (El-Shabouri 2002b). At the last step of this process is nanoparticles isolation by centrifugation.

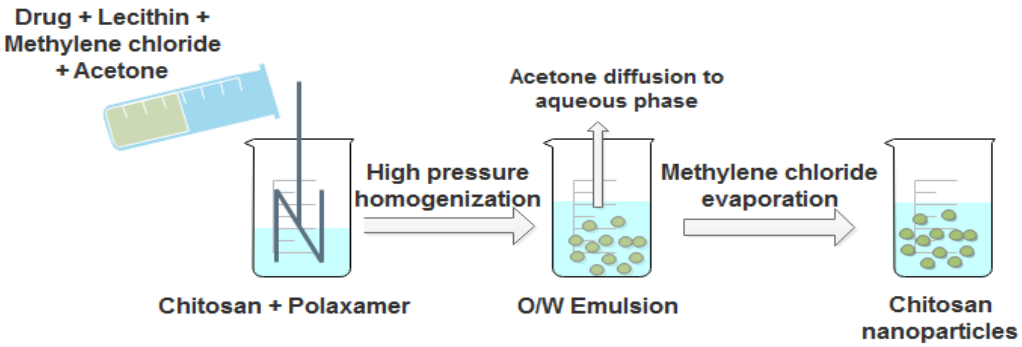

Figure 2.9. Emulsion solvent diffusion method.

Mitra et. al. used **reverse micellization** method for the first time to option of chitosan carrier on tumor targeted delivery (S. Mitra 2001b). In this method lipophilic surfactant dissolved in suitable organic solvent. Surfactants like sodium bis(ethylhexyl)

sulfosuccinate (AOT) or cetyl trimethylammonium bromide have been used. The phase which inclusive chitosan, glutaraldehyde and drug, is added to organic phase under magnetic stirring. As a result of this step reverse micelles are produced. Nanoparticles extraction is done by solvent evaporation (S. Mitra 2001b).

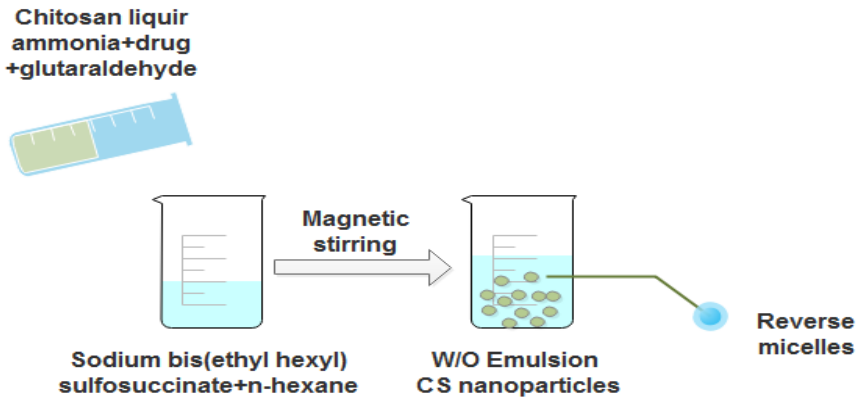

Figure 2.10. Reverse micellezation method.

Reverse micellezation method (Figure 2.10.) is in the forefront with nanoparticles sizes below 100 nm rather than other emulsification methods.

Ionic gelation, includes the electro-static interaction which is between polyions (small molecules) and oppositely charged specific cross-linkers. Ionic crosslinking mechanism come into exists from cross linkages which are interdeced by anionic molecules. Chitosan is soluble under acidic condition because protonation of its amino groups (pKa values range from 6.2 to 7 depending on the type of chitosan and conditions of measurement). In these conditions, chitosan behaves as a polycation which promotes electrostatic interactions. Ionic gelation method is one of the techniques depending on pH and the concentration values of the system. In this method, tripolyphosphate generally used as a crosslinking agent and added to chitosan solution under controlled stirring as it seen in Figure 2.11. Concentration of chitosan and tripolyphosphate is the main parameter on properties of produced nanoparticles.

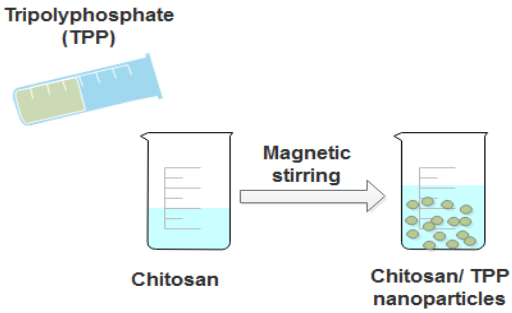

Figure 2.11. Ionic gelation method.

Polyelectrolyte complexation, requires a polyanion as it was in ionic gelation. Main difference between ionic gelation and polyelectrolyte complexation is the type of polyanion. It is called 'polyelectrolyte complexation' if macromolecules used as a polyanion. Electrostatic complex occurs at the end of this interaction. Electrostatic interaction happens between cationic chitosan and polyanion. Polysaccarides are good examples of this polyanions. Especially gluteraldehyde shows more interaction sides and negative chatge than the other polysaccharides to interact with chitosan(Avadi et al. 2010). The procedure is the same with ionic gelation.

Modified ionic gelation with radical polymerization, method involves stirring aqueous solution of chitosan and aqueous monomer solution of acrylic or merthacrylic acid at room temperature as it shown in Figure 2.12. Addition of potassium persulfate is the initiation of radical polymerization and ionic interaction occurs because of the positive charge of chitosan and negative charge of acrylic or methacrylic acid at this step. Polymerization reaction takes 6 hours. At the end of this reaction dialysis is used for removing of unreacted monomers (Yong Hu 2002).

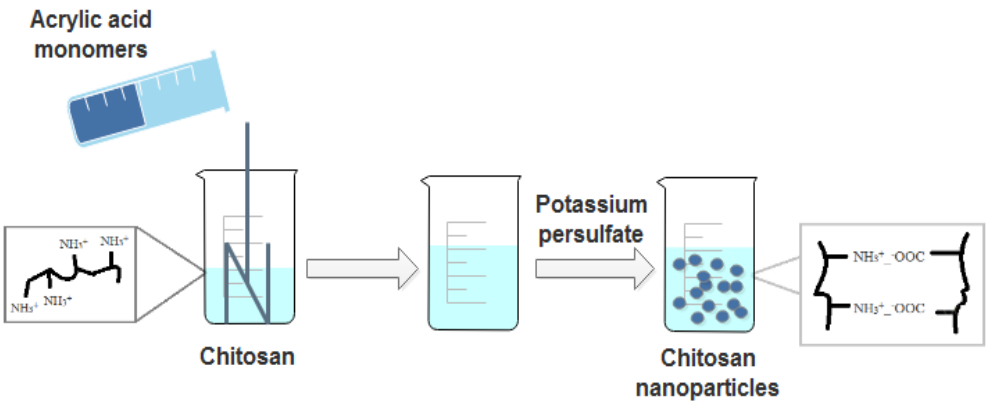

Figure 2.12. Modified ionic gelation with radical polymerization.

Desolvation, method which aimed for preparation of micron sized carriers was used for the first time in 1996 (A. Berthold 1996). Sodium sulfate adapted method is commonly used for producing chitosan nanoparticles (Hai-Quan Maoa and Kevin Y. Lina 2001) (Mansouri et al. 2006). Method is applicable for DNA and protein delivery (Yuan et al. 2009) (Syed Othman Syed Mohamad Al-Azi 2014).

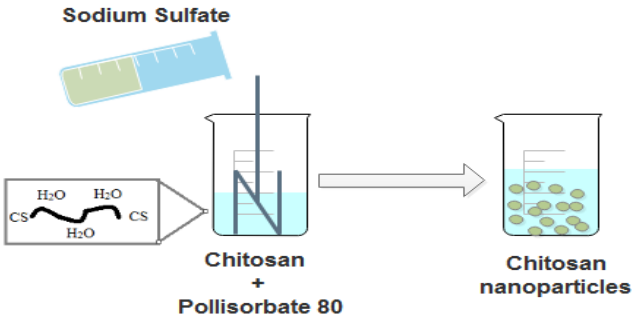

Figure 2.13. Desolvation method.

Desolvation method which is shown in Figure 2.13 based on coacervation and phase separation. Addition of desolvation agents (ethanol or aceton) cause to precipitation of nanoparticles and addition of crosslinking agent provides stabilization of nanoparticles (Raghuwanshi et al. 2012).

CHAPTER 3

MATERIALS AND METHODS

3.1. Materials

In this study, all the chemicals used were analytical grade and obtained from Sigma-Aldrich Chemical Company. These chemicals were chitosan (low molecular weight, viscosity 20.000 cps), Heptane (C_7H_{16}, M.W. 100.21 g/mol), PEO/PPO/PEO Tri block co-Polymer, Pluronic P-123 (average molecular weight 5.800g/mol), triton X-100 (MW. 628 g/mol), span 80 (M.W. g/mol), span 60 (M.W. g/mol), Sodium Dodecyl Sulfate (M.W.228g/mol), Sodium Tripoly Phosphate (as cross-linking agent), probucol, curcumin (as model hydrophobic drugs), and vancomycin hydrochloride (as model hydrophilic drug), ethanol, acetonitrile, acetic acid. The chemical structures of these chemicals are given in Figure 3.1. Model drugs are presented in Figure 3.2. Probucol is known as cholesterol lowering agent and it is effective against cardiovascular disease, restenosis. Curcumin has anti-tumourogenic, anticoagulant, antibacterial, anticancer, antioxidant activities. Vancomycin hydrochloride is an antibiotic and effective against bacterial diseases. Ultra-pure water (18.2 MΩ) was used throughout the study.

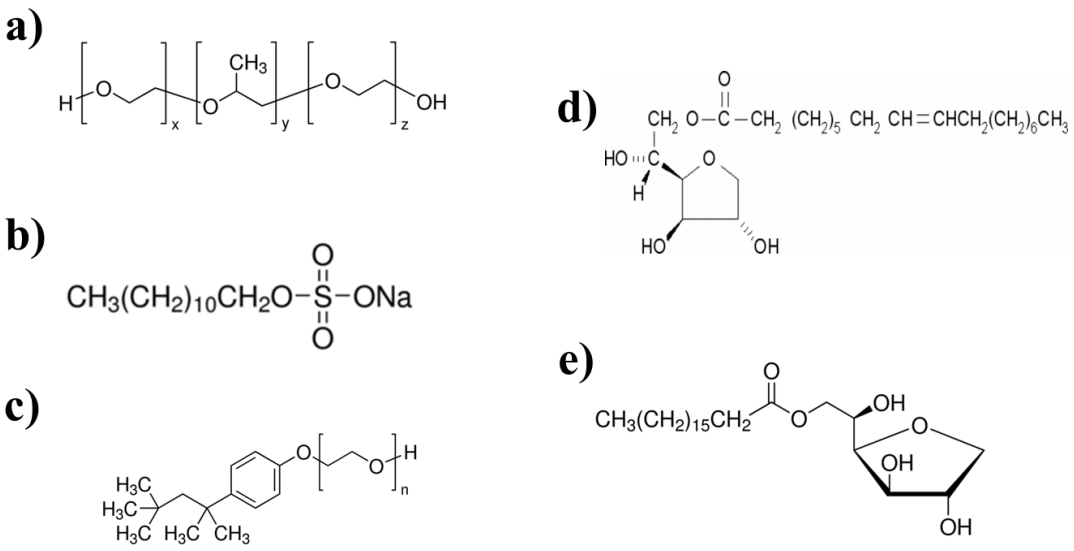

Figure 3.1. Structure of materials; a) Pluronic 123, b) Sodium Dodecyl Sulfate (SDS) c) Triton X-100 d) Span 80 e) Span 60

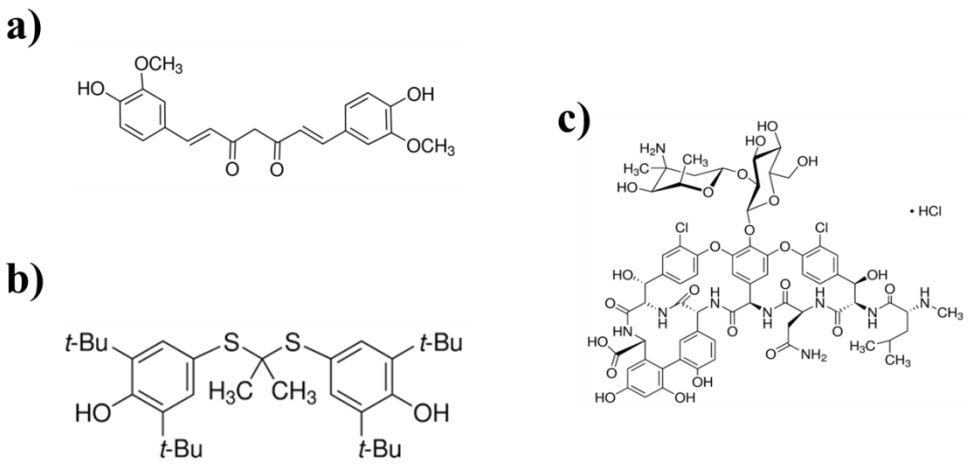

Figure 3.2. Structure of model drugs; a) Curcumin, b) Probucol, c) Vancomycin Hydrochloride

3.2. Preparation of Drug loaded P-123 Micelles

Drug loaded micelles were prepared according to the thin film hydration method as it shown in Figure 3.3. Method has superiority not only to usage on small and uniform particles and also with its simplicity. Briefly Probucol (0.001%) and P-123 (10^{-2} M) were dissolved in acetonitrile under stirring. The organic solvent removed by evaporation at 50 ^{o}C under vacuum to form a thin film. Then an aqueous solution were added to envelope drug in micelle structures.

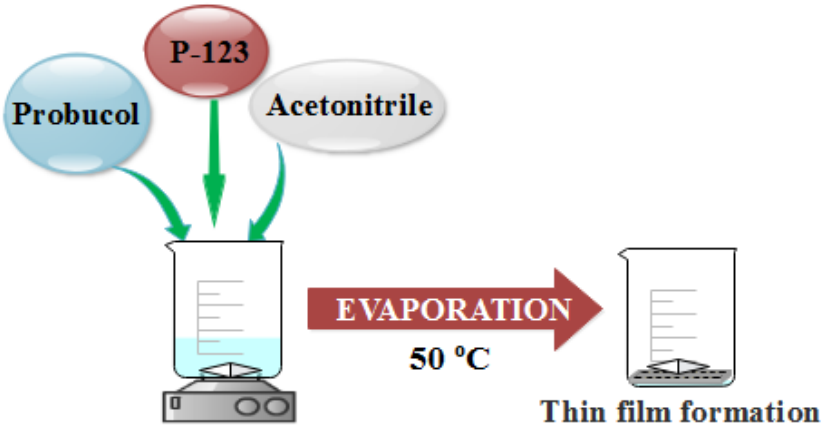

Figure 3.3. Thin film hydration method.

3.3. Production of Micelle Embedded Chitosan Nanoparticles

Initially ionic gelation method (Figure 3.4.) was used to determine the best Chitosan/TPP ratio and use for all the methods designed and produced in this study. The methods developed were to obtain chitosan nano-structures that embed drug loaded P-123 micelles in them. These methods were discussed in the following paragraphs.

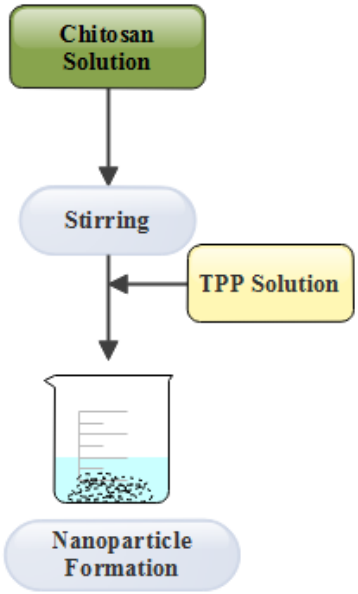

Figure 3.4. Ionic gelation method (general).

3.3.1. Oil in Water (O/W) Emulsification Coupled with Ionic Gelation Method

This method is summarized in the following flowsheet in Figure 3.5. According to the procedure given below, O/W emulsion was prepared by dispersing heptane (3%) in P-123 (10^{-2} M) solution by ultrasonic probe in the presence of SDS. Then Chitosan (1%, 0.5% (w/v) in 1% acetic acid) and TPP solutions were added and stirred for about 30 minutes to from chitosan layer around oil droplets stabilized by P-123 and SDS molecules. In the case of drug, Probucol dissolved in heptane as 0.001% (w/v) and added to P-123 solution before emulsification. Expected nanoparticle structure is given in Figure 3.7.

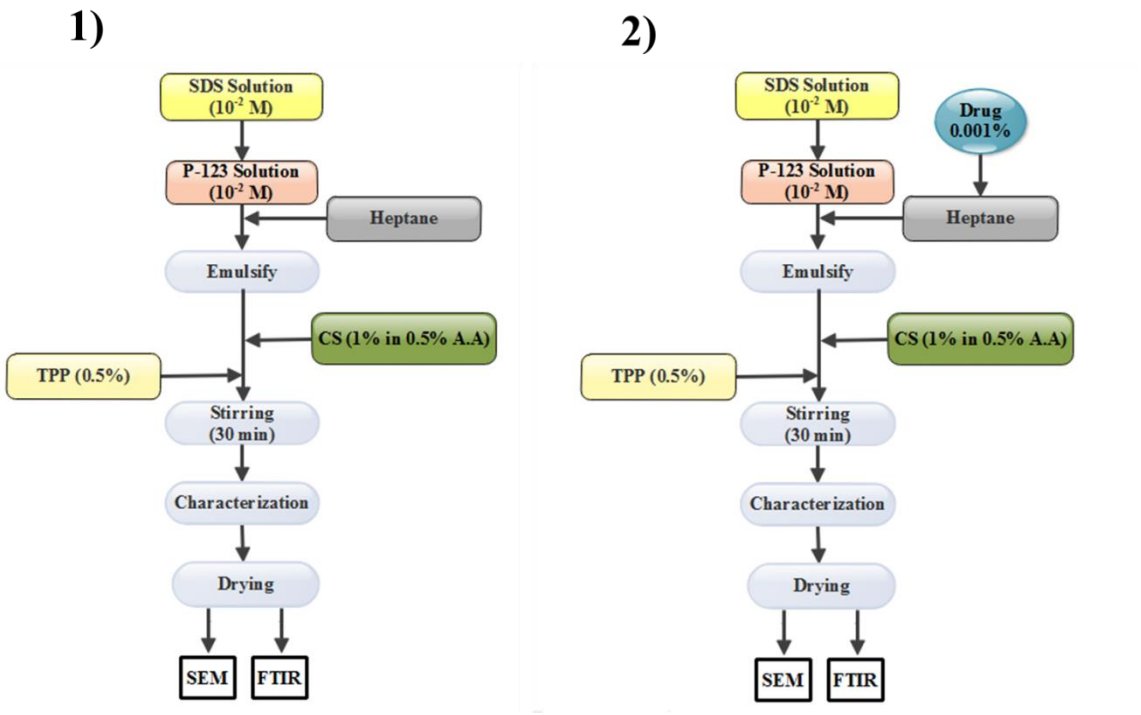

Figure 3.5. Oil in Water (O/W) Emulsification Coupled with Ionic Gelation Method

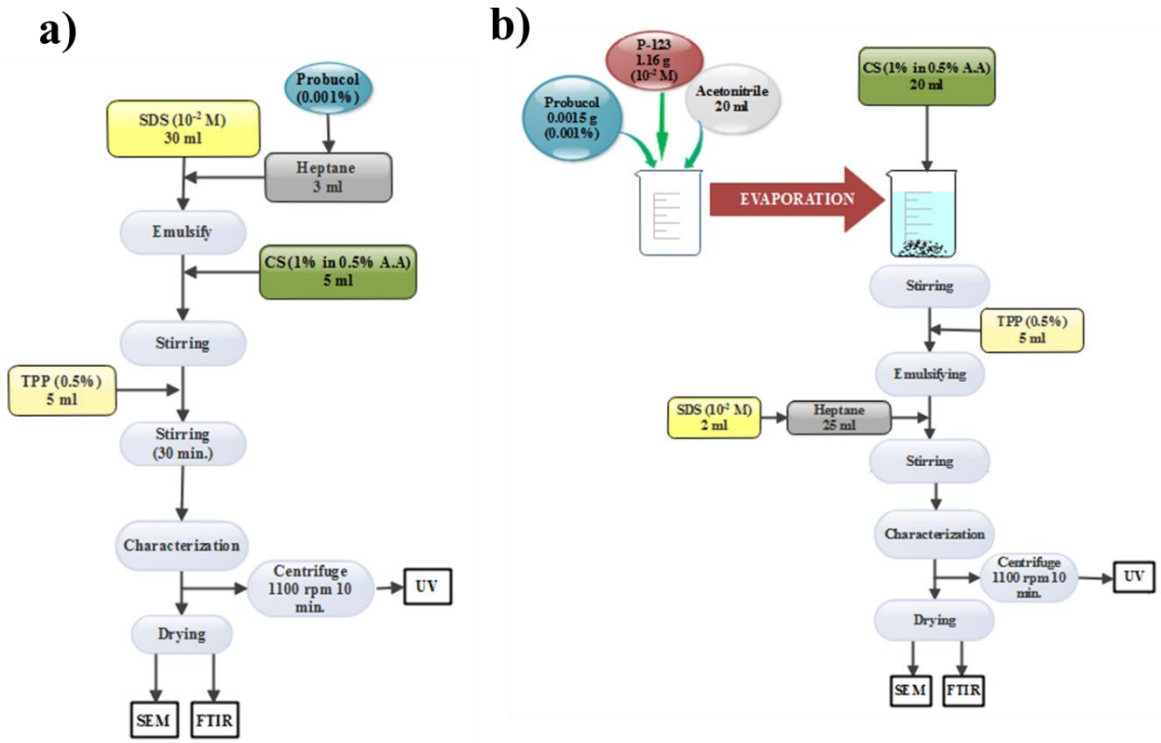

Figure 3.6. Oil in Water (O/W) Emulsification Coupled with Ionic Gelation Method conditions **(continue on next page)**

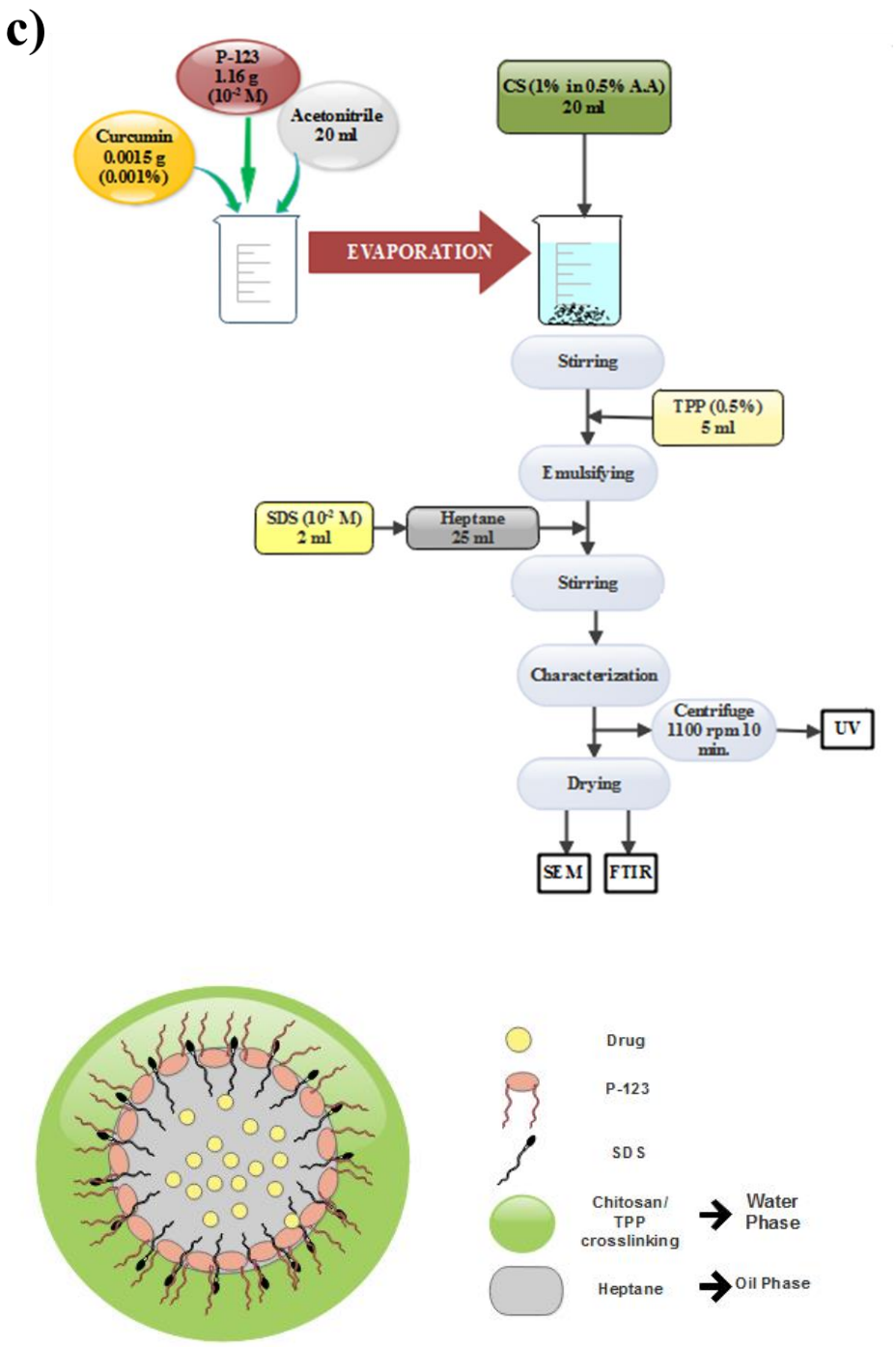

Figure 3.7. Schematic picture of drug loaded micelle embedded chitosan nanoparticle produced by Oil in Water (O/W) Emulsification Coupled with Ionic Gelation Method

3.3.2. Water in Oil (W/O) Emulsification Coupled with Ionic Gelation Method

Chitosan (1% (w/v) in 1% acetic acid, 0.5% in 1% acetic acid) solution was stirred overnight to ensure total solubility. For the same purpose 10^{-2} M P-123 solution was stirred overnight and used for creation of micelles. As a crosslinking agent 0.5% (w/v) TPP solution was used in this method. Chitosan solution was added to 15 ml heptane in a beaker. After ultrasonic probe treatment 10^{-2} M P-123 solution was added. 0.5% TPP solution was added for the purpose of crosslinking. Suspension was stirred for 30 minutes to ensure reaction completion (Figure 3.8.).

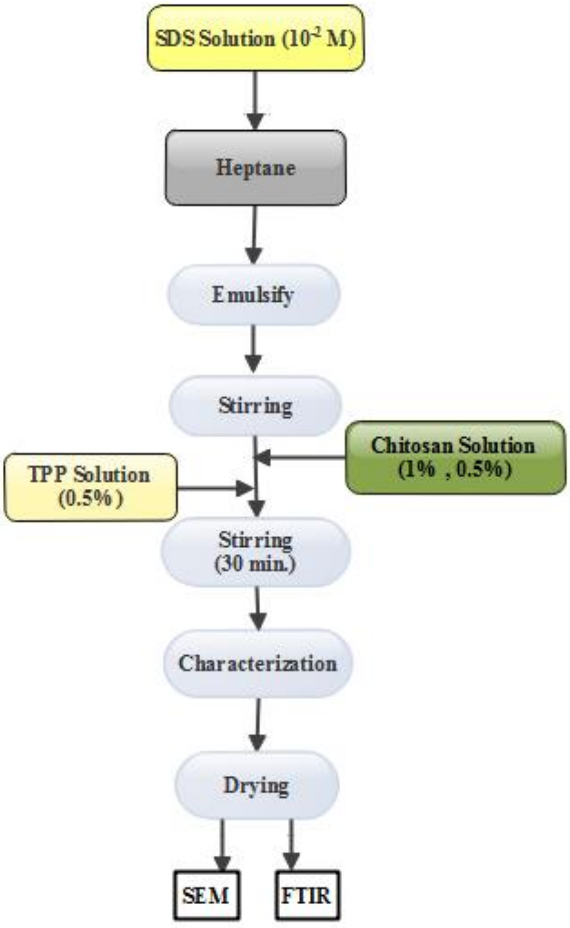

Figure 3.8. Water in Oil (W/O) Emulsification Coupled with Ionic Gelation Method

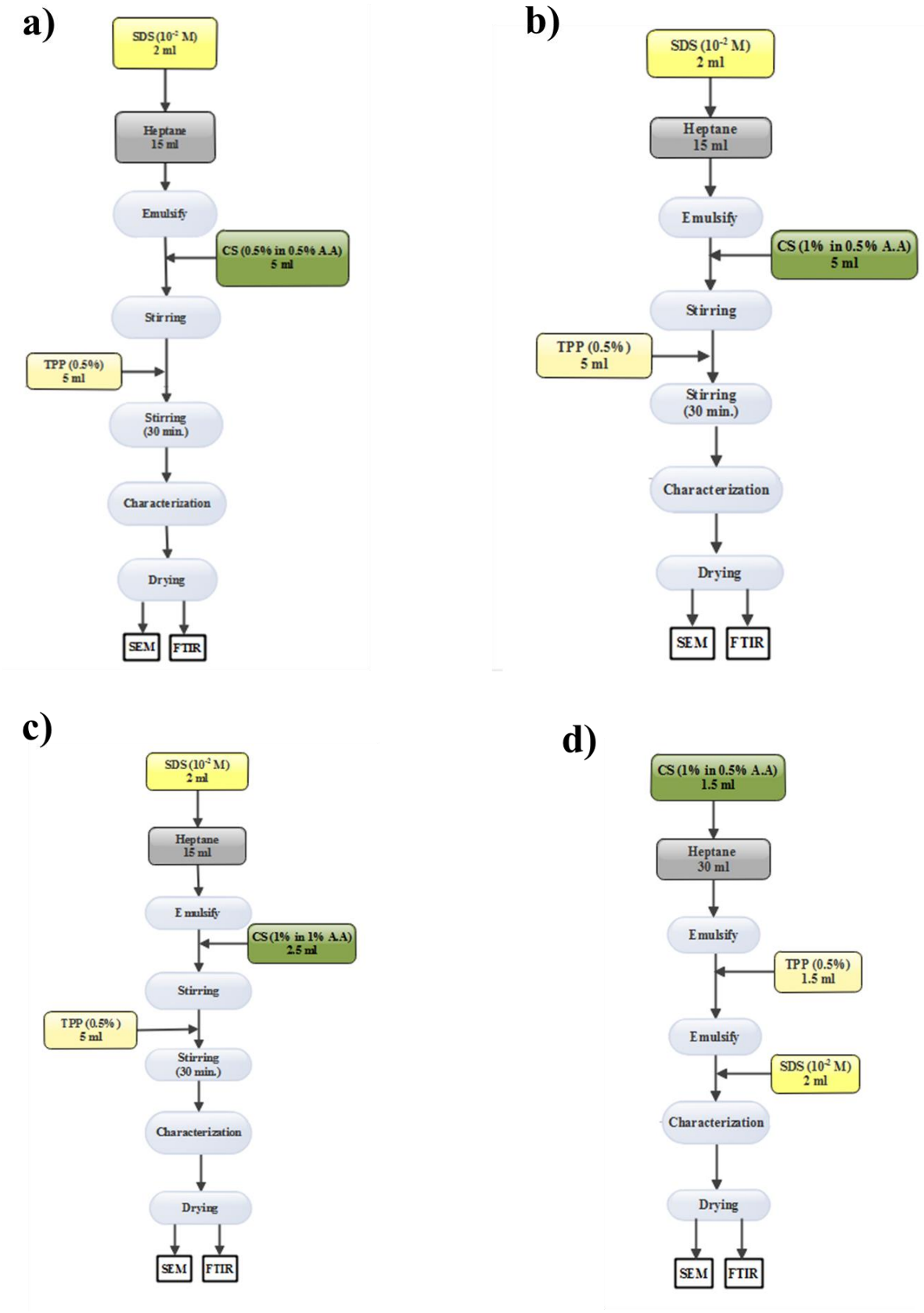

Figure 3.9. Water in Oil (W/O) Emulsification Coupled with Ionic Gelation Method conditions. **(continue on next page)**

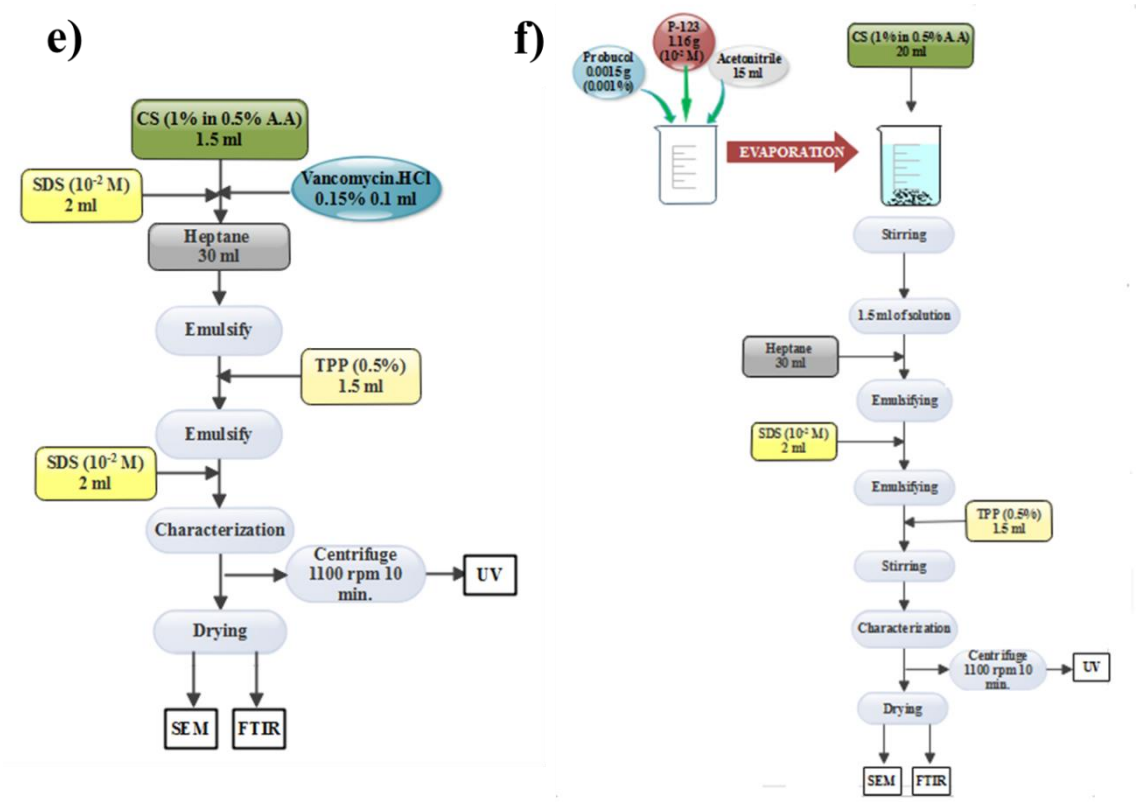

3.3.3. Oil in Water in Oil (O/W/O) Emulsification Coupled with Ionic Gelation Method

This method is summarized in the following flowsheets in Figure 3.10 and 3.11. Chitosan (1% (w/v) in 1% acetic acid, 0.5% in 1% acetic acid) solution was stirred overnight to ensure total solubility. For the same purpose 10^{-2} M P-123 solution was stirred overnight and used for creation of micelles. As a crosslinker agent 0.5% (w/v) TPP solution was used in this method. Firstly chitosan solution (1% and 0.5%) and 10^{-2} M P-123 solution added to a beaker under constant stirring. Heptane added drop by drop. After addition of heptane, SDS solution added for emulsification. Suspension treated with ultrasonic probe. During the treatment of ultrasonic probe, TPP (0.5%) solution added in a way to CS/TPP ratio 2. After addition of TPP, second oil phase (heptane) added under constant stirring. Some experiments include second SDS solution addition in different steps of process for the purpose of dispersion effect. For the formation of chitosan nanoparticles suspension was stirred 30 minutes. In order to obtain drug loaded micelle embedded chitosan nanoparticles, 0.001% Probucol was dissolved in 1 ml heptane.

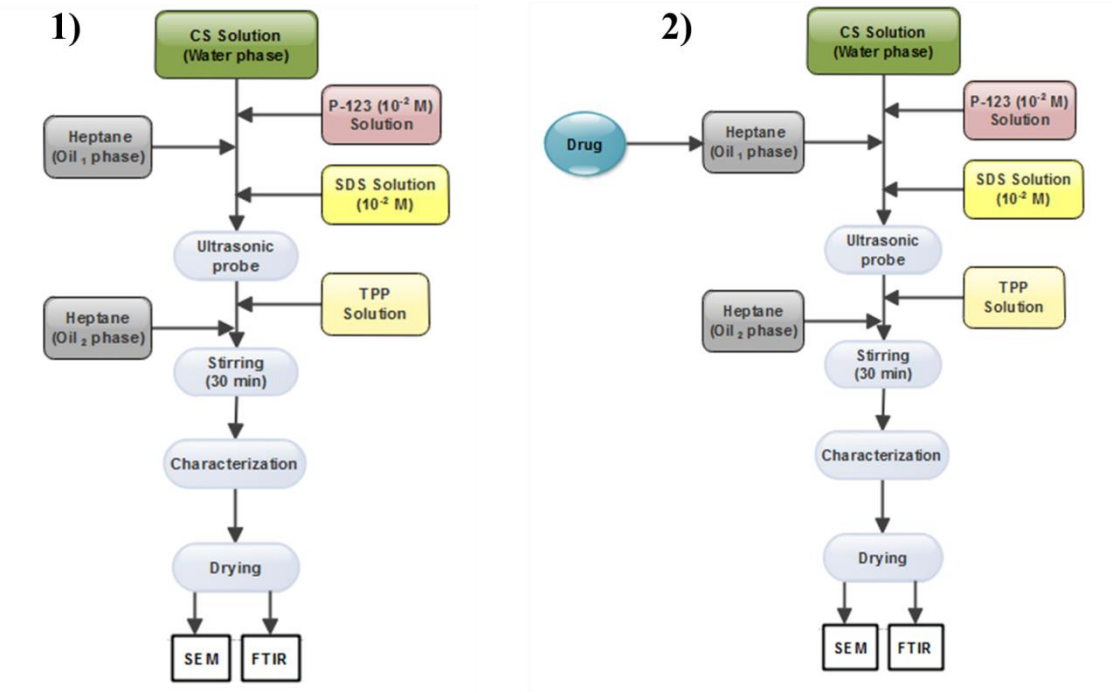

Figure 3.10. O/W/O Emulsification coupled with Ionic Gelation method
a) without drug b) with drug

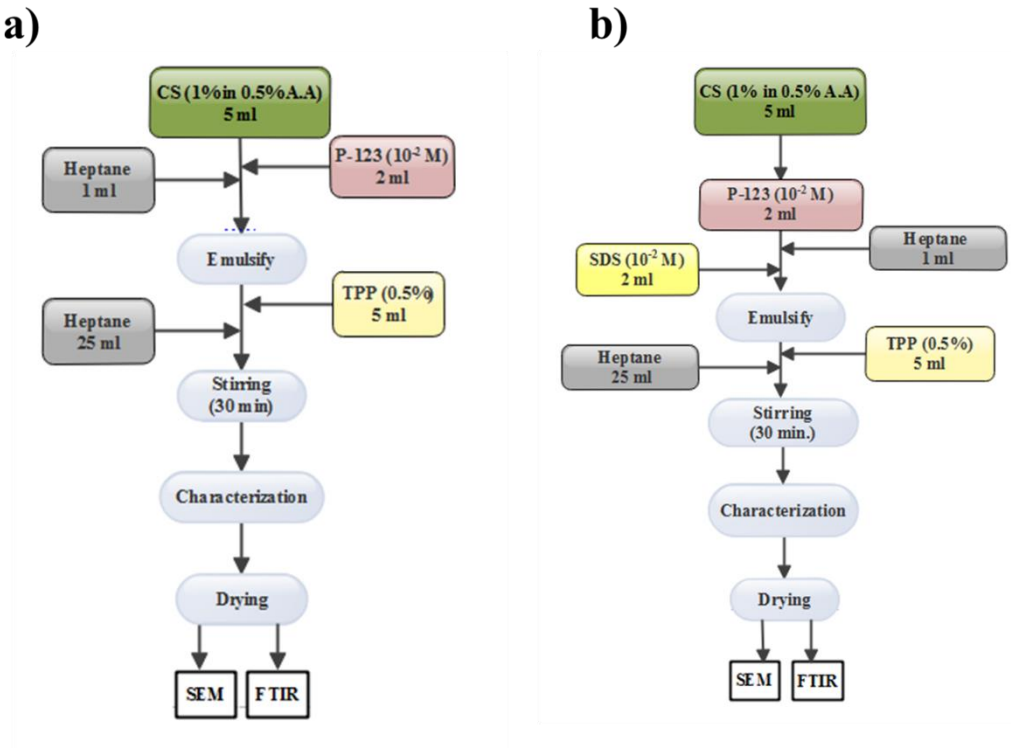

Figure 3.11. O/W/O Emulsification coupled with Ionic Gelation method conditions.
(continue on next pages)

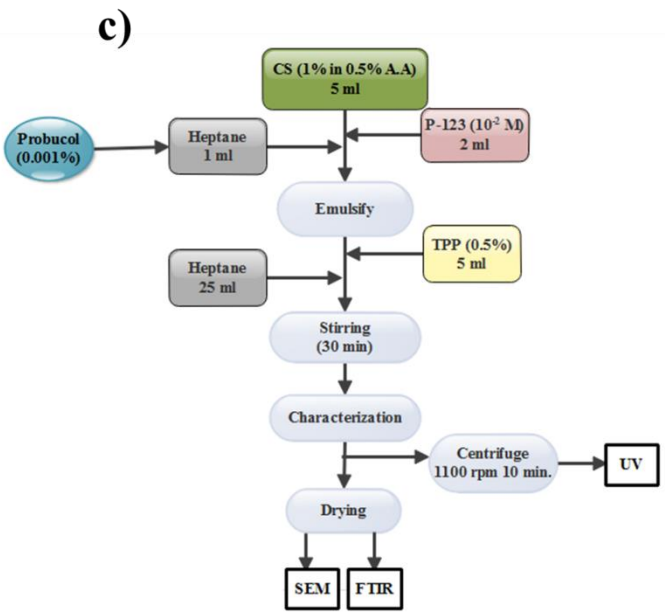
c)
CS (1% in 0.5% A.A)
5 ml
Probucol
(0.001%)
Heptane
1 ml
P-123 (10^{-2} M)
2 ml
Emulsify
TPP (0.5%)
5 ml
Heptane
25 ml
Stirring
(30 min)
Characterization
Centrifuge
1100 rpm 10 min.
UV
Drying
SEM
FTIR

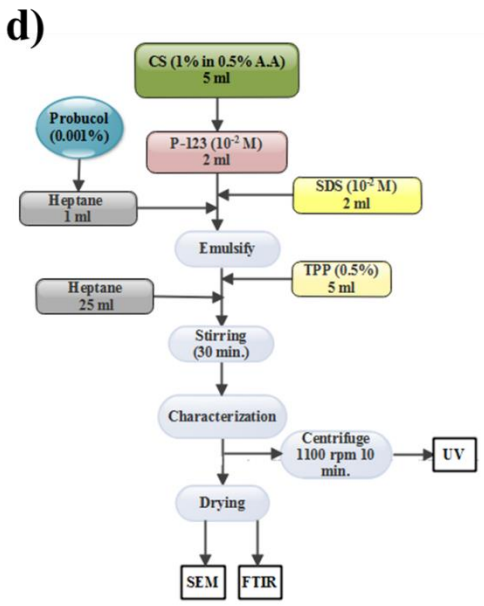
d)
CS (1% in 0.5% A.A)
5 ml
Probucol
(0.001%)
P-123 (10^{-2} M)
2 ml
SDS (10^{-2} M)
2 ml
Heptane
1 ml
Emulsify
TPP (0.5%)
5 ml
Heptane
25 ml
Stirring
(30 min.)
Characterization
Centrifuge
1100 rpm 10
min.
UV
Drying
SEM
FTIR

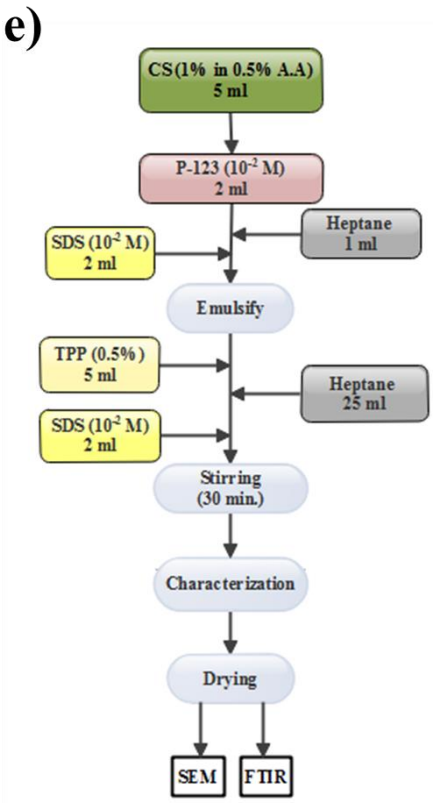
e)
CS (1% in 0.5% A.A)
5 ml
P-123 (10^{-2} M)
2 ml
SDS (10^{-2} M)
2 ml
Heptane
1 ml
Emulsify
TPP (0.5%)
5 ml
Heptane
25 ml
SDS (10^{-2} M)
2 ml
Stirring
(30 min.)
Characterization
Drying
SEM
FTIR

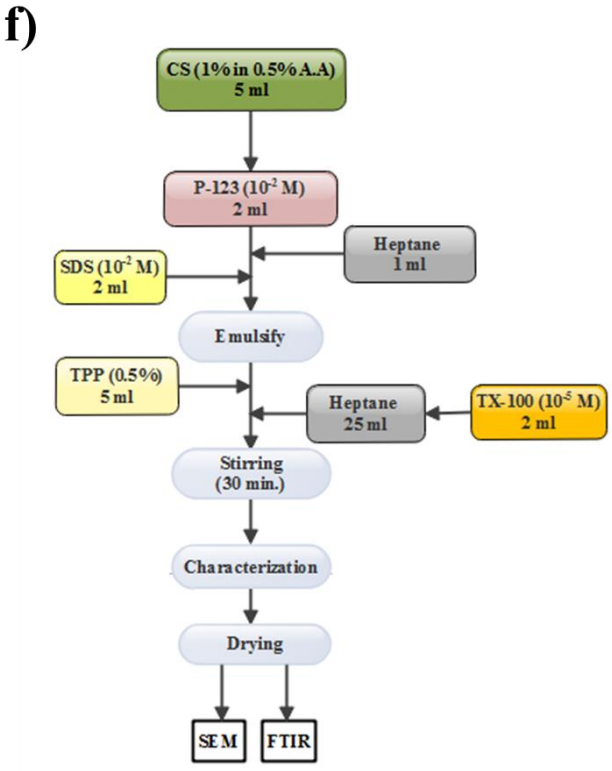
f)
CS (1% in 0.5% A.A)
5 ml
P-123 (10^{-2} M)
2 ml
SDS (10^{-2} M)
2 ml
Heptane
1 ml
Emulsify
TPP (0.5%)
5 ml
Heptane
25 ml
TX-100 (10^{-5} M)
2 ml
Stirring
(30 min.)
Characterization
Drying
SEM
FTIR

g)

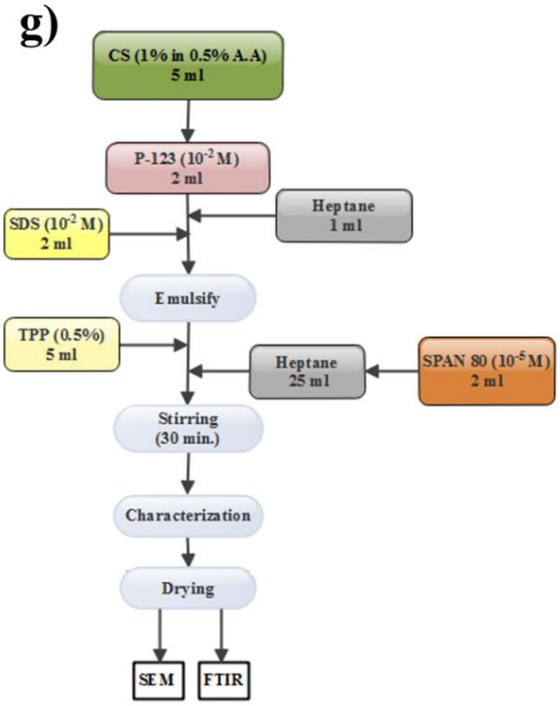
CS (1% in 0.5% A.A)
5 ml
P-123 (10^{-2} M)
2 ml
Heptane
1 ml
SDS (10^{-2} M)
2 ml
Emulsify
TPP (0.5%)
5 ml
Heptane
25 ml
SPAN 80 (10^{-5} M)
2 ml
Stirring
(30 min.)
Characterization
Drying
SEM
FTIR

h)

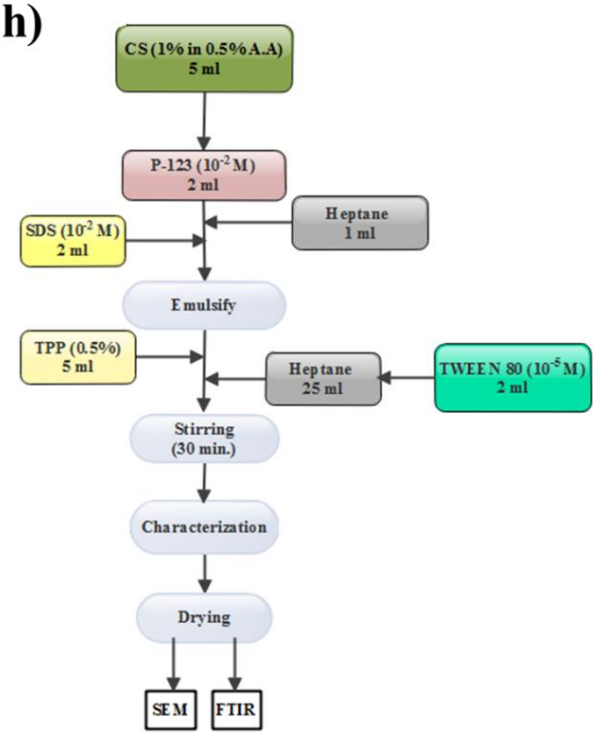
CS (1% in 0.5% A.A)
5 ml
P-123 (10^{-2} M)
2 ml
Heptane
1 ml
SDS (10^{-2} M)
2 ml
Emulsify
TPP (0.5%)
5 ml
Heptane
25 ml
TWEEN 80 (10^{-5} M)
2 ml
Stirring
(30 min.)
Characterization
Drying
SEM
FTIR

ı)

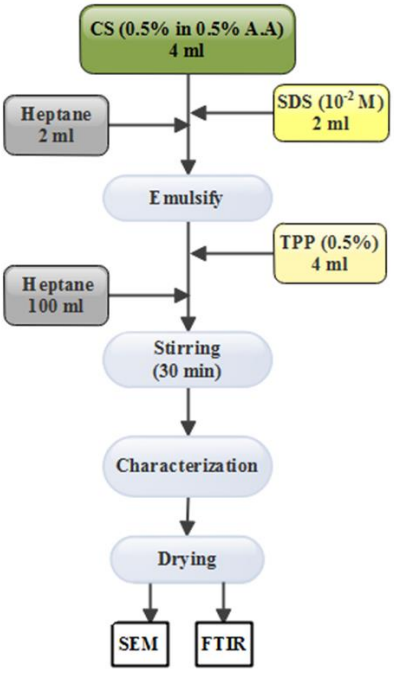
CS (0.5% in 0.5% A.A)
4 ml
Heptane
2 ml
SDS (10^{-2} M)
2 ml
Emulsify
TPP (0.5%)
4 ml
Heptane
100 ml
Stirring
(30 min)
Characterization
Drying
SEM
FTIR

j)

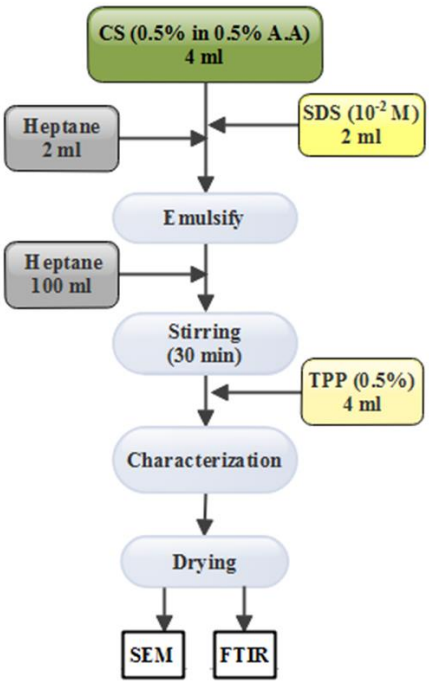
CS (0.5% in 0.5% A.A)
4 ml
Heptane
2 ml
SDS (10^{-2} M)
2 ml
Emulsify
Heptane
100 ml
Stirring
(30 min)
TPP (0.5%)
4 ml
Characterization
Drying
SEM
FTIR

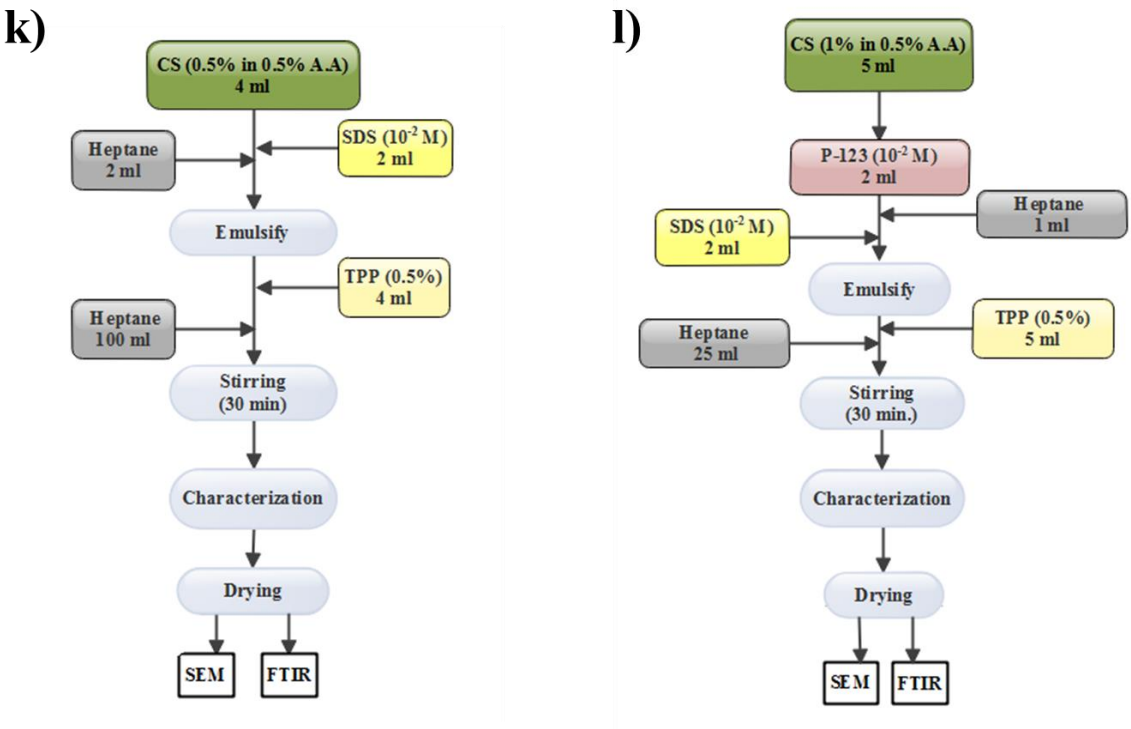

As a consequence of O/W/O emulsification and ionic gelation process proposed structure of drug loaded micelles embedded chitosan nanoparticles are shown in Figure 3.12.

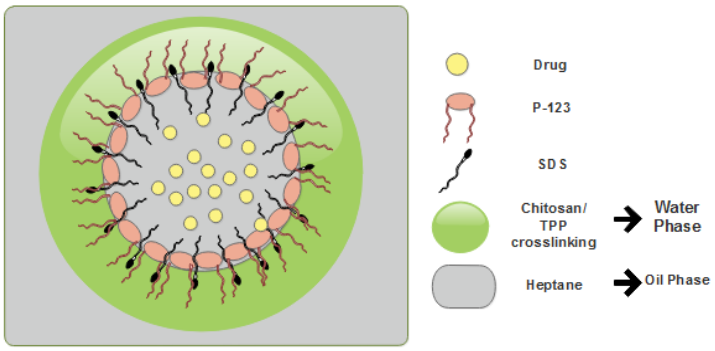

Figure 3.12. Schematic picture of drug loaded micelle embedded chitosan nanoparticle produced by O/W/O Emulsification coupled with Ionic Gelation method.

3.3.4. Spontaneous Emulsion Coupled with Ionic Gelation Method

Chitosan (1% (w/v) in 1% acetic acid, 0.5% in 1% acetic acid) solution was stirred overnight to ensure total solubility. For the same purpose 10^{-2} M P-123 solution was stirred overnight and used for creation of micelles. As a crosslinking agent 0.5% (w/v) TPP solution was used in this method. Firstly surfactant solution (SDS or CTAB 10^{-2} M) added to ethanol to creation for spataneous emulsion. Under constant stirring oil phase added to solution and relying on the crosslinking mechanism chitosan and TPP added for the formation of nanoparticles.

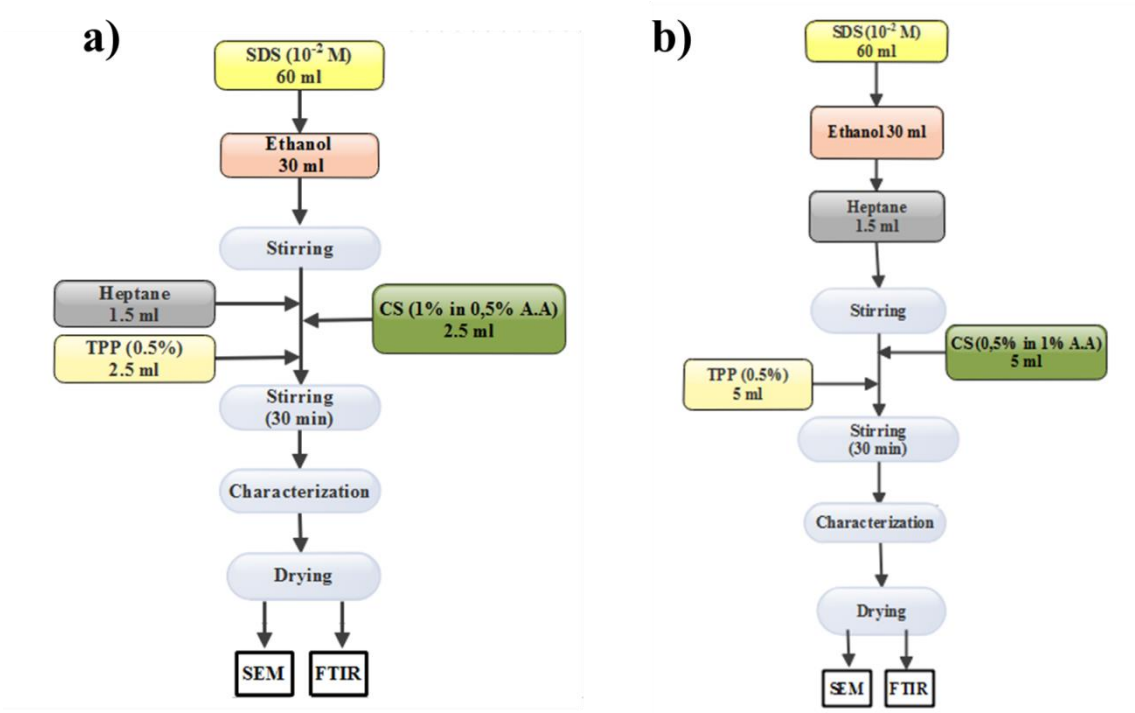

Figure 3.13. Spontaneous Emulsion Coupled with Ionic Gelation Method conditions**. (continue on next pages)**

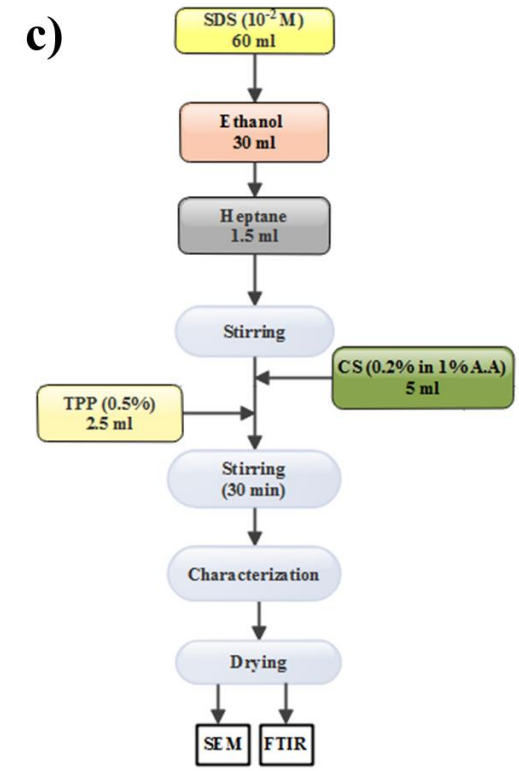
c)
SDS (10^{-2} M) 60 ml
Ethanol 30 ml
Heptane 1.5 ml
Stirring
CS (0.2% in 1% A.A) 5 ml
TPP (0.5%) 2.5 ml
Stirring (30 min)
Characterization
Drying
SEM
FTIR

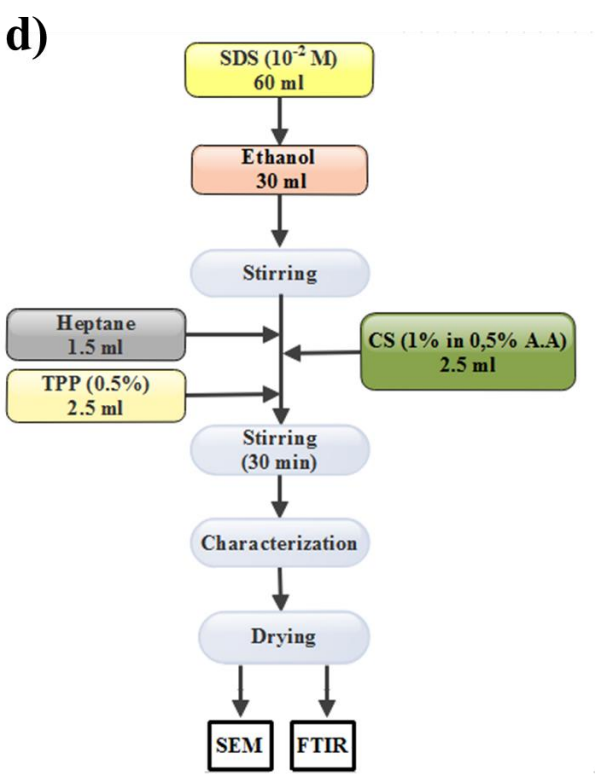
d)
SDS (10^{-2} M) 60 ml
Ethanol 30 ml
Stirring
Heptane 1.5 ml
CS (1% in 0,5% A.A) 2.5 ml
TPP (0.5%) 2.5 ml
Stirring (30 min)
Characterization
Drying
SEM
FTIR

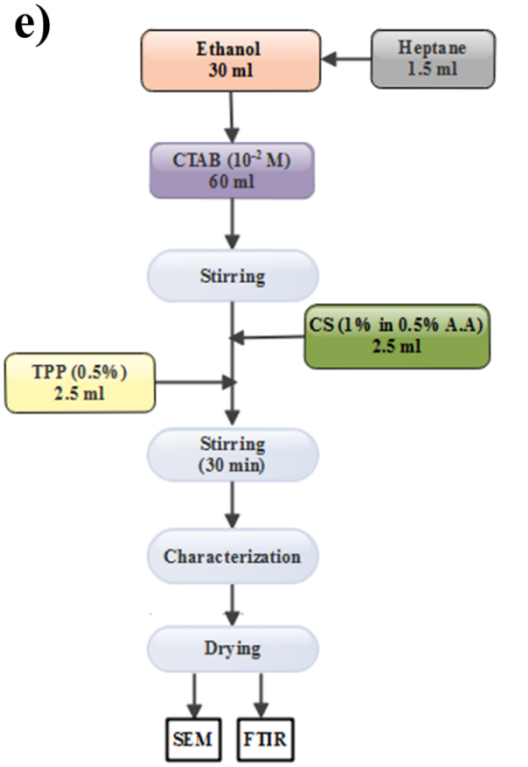
e)
Ethanol 30 ml
Heptane 1.5 ml
CTAB (10^{-2} M) 60 ml
Stirring
CS (1% in 0.5% A.A) 2.5 ml
TPP (0.5%) 2.5 ml
Stirring (30 min)
Characterization
Drying
SEM
FTIR

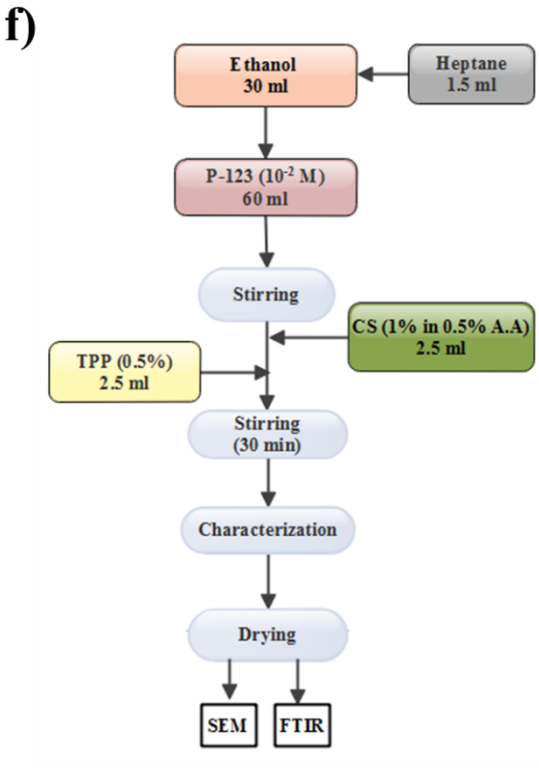
f)
Ethanol 30 ml
Heptane 1.5 ml
P-123 (10^{-2} M) 60 ml
Stirring
CS (1% in 0.5% A.A) 2.5 ml
TPP (0.5%) 2.5 ml
Stirring (30 min)
Characterization
Drying
SEM
FTIR

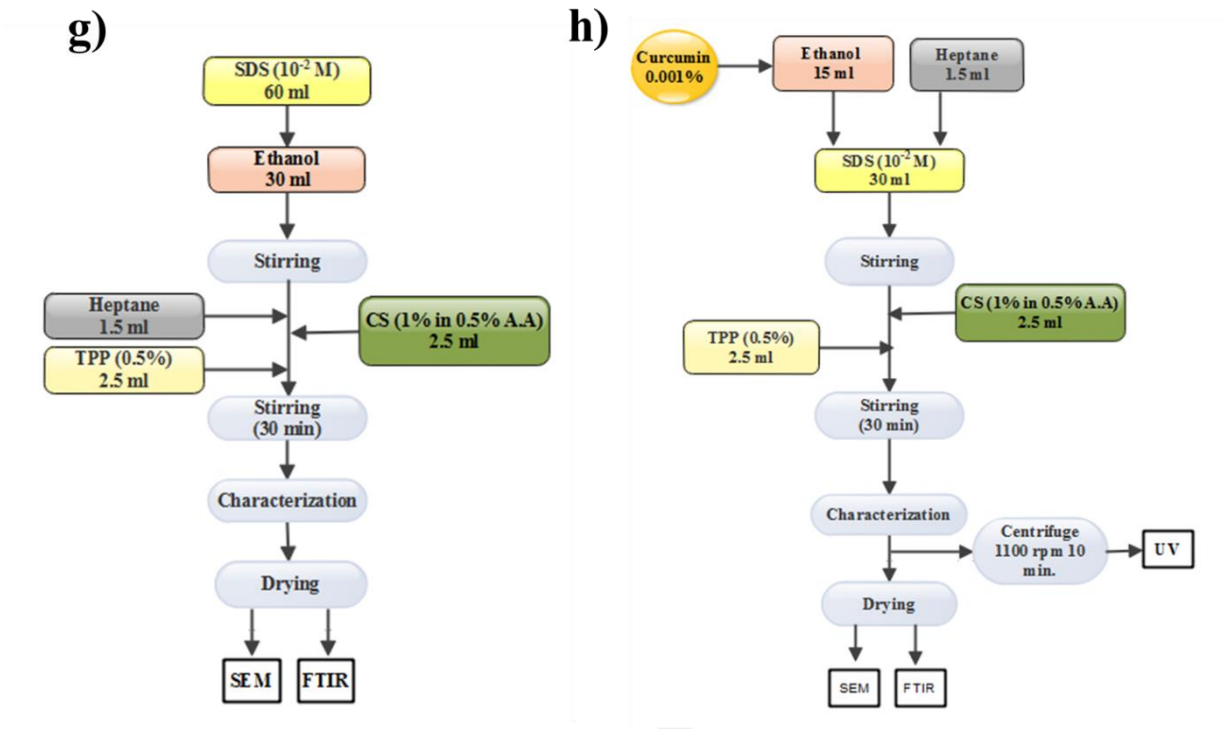

3.3.5. Thin Film Hydration Coupled with Ionic Gelation Method

This method is summarized in the following flowsheet in Figure 3.14. For the first step of the process SDS and P-123 micelles were loaded with drug. Loading drug into micelles was achived by 0.05717 g SDS (as 10^{-2} M in final concentration), P-123 (as 10^{-2} M in final concentration) and drug (0.001% w/v) dissolution in acetonitrile before evaporation. 20 ml chitosan solution (0.5% w/v) in acetic acid (1%) was added into the evaporated dissolution which includes drug loaded SDS and P-123 micelles as a thin film. For the purpose of chitosan nanoparticles formation 20 ml 0.5% TPP solution added under constant stirring. Particles were dispersed in oil phase and stabilized with SDS addition and dried for the characterization.

For the comprasion of loaded P-123 micelles and SDS+P-123 micelles, first experiment (STEM images shown in figure 4.12. (a) in the result and discussion part) was done with only P-123 (10^{-2} M) and drug in evaporation step of the process.

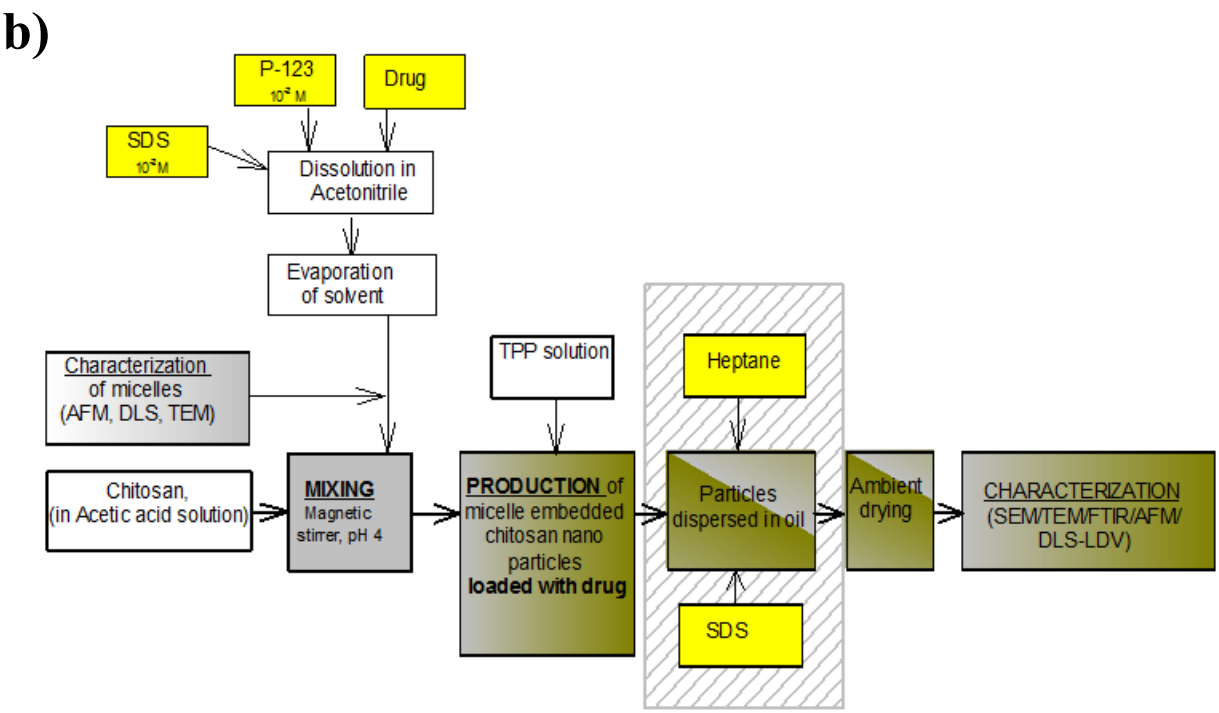

Figure 3.14. Thin film hydration coupled with Ionic Gelation Method

3.4. Characterization of P-123 Micelles and Micelle Embedded Chitosan nanoparticles

3.4.1. Surface Tension Measurements

Surface tension measurements of Pluronic-123 solutions were conducted using Kruss Model Digital Tensiometer (K10ST) with the Du-Noüy Ring method to determine critical micelle concentration of Pluronic-123. For this purpose several different concentrations (10^{-2}- 10^{-7} M) of Pluronic-123 were used and the Critical micelle concentration of Pluronic-123 was determined.

3.4.2. Dynamic Light Scattering Analysis

Size and zeta potential measurements of Pluronic-123 micelles were carried out using Malvern Zeta Sizer Nano ZS. The device employs a combination of laser Doppler velocimetry and Phase Analysis Light Scattering (PALS). Malvern Zeta Sizer uses dynamic light scattering method and working principle based on the fact that spatial

distribution of scattered light is a function of the particle size of the analyzed sample. Size of particles which are measured by the method is inversely proportional to angle seen after the particles scatter light. In other words, small particles scatter light at small angles while large particles scatter light at small angles relative to the laser beam. These particles pass through a focused laser beam during the laser diffraction measurement. A series of photosensitive detectors are used to get the angular intensity of scattered light. Particle size is calculated by using the map of scattering intensity versus angle. Particles are moving because of Brownian motion which is due to random collision with the molecules of the liquid that surrounds the particle. Stokes-Einstein equation defines the relationship between size of particle and its speed due to Brownian motion and Zeta Sizer uses the relationship to obtain size. Malvern Zeta Sizer Nano ZS (Figure 3.7) is used to obtain zeta potential by using Henry equation.

3.4.3. SEM Analysis

Scanning Electron Microscopy (SEM) was used for the determination of surface morphologies and structural integrity of micro and/or nano sized particles. SEM works based on electron sample interaction. It gives an opportunity for scanning samples with a focused beam of electrons. In this study SEM analysis carried out by Philips XL-30S FEG instrument in vacuum environment. Conductivity of the samples were supplied by coating Au. Sample surface images were recorded at different areas and magnifications.

3.4.4. STEM Analysis

Scanning Transmission Electron Microscopy (STEM) analysis was performed by a Quanta 250FEG type instrument. The reflected electron beam is limited by a raster across the surface of the sample and the image is obtained by counting backscattered electrons. For this analysis, a drop of nanoparticle sample was placed on a carbon grid (200 mesh) and dried under vacuum at 30^{o}C. The images were recorded at different areas and magnifications.

3.4.5. TEM Analysis

Transmission Electron Microscopy (TEM) was used for the investigation of surface and morphology of chitosan and micelle embedded chitosan nanoparticles. TEM has priority on imaging samples with a great magnification rather than SEM and other electron microscope techniques so it makes TEM the best way to determine morphological properties of nanoparticles and micelles in samples. In this study JEOL-JEM 1220 type of TEM was used. Samples were dropt on carbon grid and dried. Different magnification and areas were chosen for the imaging.

3.4.6. FTIR Analysis

Fourier Transform Infrared Spectroscopy (FTIR) was used to qualitative analysis of micelle embedded chitosan nanoparticles. Presence or absence of functional groups was investigated. FTIR spectroscopy based on vibrational energy as a consequence of radiation absorption on atoms. Vibrational energy leads to determine functional groups and bonds in compounds.

Analysis was performed using FTIR spectra by using Perkin Elmer Spectrum 100 FTIR spectrometer in a frequency range 4000-400 cm^{-1} with 4 scans at resolution 4 cm^{-1}. KBr pellet method was used for the FTIR analysis of solid samples and ATR method for the liquid samples in a frequency range 4000-510 cm^{-1}. For the preparation the solid samples were dried in petri dish under vacuum. 0.25 g KBr and 0.1 g dried sample to provide homogenization and pressed. The characteristic peaks of pure materials used in this study to produce micelle embedded chitosan nanoparticles were given in Figure 3.15 and discussed in the following paragraphs.

The FTIR spectrum of chitosan shows the chracteristic peaks assigned to polysaccharide structures. Main signals in the spectrum are: a strong and broad band due to the axial O-H and N-H stretching centered at 3440 cm^{-1}, C-H stretching bands registered at 2870-2880 cm^{-1}, the absorption centered at 1655 cm^{-1} attributable to the axial C=O stretching of the acetamido groups (named amide I). The one at 1580 cm^{-1} attributable to the angular deformation of N-H bonds of the amino groups, the bands at 1420-1477 cm^{-1} resulting from the coupling of C-N axial stretching and N-H angular deformation, the sharp band at 1377 cm^{-1} assigned to the CH_3 symmetrical deformation

mode. Finally, finger print bands, extremely useful for evidencing chitosan presence even in low amounts (for instance for chitosan coatings deposition), are due to skeletal signals (vibrations of glycosidic bonds, C-O and C-O-C stretching) absorbing between 1150 cm^{-1} and 900 cm^{-1} (Corazzari et al. 2015).

TPP spectrum showing a broad peak at 3413 cm^{-1} could be attributed to overlapping of N-H and O-H stretching, vibration. Similarly, strong peak at 1141.38 cm^{-1} designated the stretching vibration of PO_2 group and 922.92 cm^{-1} antisymmetric stretching vibration of the P-O-P bridge (Walke et al. 2015).

FTIR spectrum of P-123; the main signal situate at 2962 cm^{-1} shows the C-H stretching, peaks at 1372cm^{-1} attribute C-H rocking. Signal at 1438 cm^{-1} shows C-H bending on the structure and the peak at 923 cm^{-1} is the proof of the presence of O-H bending (Jindal and Mehta 2015).

In the FT-IR spectrum of SDS, the two strong absorbance peaks at 2921 and 2852 cm^{-1} were from the asymmetric and symmetric stretching of $-CH_2$, respectively, the shoulder peak at 2956 cm^{-1} was from the asymmetric C-H stretching mode of the terminal $-CH_3$ groups, and the peaks at 1217 and 1083 cm^{-1} were from the asymmetric and symmetric stretching vibrations of S=O, respectively (Sarma and Mohanta 2015).

Probucol spectra shows sharp characteristic peaks at 2959, 1423 and 1309 cm^{-1}. (Ajun et al. 2009).

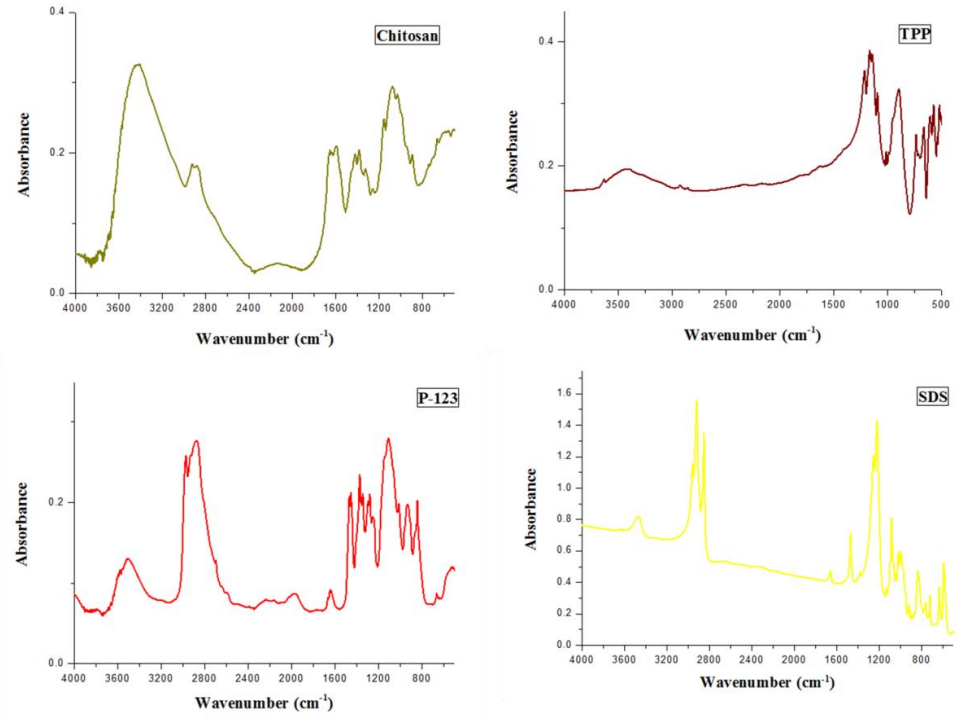

Figure 3.15. FTIR Spectras of all pure materials.**(continue on next page)**

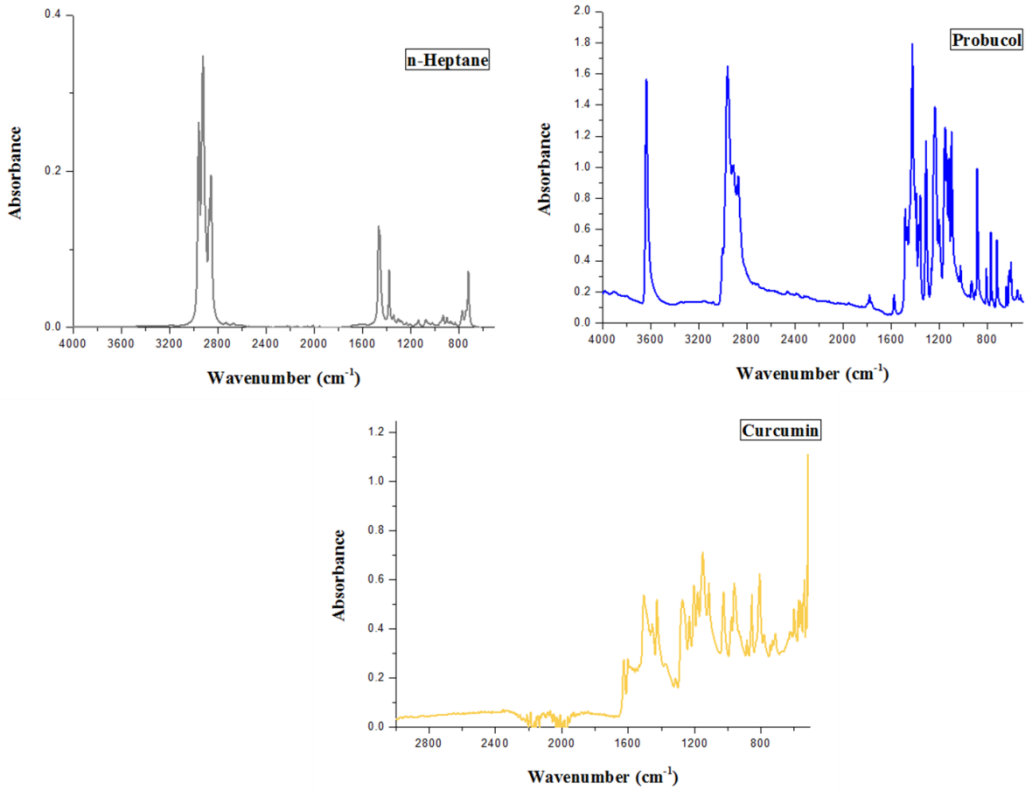

3.4.7. Determination of Drug Concentration: UV-Vis Analysis

Ultraviolet spectroscopy is the technique which based on sample-light interaction. Different wavelength of light interact with the sample and gives information about the special structures of the samples. In this study Carrian Varry type of ultraviolet spectrometer was used to determine absence or presence of drug in the solid samples. For UV measurements standart solutions of drugs were prepared to obtain calibration curves. Samples were measured between wavelength with 200-450 nm according to drugs absorption at 417 and 242 nm for Curcumin and Probucol respectively. In order to constitute of calibration curve (Figure 3.16), solutions which include different concentrations of drug were preperad from a main solution which was obtained by thin film hydration method as in Figure 3.17.

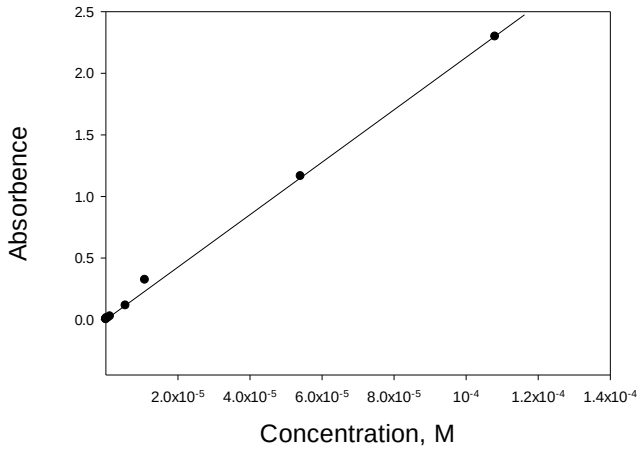

Concentration	Absorbance
5.43E-09	0.00314
1.08E-08	0.00579
5.43E-08	0.00865
1.08E-07	0.01343
5.43E-07	0.01508
1.08E-06	0.0278
5.43E-06	0.11615
1.08E-05	0.32422
5.43E-05	1.16591

Figure 3.16. Calibration curve of standart solutions with different concentrations (for Probucol)

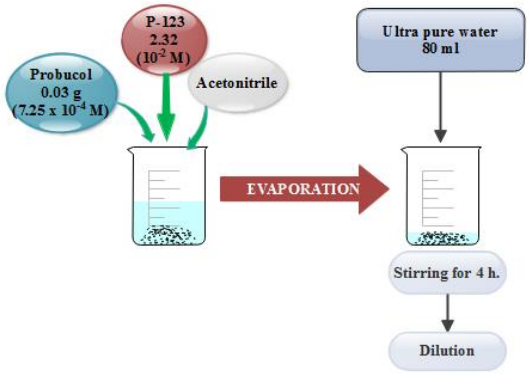

Figure 3.17. Preperation of standart solutions with different concentrations (for Probucol)

3.5. Drug Uptake and Release Studies

Drug uptake capacity of nanoparticles were determined using UV-analysis of supernatants obtained during synthesis of nanoparticles. The amount of unloaded drug was determined and substracted from initial amounts.

Drug release studies were done using UV-analysis of supernatants obtained after the repalecement of nanoparticles in simulated body fluid solution. For this reason, 0.4 g dried sample was added to 100 ml of simulated body fluid with fixing pH (as 6.8 and 7.4) and temperature (37°C) and stirred. Small amount of samples were withdrown at preset time intervals for 26 hrs. And analyzed by Uv-vis (Figure 3.18.).

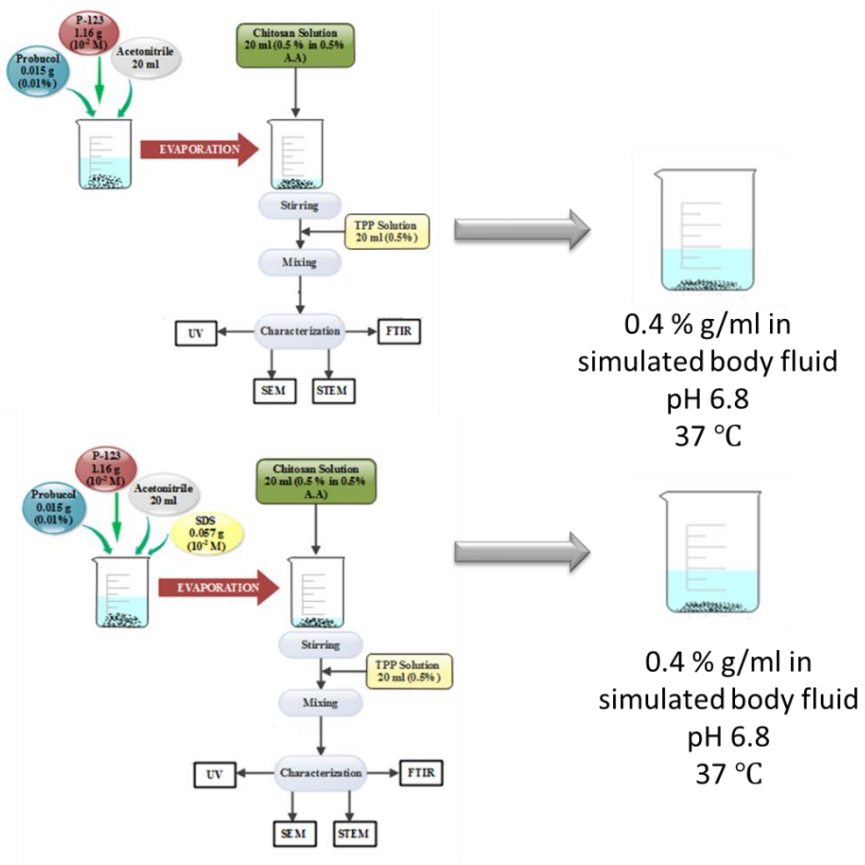

Figure 3.18. Drug release studies from micelle embedded chitosan nanoparticles.

CHAPTER 4

RESULTS & DISCUSSION

4.1. Characterization of P-123 micelles

Initially, surface tension measurements were performed to determine the association behavior of the P-123 molecules in aqueous solution and the result is presented in Figure 4.1-a. It is seen that the surface tension behavior of P-123 could roughly be divided into 3 concentration regions: In Region I where the surface tension decreases steadily with the increasing concentration, P-123 molecules are in their single form. Region II is the transition region where the P-123 molecules most probably form dimmers and trimers. In Region III where the surface tension remains constant with changes in concentration, the P-123 molecules are in the form of micelles. The critical micelle concentration (CMC) value determined from the figure was 10^{-4} M.

Figure 4.1-b gives the size distribution result of P-123 micelles obtained by DLS (10^{-3} M). It is clearly seen that the average size of micelles were found to be around 20 nm. The size of micelles were also observed by AFM and STEM images (Figures 4.1-c and d). These results also show that the size of P-123 micelles are around 20 nm. In the case of TEM images, however, P-123 micelles seem to come together and form loose aggregates and therefore structures look larger then 20 nm.

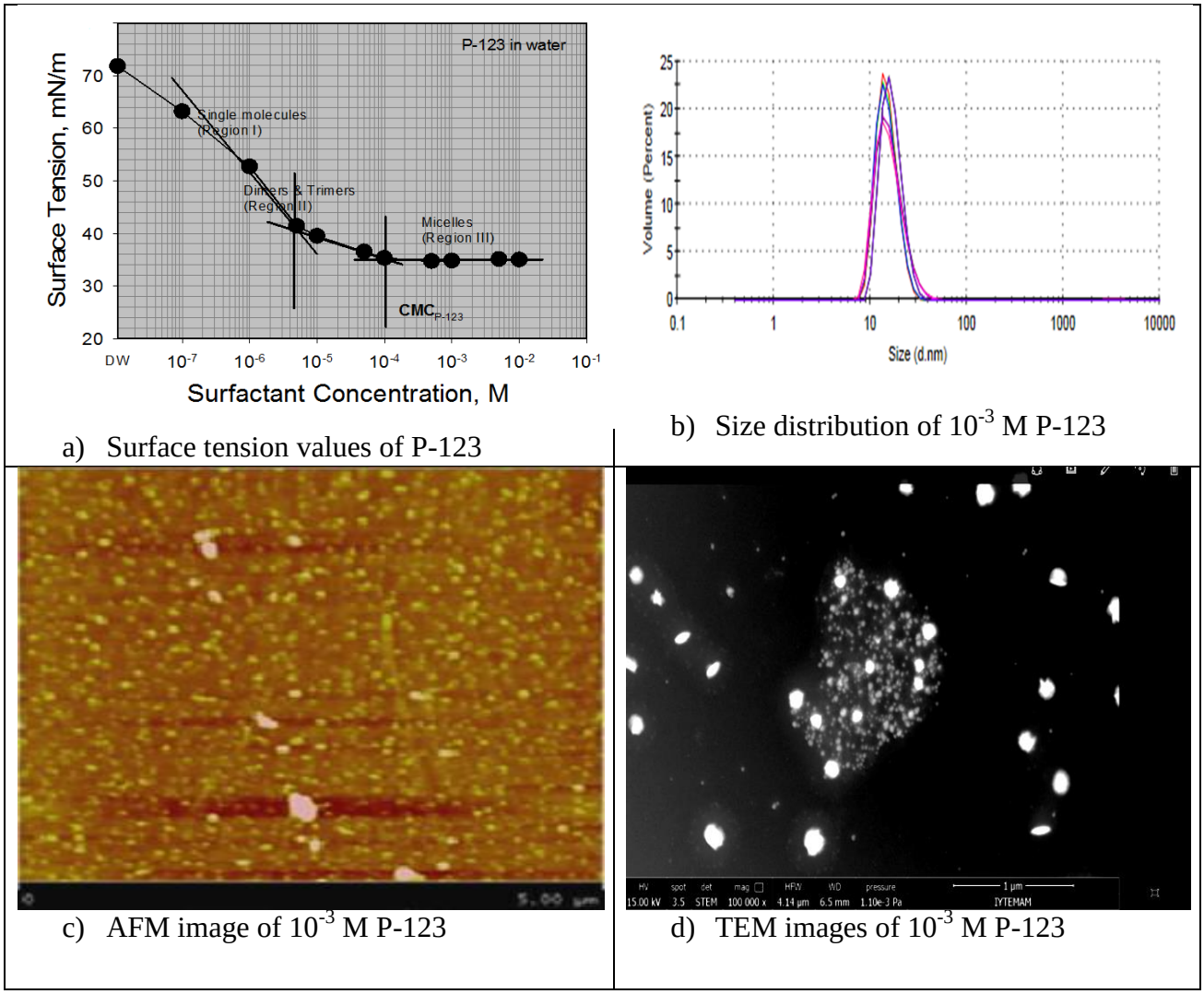

a) Surface tension values of P-123

b) Size distribution of 10^{-3} M P-123

c) AFM image of 10^{-3} M P-123

d) TEM images of 10^{-3} M P-123

Figure 4.1. Characterization of P-123 micelles; a) Surface tension values of P-123 solutions,b)size distribution of P-123 micelles by DLS c)AFM image of 10^{-3} M P-123 d)TEM picture of P-123 micelles.

4.1.1. Modification of P-123 Micelles by SDS

The size and surface properties of P-123 micelles were modified by a simple anionic surfactant Sodium dodecyl sulfate, SDS. The P-123&SDS micelles were found to be smaller (~5 nm) and more negatively charged. These results were presented in Figure 4.2-a and b.

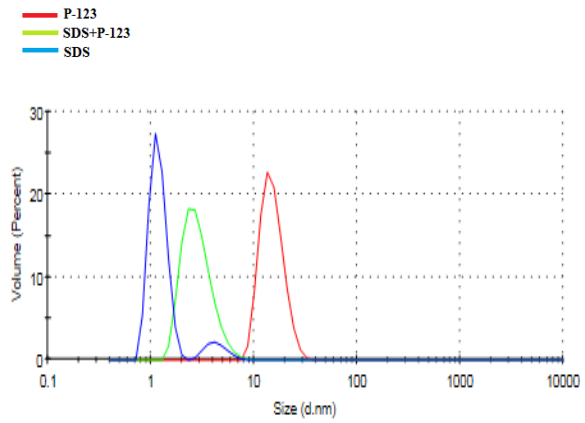

(a) Size distribution of P-123, SDS, P123+SDS micelles by DLS.

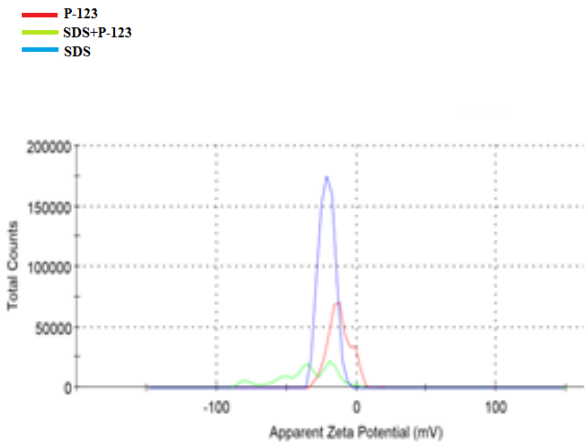

(b) Charge of P-123, SDS, P123+SDS micelles

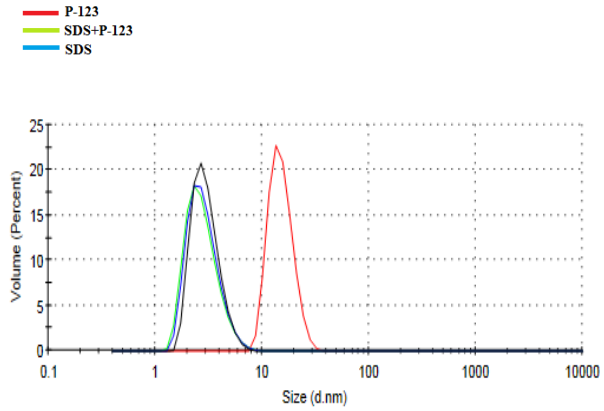

(c) Size of P-123, SDS, P123+SDS micelles loadded with Probucol

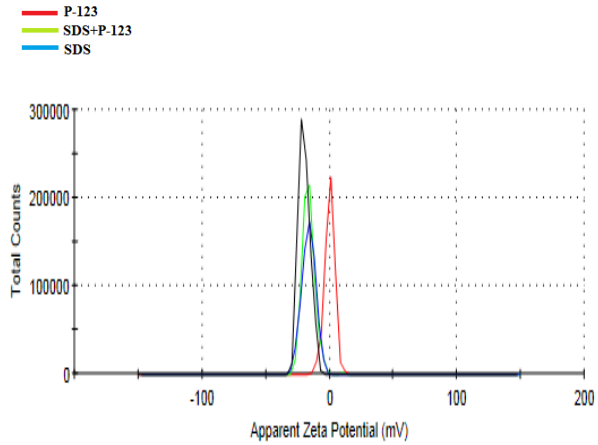

(d) Charge of P-123, SDS, P123+SDS micelles loadded with Probucol

Figure 4.2. a) Size distribution and b) charge of P-123 micelles without drug c) Size and e)charge of P-123 micelles loaded with drug in the absence and presence of SDS.

4.1.2. Characterization of Drug Loaded P-123 Micelles

The similar type of characterization was also conducted by loading drug into P-123 micelles and the results are presented in the same figure 4.2. It is seen that the presence of drug do not change the size and surface properties of micelles. Therefore chitosan was expected to deposit on the micelle surfaces and produce chitosan particles. STEM images for these particles are given in the Figure 4.3.

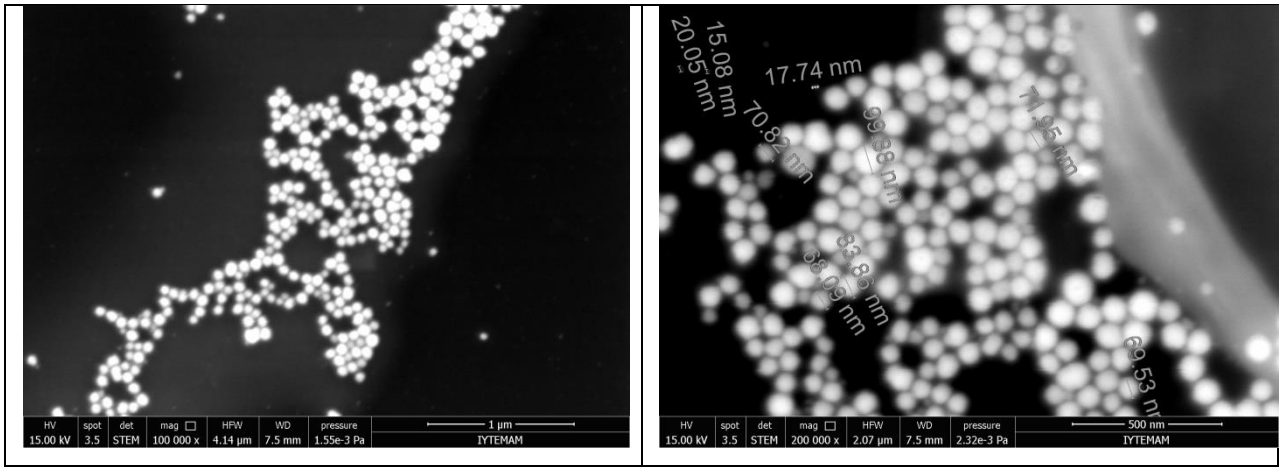

Figure 4.3. STEM images of P-123 micelles loaded with drug.

4.2. Characterization of Micelle Embedded Chitosan Nanoparticles

4.2.1. Oil in Water (O/W) Emulsification Coupled with Ionic Gelation Method

In this method, drug loaded chitosan nano particles were produced and the SEM images and FTIR analysis of these particles were presented in Figures 4.4 and 4.5. Here, two different methods were used to envelope drug in chitosan nanoparticles using two types of hydrophobic drugs. The details of these methods are discussed in "Materials and Methods" Chapter (Chapter 3). One method was based on the dissolution of drug in oil phase to produce O/W emulsion and built a chitosan layer around it. The other method was based on the preparation of drug loaded P-123 micelles in water solution first and then production of chitosan layer around it. These particles were then placed in oil phase to freeze the boundries (kind of freeze dry) of the particles. As it is seen from the SEM images that the particles are larger and there is a strong agglomeration when drug was dissolved in oil phase (Figure 4.4-a). However, the particles were much smaller and dispersed when drug, Probucol, was enveloped in P-123 micelles and chitosan coverage of these micelles. That is drug loaded micelle embedded chitosan nano particles are able to produce successfully by this method. However, it was not that successful in the case of Curcumin.

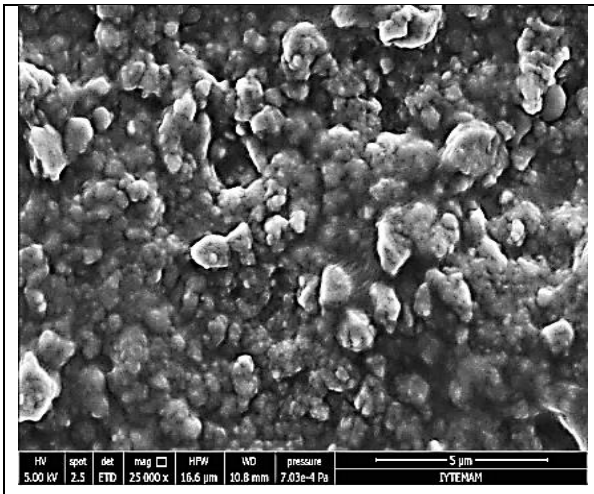

a) Probucol dissolved in oil phase, without P-123 micelles.

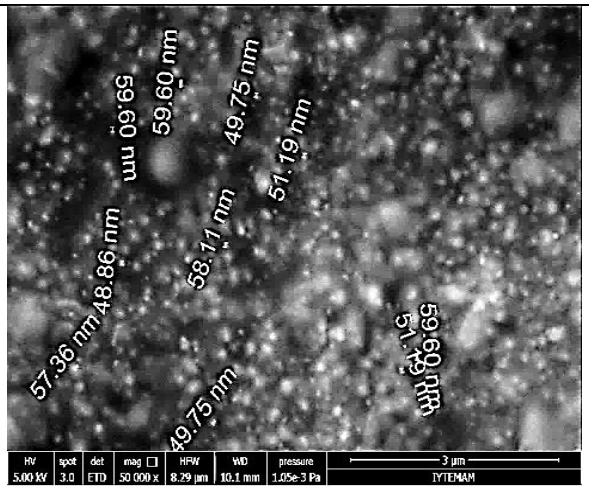

b) Probucol loaded in P-123 micelles by thin film hydration method.

.

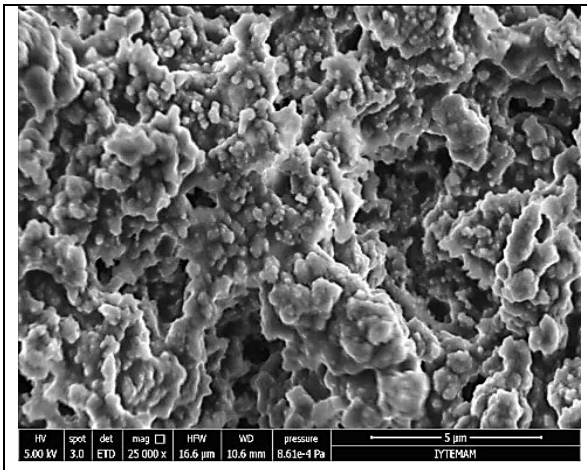

c) Curcumin loaded in P-123 micelles by thin film hydration method

Figure 4.4. SEM images of drug loaded chitosan nanoparticles by different methods

The FTIR analysis of these materials, drug loaded micelle embedded chitosan nano particles were done and given in Figures 4.5-a,b and c (for the best result of this method). In these figures the FTIR peaks of each substance that makes the nanoparticle were given together to compare and comment on the results. In addition, the FTIR analysis of each substance is also given separately in Appandix A.

The characteristic FTIR spectrum of P-123 was as follows; the main signal situate at 2962 cm^{-1} shows the C-H stretching, peaks at 1372cm^{-1} attribute C-H rocking. Signal at 1438 cm^{-1} shows C-H bending on the structure and the peak at 923 cm^{-1} is the proof of the presence of O-H bending (Jindal and Mehta 2015). The characteristic FTIR spectrum of Probucol shows sharp characteristic peaks at 2959, 1423 and 1309 cm^{-1}. (Ajun et al. 2009). So, these spectrums can be seen there are overlaped spectrums.

So, it is seen from the Figures 4.5-a and b that the characteristic spectrums of both the drug (Probucol) and P-123 micelles overlape. However, the intesities of the peaks shows that these two materials are in the structure of the nanoparticles produced.

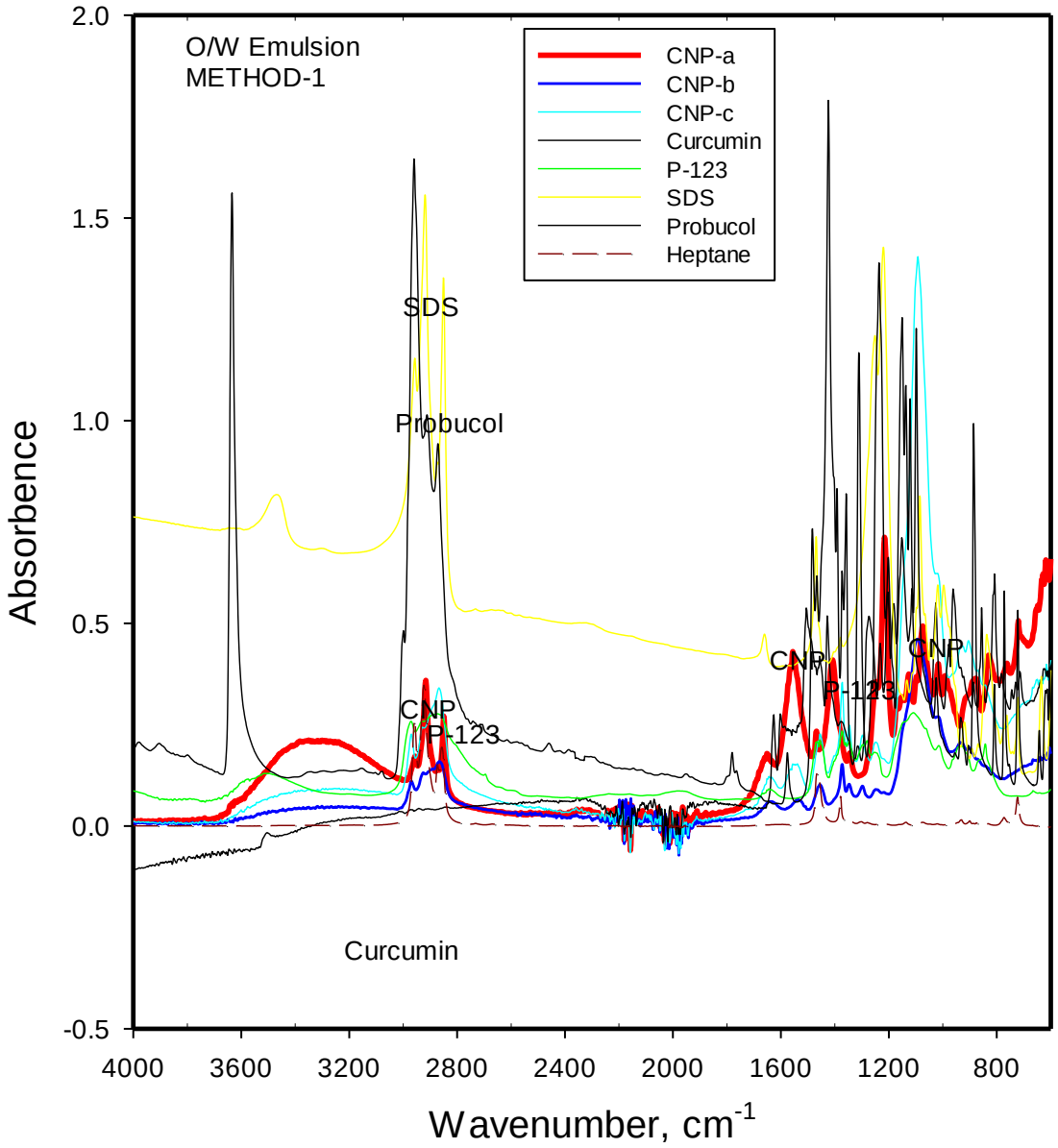

Figure 4.5-a. FTIR spectra of Oil in Water Emulsification Coupled with Ionic Gelation Method

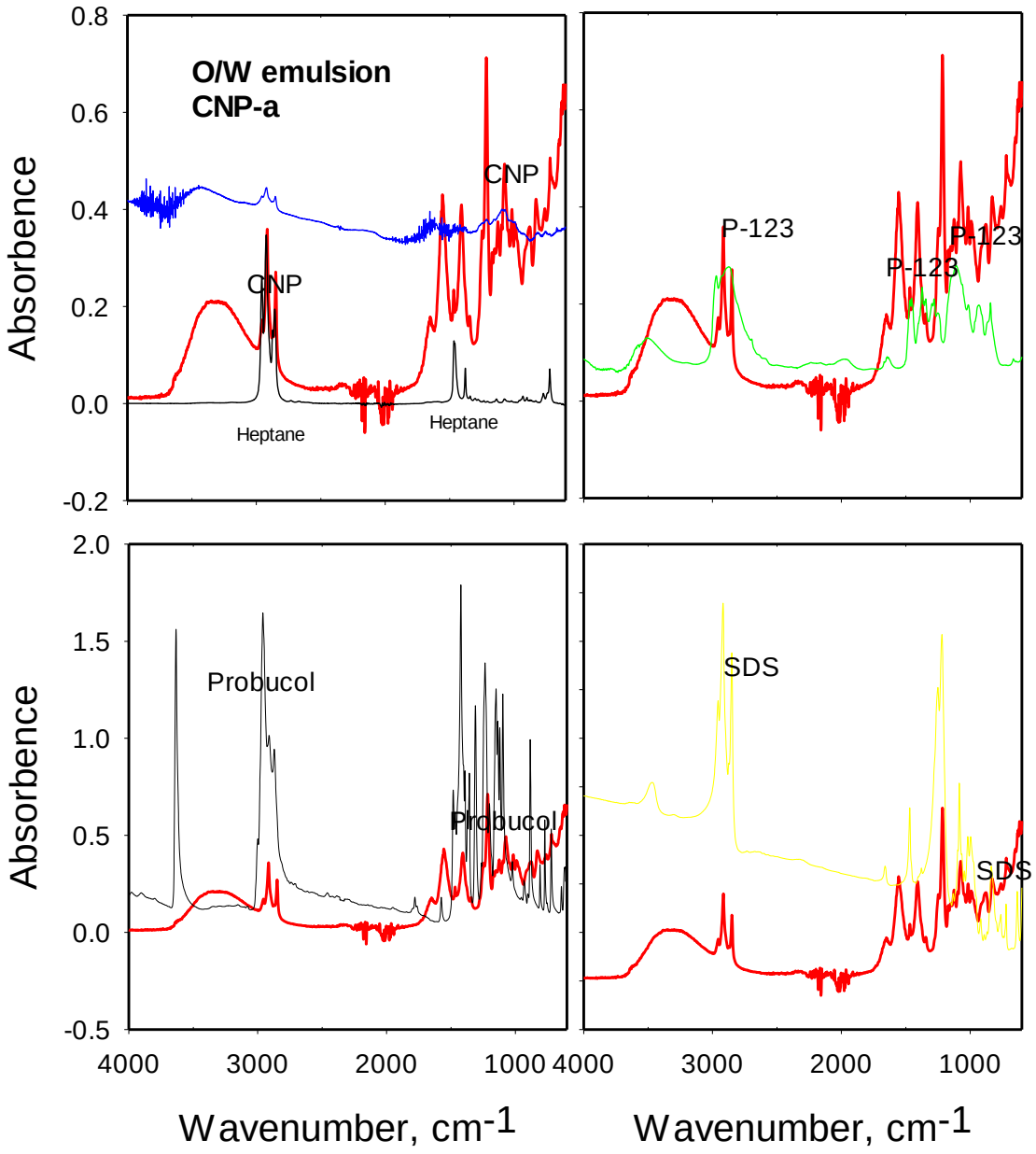

Figure 4.5-b. FTIR spectra of Oil in Water Emulsification Coupled with Ionic Gelation Method

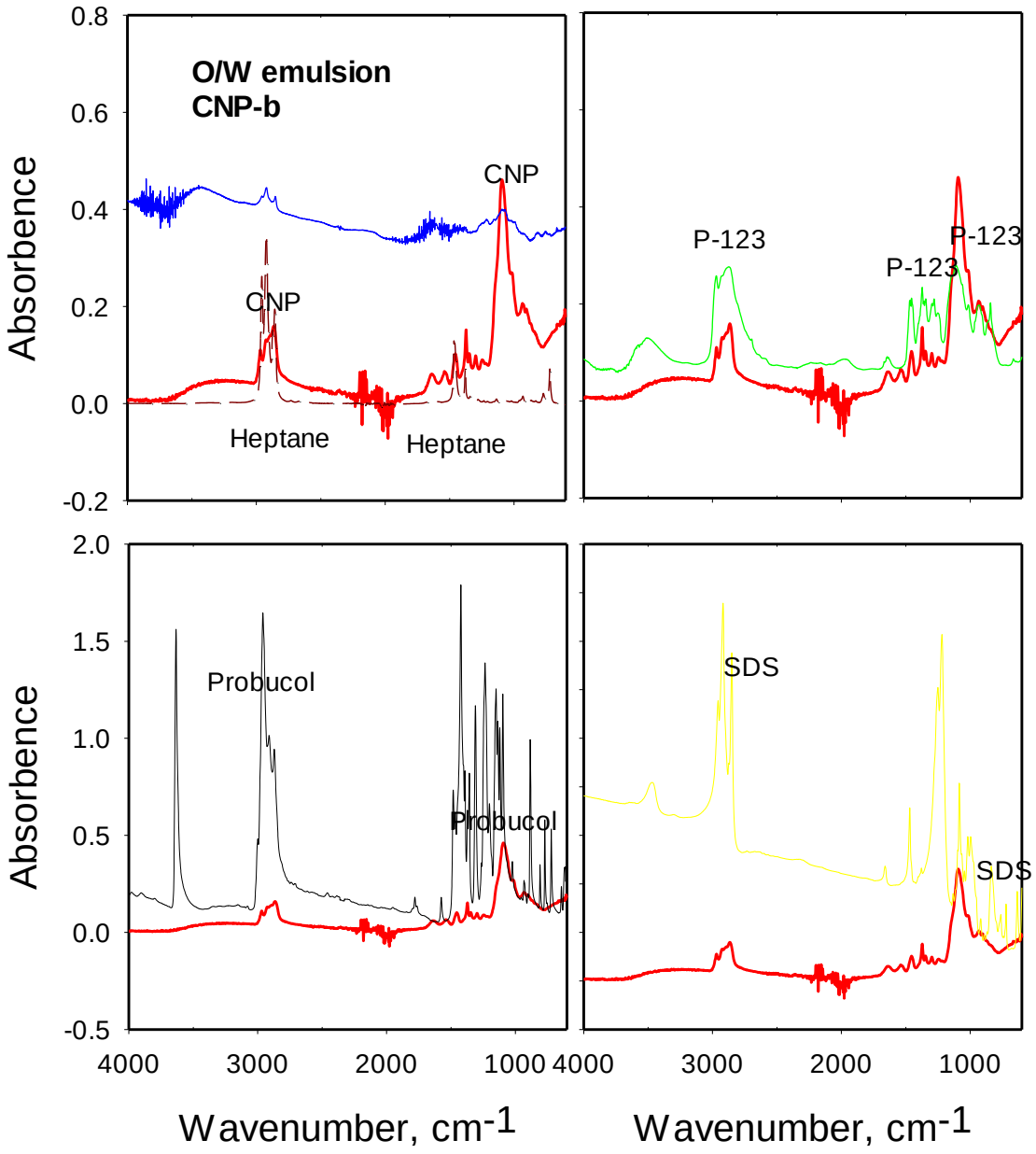

Figure 4.5-c. FTIR spectra of Oil in Water Emulsification Coupled with Ionic Gelation Method

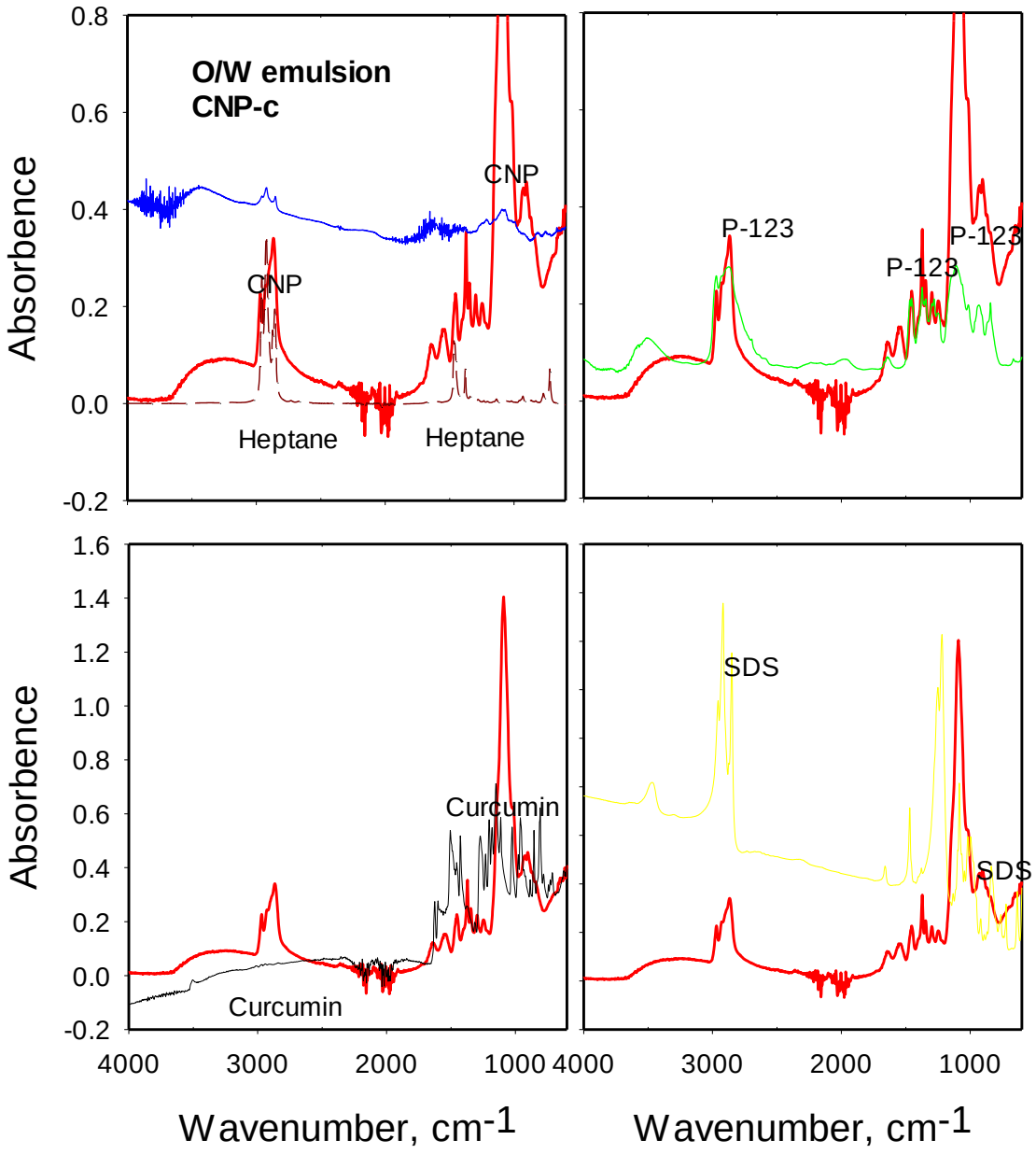

Figure 4.5-d. FTIR spectra of Oil in Water Emulsification Coupled with Ionic Gelation Method

4.2.2. W/O Emulsification Coupled with Ionic Gelation Method

In this method, several experimental conditions were tested and the results of these analysis were presented in the following figures as SEM images and FTIR analysis. The procedure of these methods were discussed in Chapter 3 in detail. In this method, the following conditions were tested.

1. Effect of chitosan percentage,
2. Effect of W/O ratio
3. Addition of a hydrophilic drug & hydrophobic drug.

The results of these analysses were presented in the Figures 4.7, 4.8, 4.9 and 4.10. As it is seen from the figures that the production of chitosan nanoparticles were possible if the chitosan percentage was low (0.5%) and W/O ratio was 1/6. However, there was a strong agglomeration for all the cases. The presence of the drugs (hydrophilic or hydrophobic) did not change the situation. Therefore, this method was also found to be not suitable to produce chitosan nanopartles that embed drug loaded micelles.

FTIR analysses of these particles were given in Figure 4.9 to analyze particle structure.

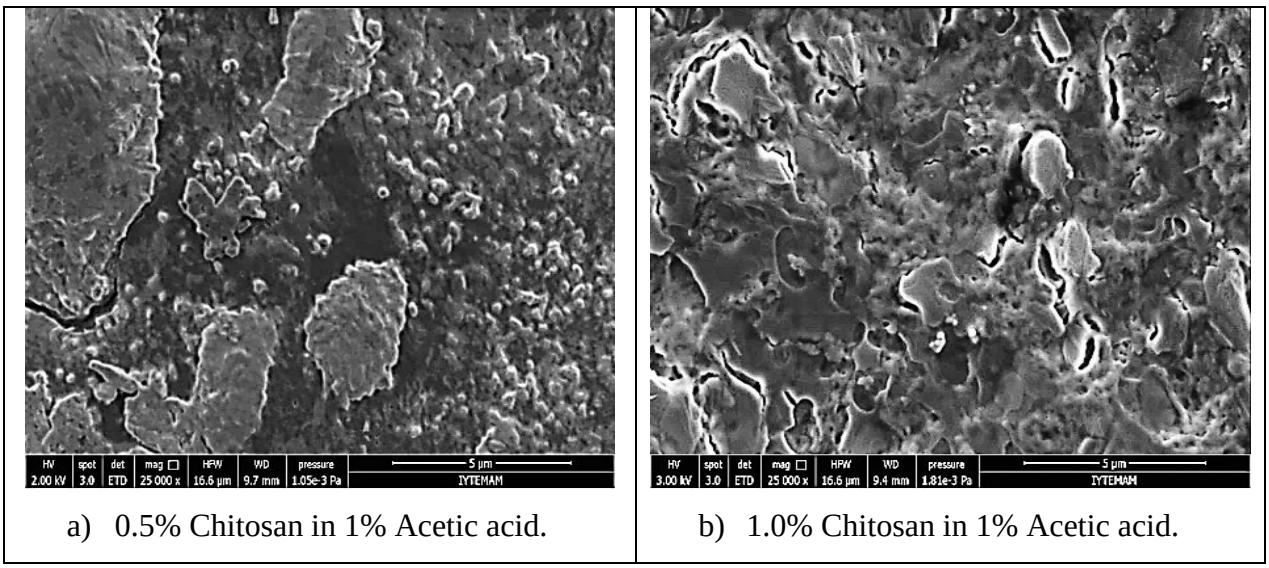

a) 0.5% Chitosan in 1% Acetic acid.

b) 1.0% Chitosan in 1% Acetic acid.

Figure 4.6. SEM images of effect of chitosan percentage on the production of nanoparticles by W/O emulsification method.

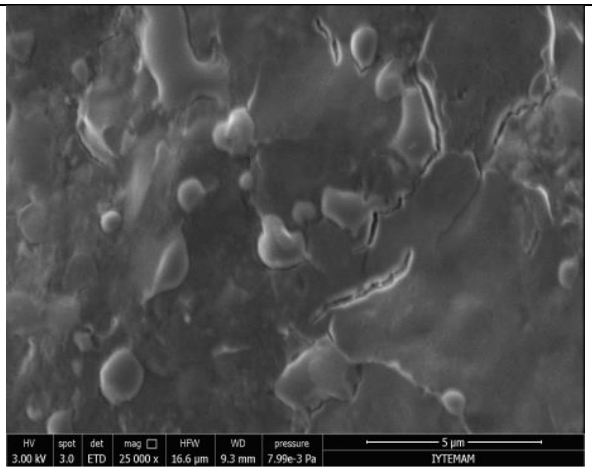

a) W/O ratio= 4/5.

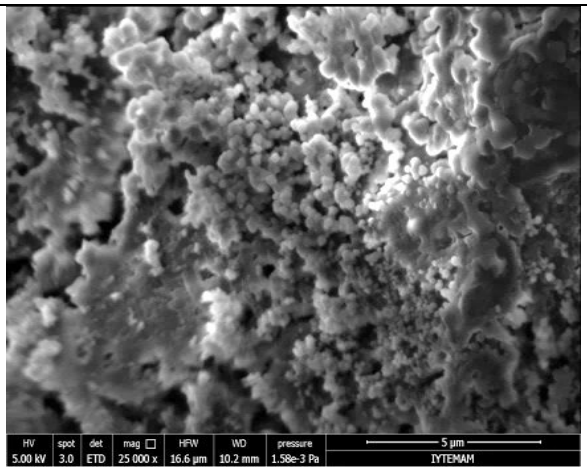

b) W/O ratio = 1/6.

Figure 4.7. SEM images effect of W/O ratio on the production of nanoparticles by W/O emulsification method (1% CS, 0.5% TPP).

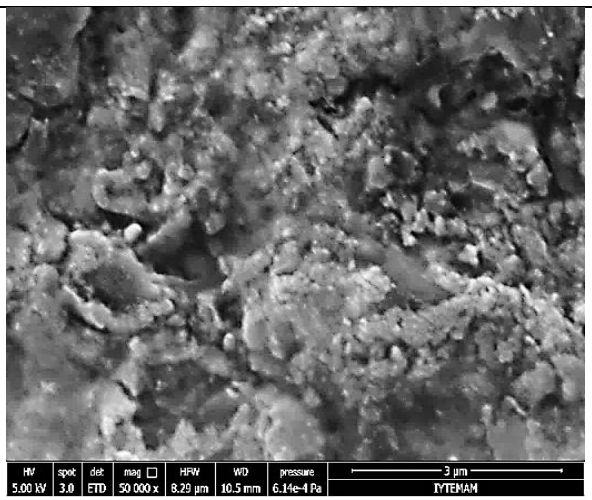

a) Vancomycin Hydrochloride (Hydrophilic drug)

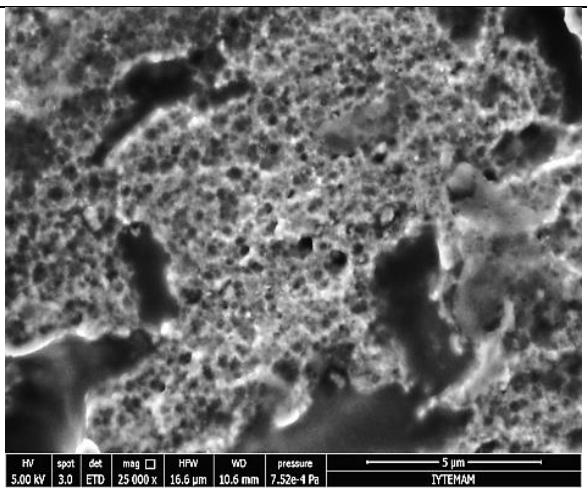

b) Probucol (Hydrophobic drug)

Figure 4.8. SEM images of production of hydrophilic and hydrophobic drug loaded chitosan nanoparticles (1% CS, 0.5% TPP).

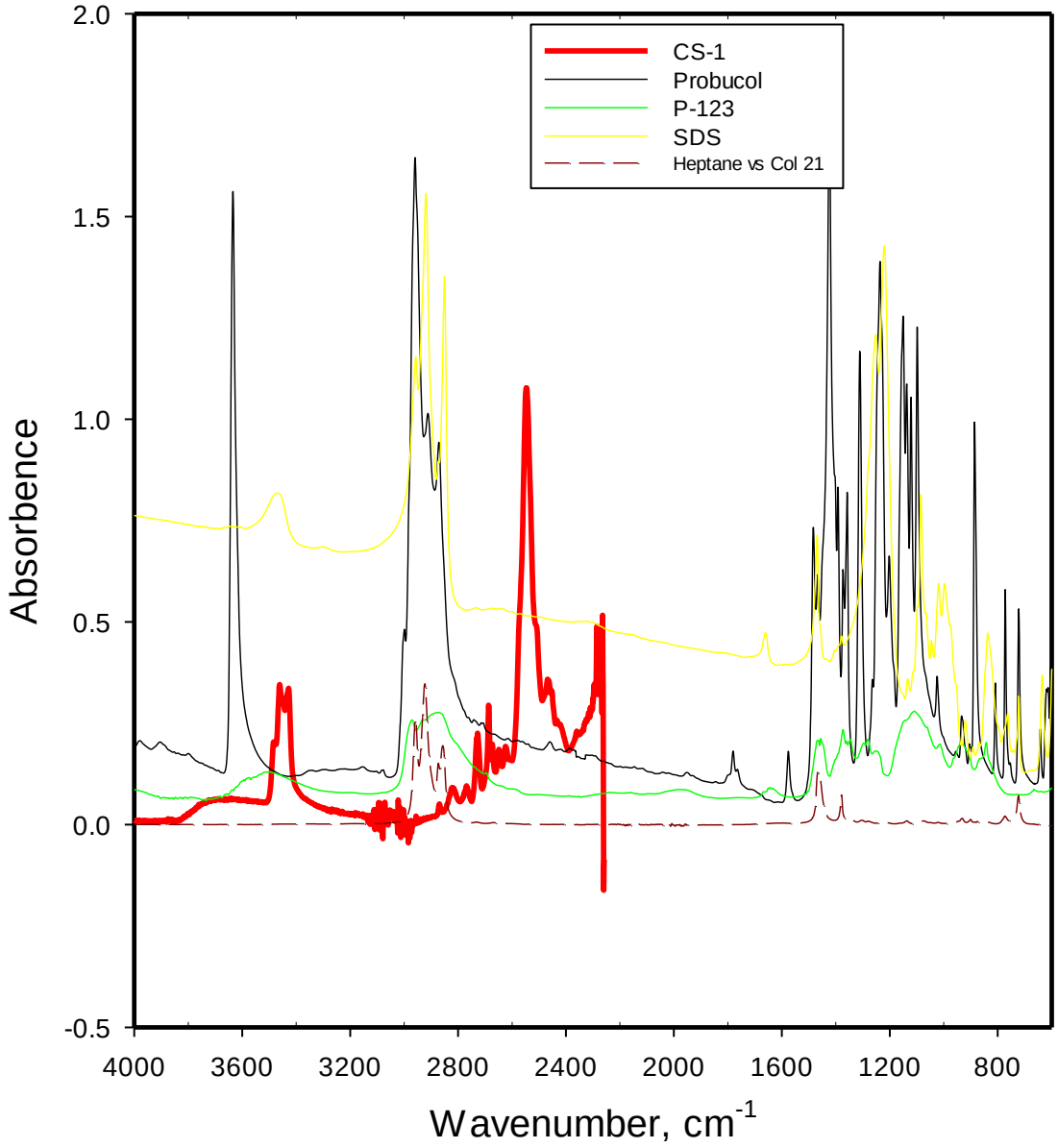

Figure 4.9-a. FTIR spectra of Water in Oil Emulsification Coupled with İonic Gelation Method with probucol

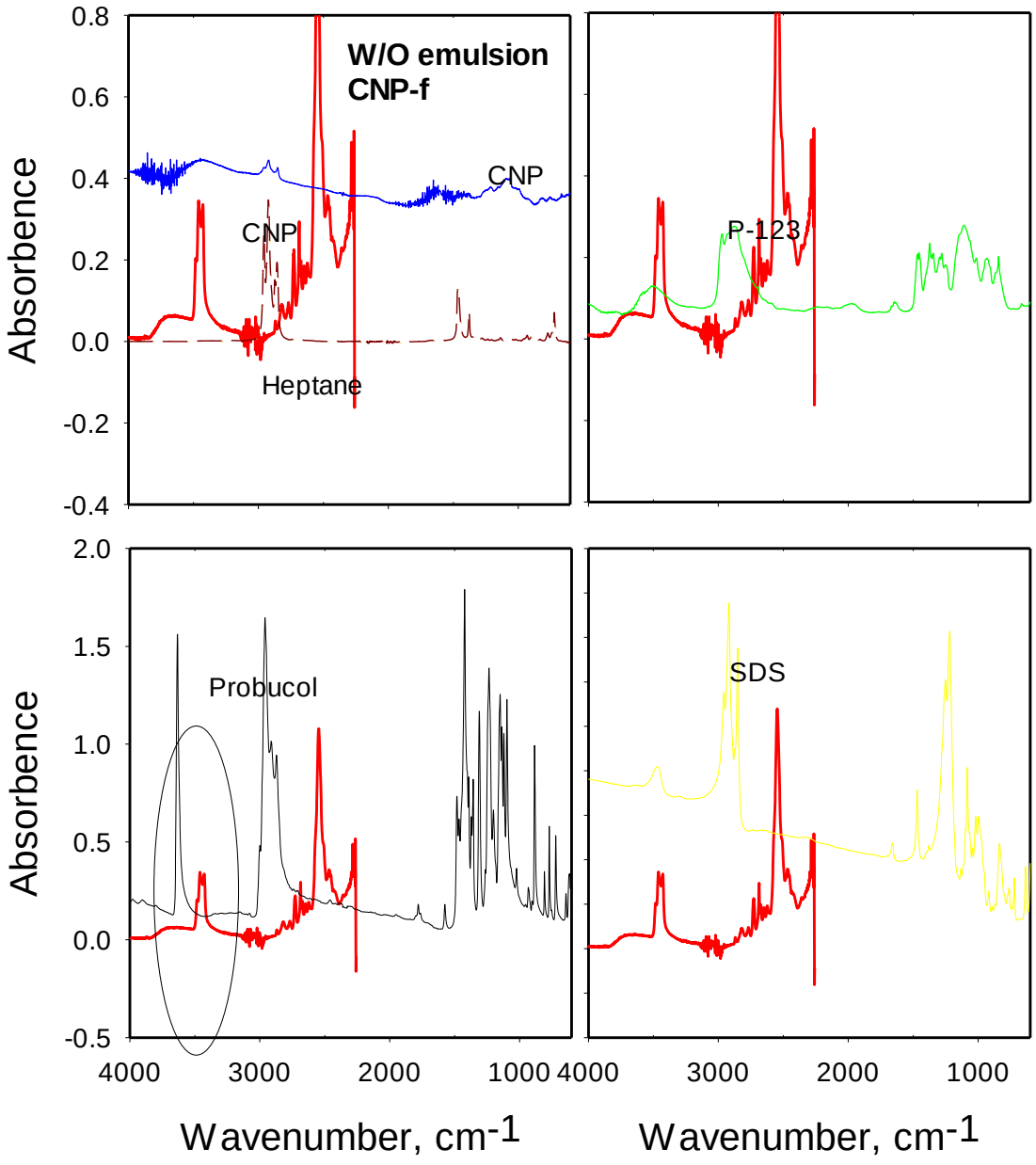

Figure 4.9-b. FTIR spectra of Water in Oil Emulsification Coupled with İonic Gelation Method with probucol

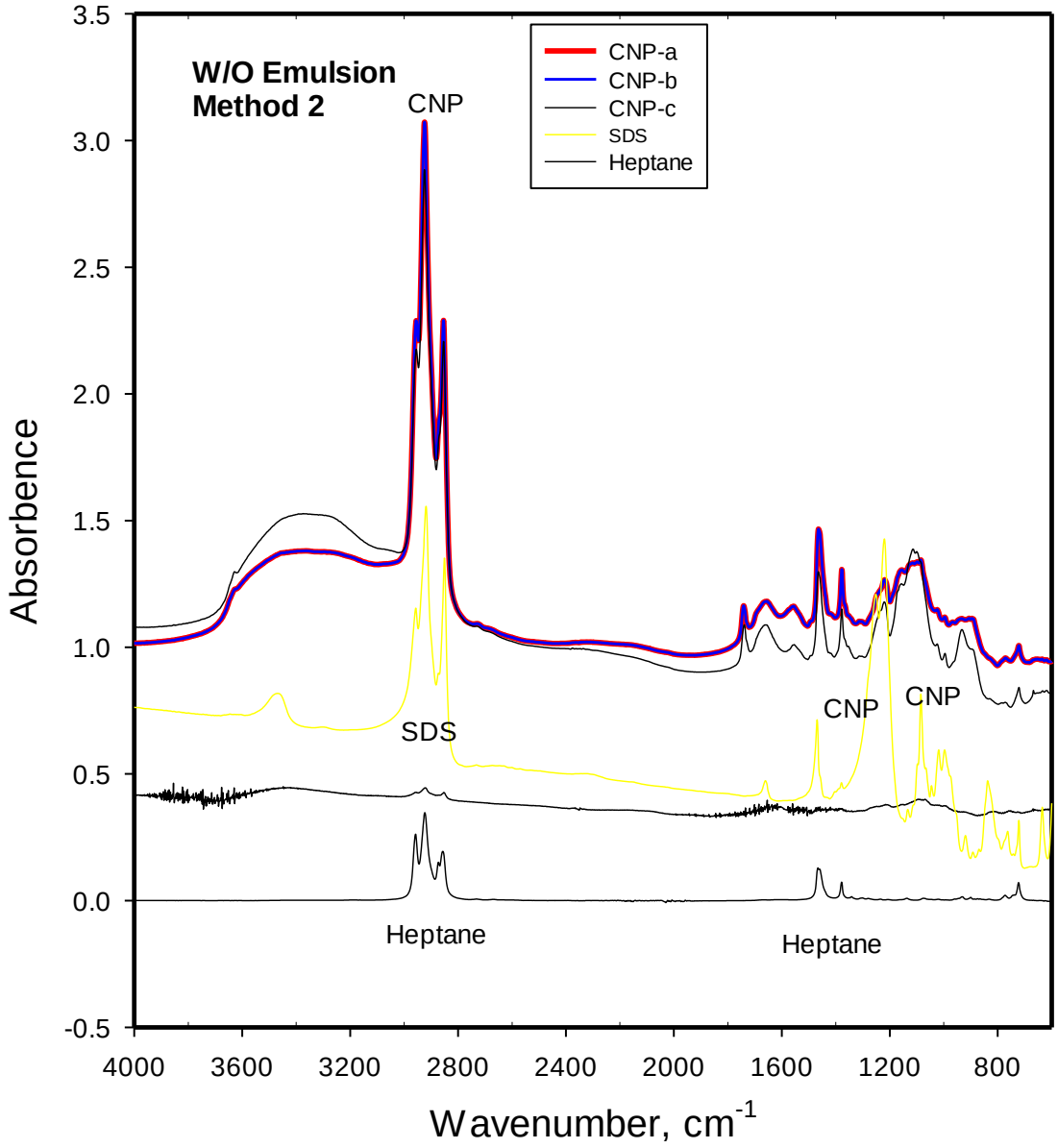

Figure 4.9-c. FTIR spectra of Water in Oil Emulsification Coupled with İonic Gelation Method without drug

4.2.3. Oil - Water - Oil (O/W/O) Emulsification Coupled with Ionic Gelation Method

In this method, several experimental conditions in the absence and presence of drug (Probucol, as a hydrophobic drug) were tested and the results of these analysis were presented in the following figures (4.10., 4.11., 4.12., 4.13.) as SEM images. In addition, TEM images, FTIR analysis and UV-Vis analysis were also presented for

some conditions. The procedure of these methods were discussed in Chapter 3. in detail. In this method, the conditions tested can be listed as below.

1) P-123 and P-123+SDS at O/W interface to make oil in water stable.
2) Surfactant type as SDS, Span 80, Tween 80, T X-100, CTAB as dispersant
3) Changing the addition step of TPP to the solution.
4) Changing the percentage of chitosan as 1% and 0.5%.

In the first condition tested it can be seen that the chitosan can be in nanoparticle form only when the mixture of P-123 + SDS was at the interface in the presence of Probucol. However, the particles are like in the muddy environment which is undesirable.

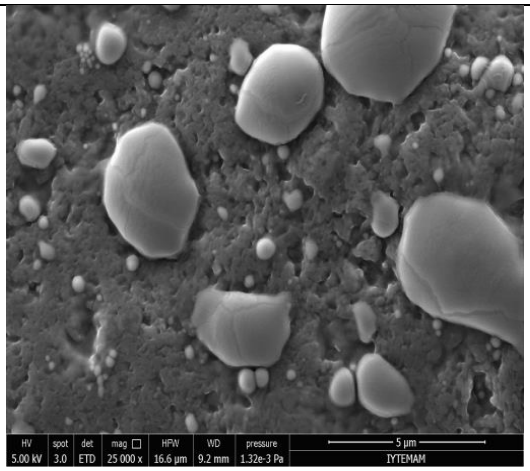

a) P-123 at the interface, without drug.

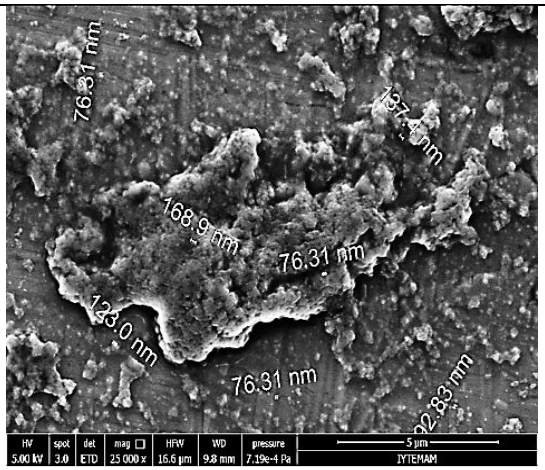

b) P-123 + SDS at the interface, without drug.

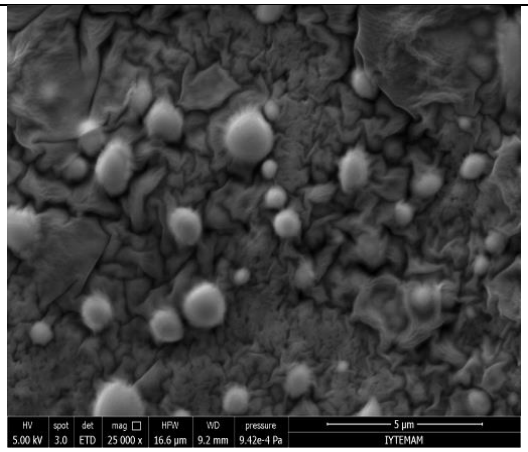

c) P-123 at the interface and Probucol loading.

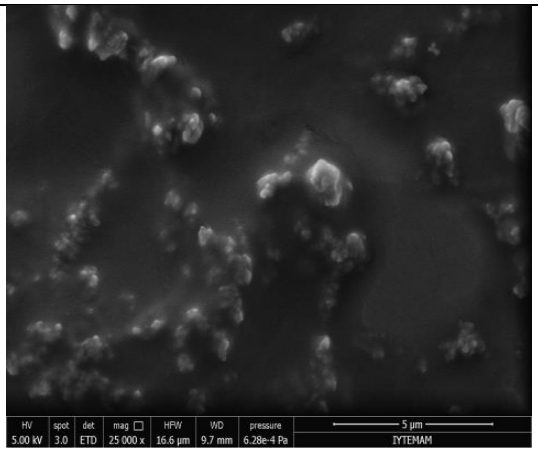

d) P-123 + SDS at the interface and Probucol loading.

Figure 4.10. SEM images of P-123 (10^{-2}M) and P-123 (10^{-2}M) +SDS (10^{-2} M) at O/W interface (1% CS, 0.5%TPP).

This method was tested in the absence of drug loaded P-123 micelles with other surfactants and the results of these tests were presented in Figure 4.11. As it is seen that chitosan was in particle form for all the cases if there is no loaded P-123 micelle. But, the particles were agglomerated and nonspherical.

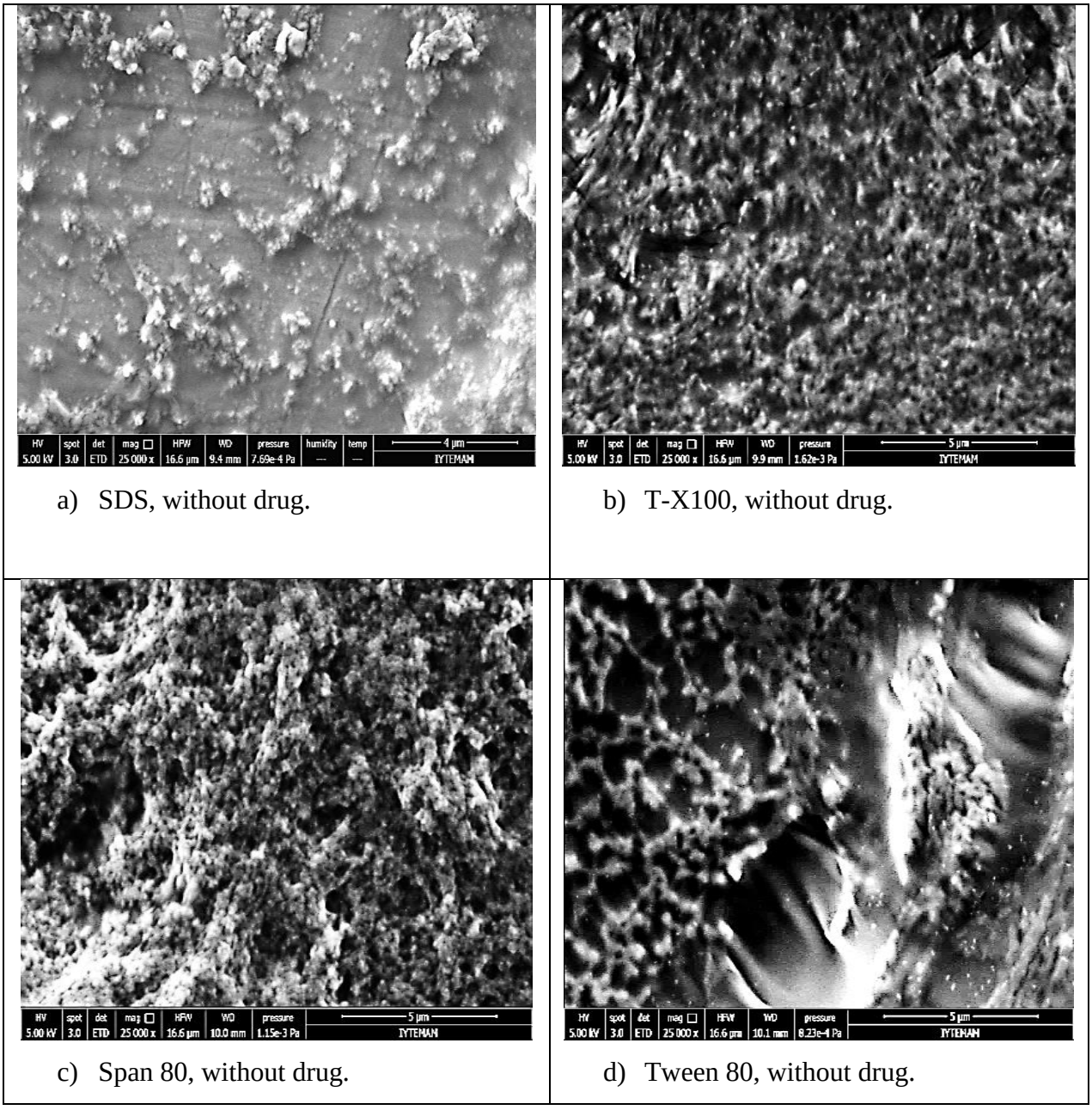

a) SDS, without drug.

b) T-X100, without drug.

c) Span 80, without drug.

d) Tween 80, without drug.

Figure 4.11. Surfactant type as SDS, Span 80, Tween 80, T X-100, CTAB as dispersant

Similar type of synthesis was also performed by changing the concentration of chitosan solution and the addition order (before and after oil phase) of TPP to the system. These results were presented in 4.12 and 4.13 as SEM images. As it is seen in Figure 4.12. and 4.13. that neither the change of chitosan concentration nor the change of TPP addition order affect the system. There was a strong agglomeration for all the

cases. FTIR results of these tests were also given in Figure 4.14a, 4.14b,4.14c. Therefore this method was also found to be not suitable to form these type of chitosan nanoparticles.

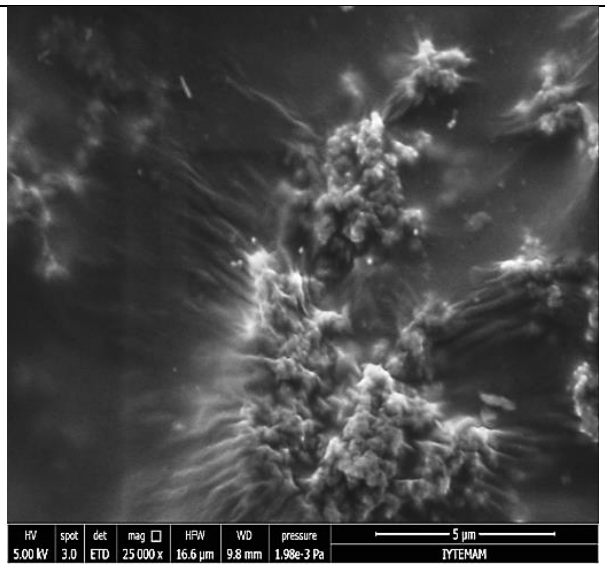

I) TPP addition before heptane (oil phase).

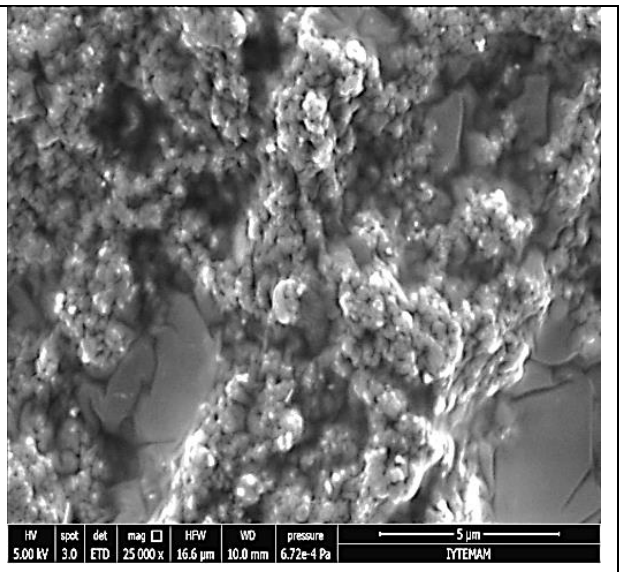

J) TPP addition after heptane (oil phase).

Figure 4.12. Changing the addition step of TPP to the solution

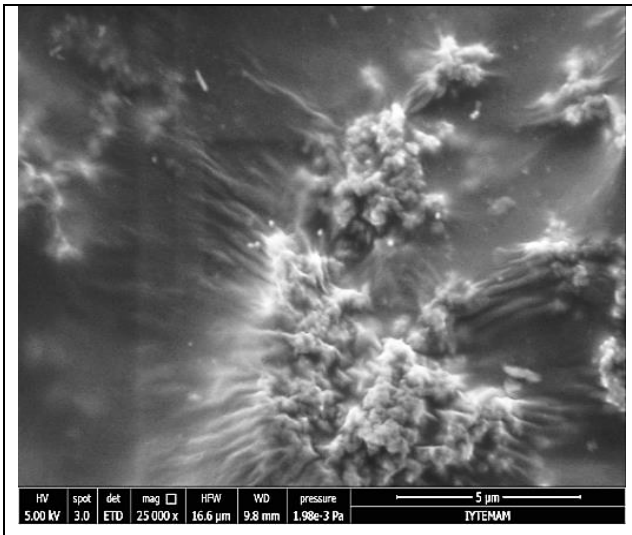

k) 0.5% CS

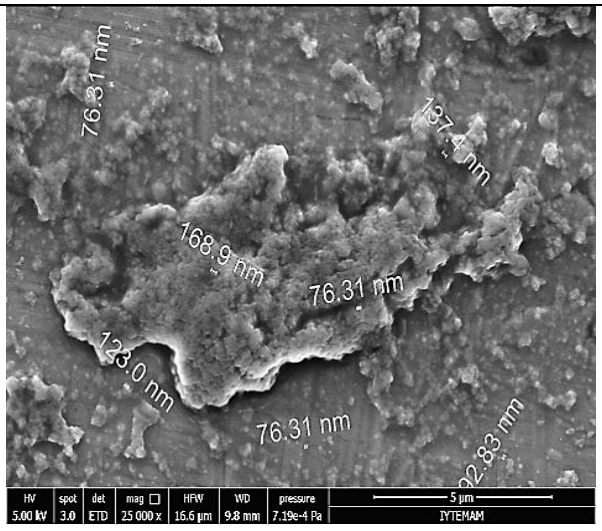

l) 1.0% CS

Figure 4.13. Changing the percentage of chitosan as 1% and 0.5%.

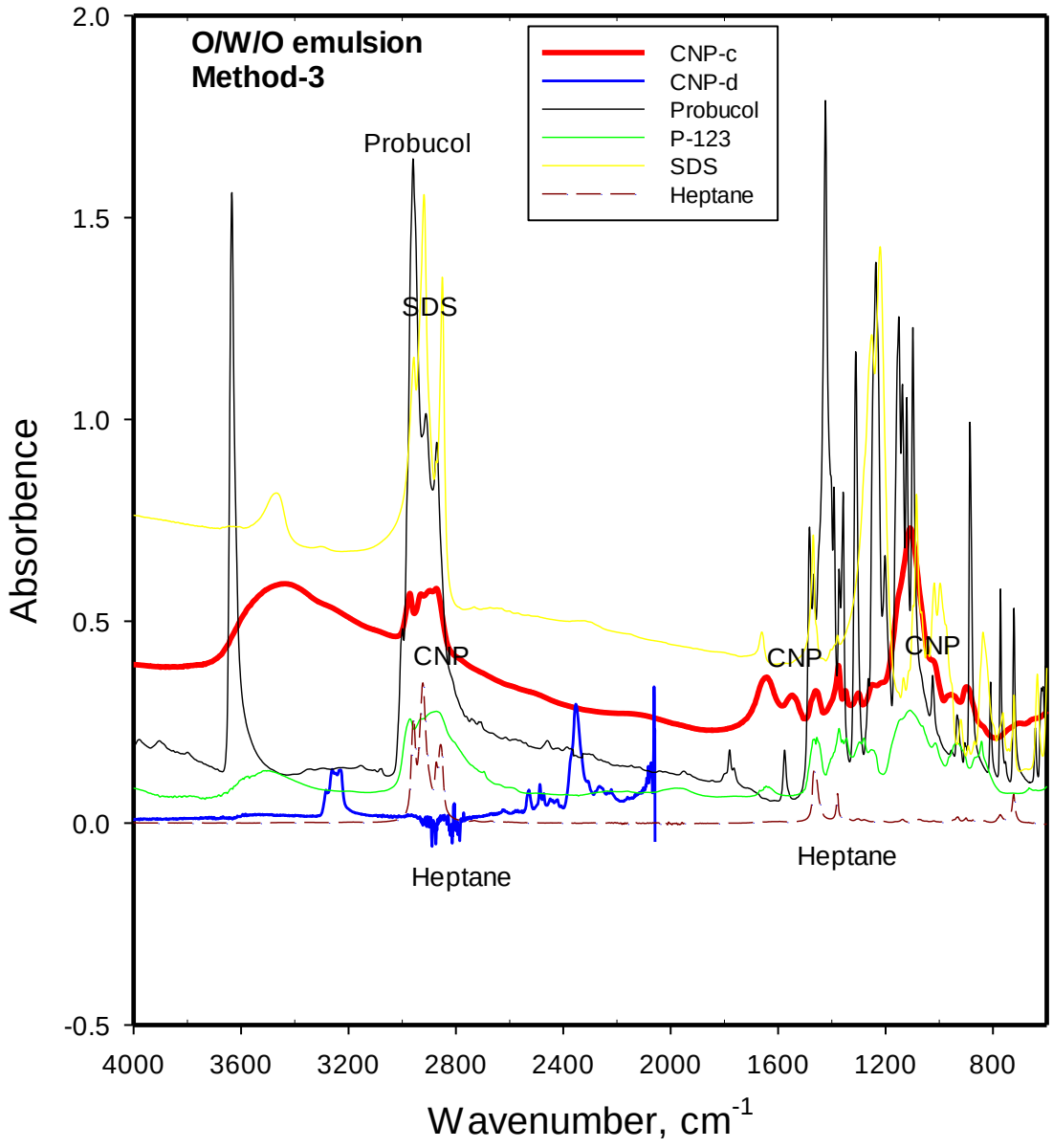

Figure 4.14-a. FTIR spectras of Oil in Water in Oil Emulsification Coupled with İonic Gelation Method (flowsheet c,d)

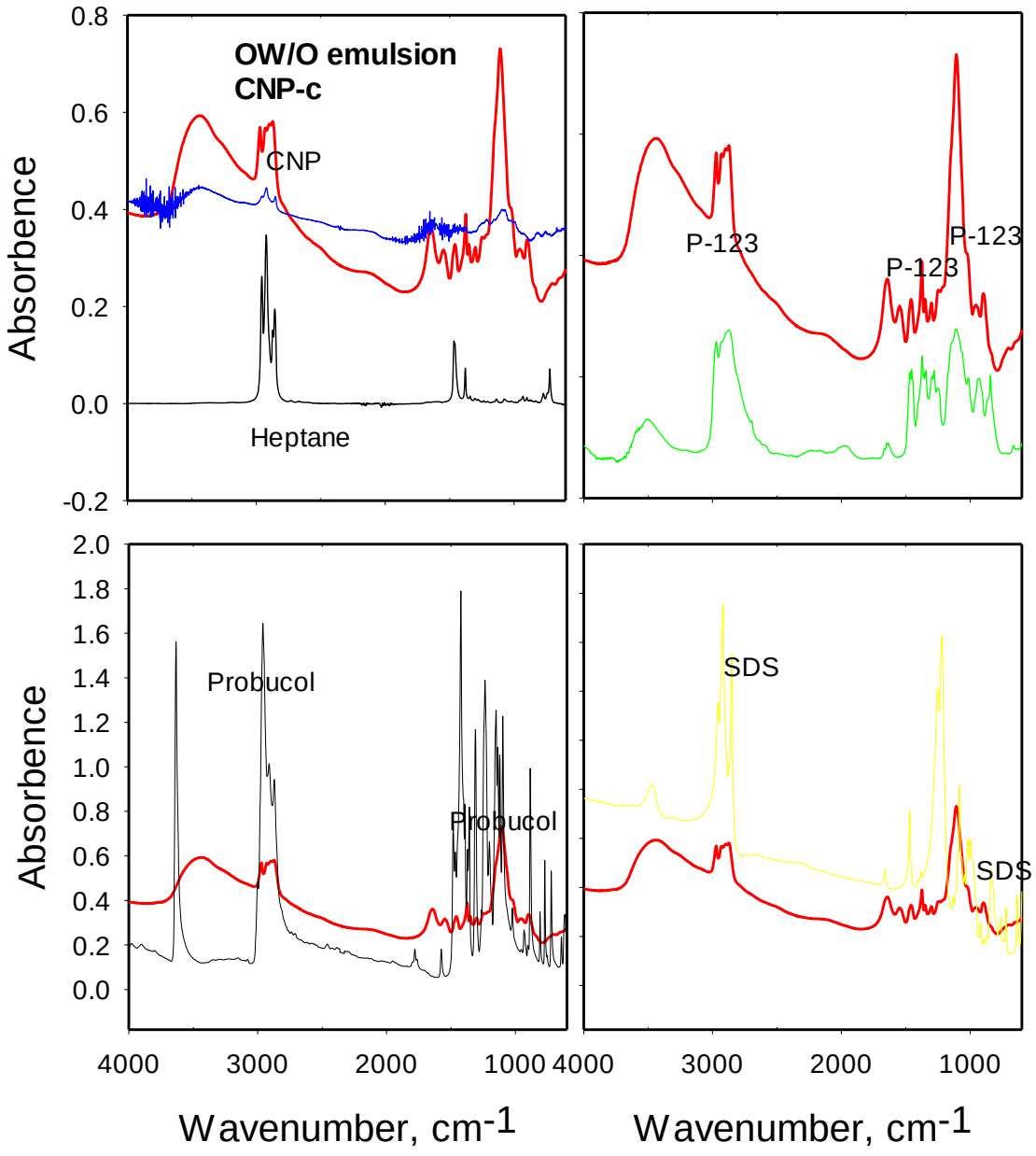

Figure 4.14-b. FTIR spectra of Oil in Water in Oil Emulsification Coupled with İonic Gelation Method with drug

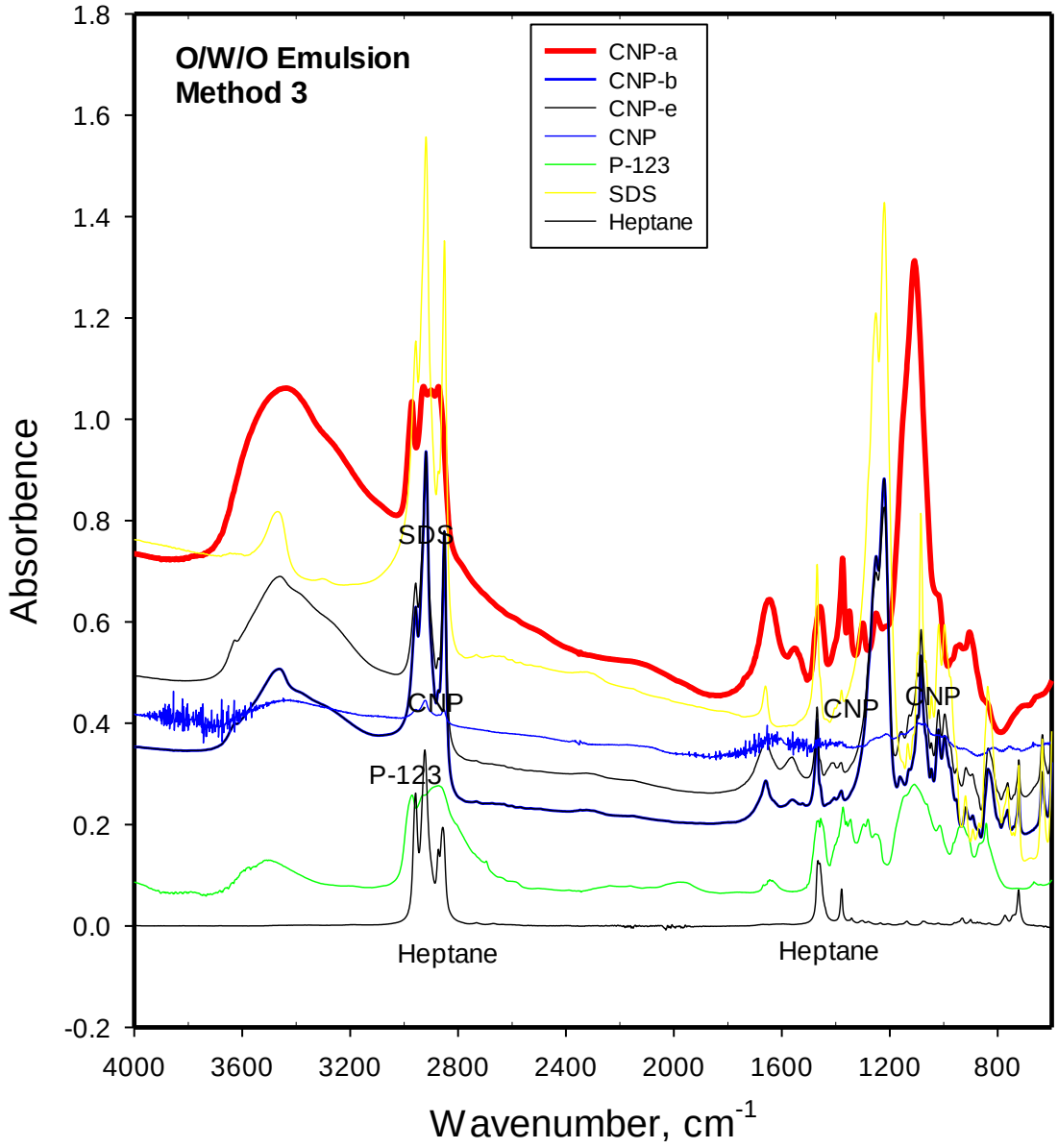

Figure 4.14-c. FTIR spectra of Oil in Water in Oil Emulsification Coupled with İonic Gelation Method without drug (flowsheet a,b,e).

4.2.4. Spontaneous Emulsion Coupled with Ionic Gelation Method

In this method, spontaneous oil in water emulsion was obtained and then chitosan was condenced on droplets. The details of the method were discussed in Chapter 3. In this method, three types of surfactant were used to provide stability of droplets in aqueous solution. These surfactants were SDS with negative charge, CTAB with positive charge and P-123 with no charge (or slightly negative or positive

depending on the system). The results of these studies are given in the following figures as SEM images. However, it was observed that this is not a good way to produce spherical and stable chitosan nano particles. The particles obtained were not even spherical in the presence of a hydrophobic drug, curcumin. This drug was dissolved in ethanol and given to the oil phase.

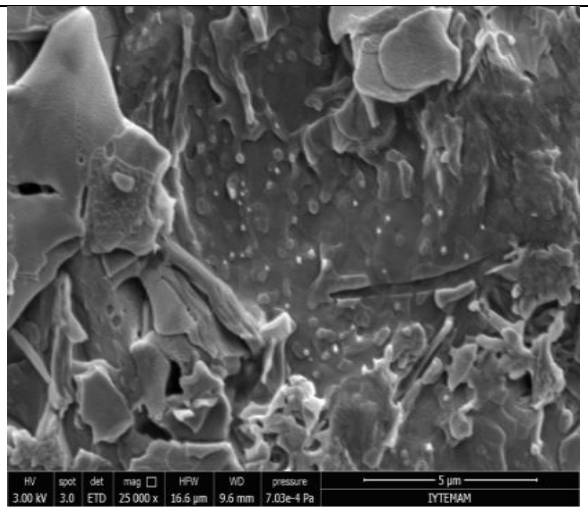

a) SDS, 2.5 ml Chitosan

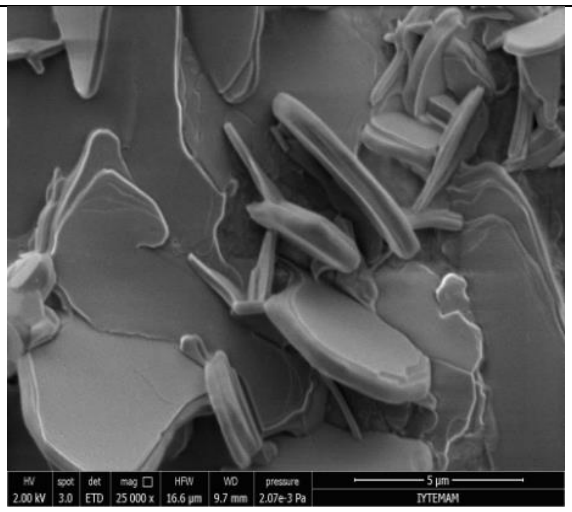

b) SDS, 5 ml Chitosan

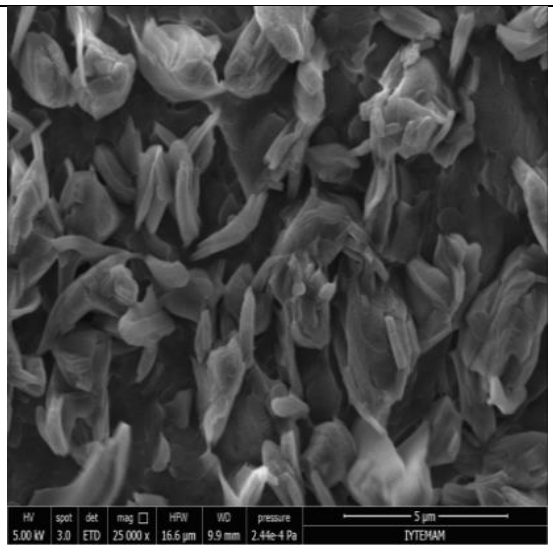

c) SDS, 25 ml Chitosan

Figure 4.15. SEM images of spontaneous emulsion in the presence of SDS.

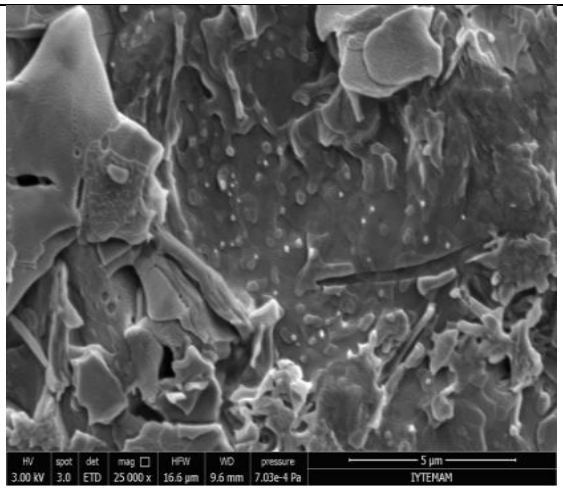

d) With SDS (10^{-2} M)

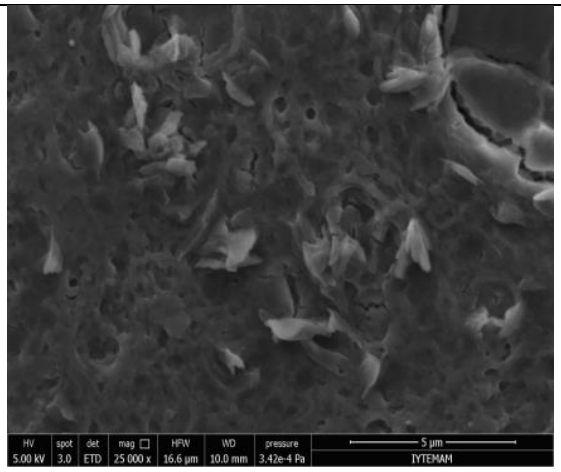

e) With CTAB (10^{-2} M)

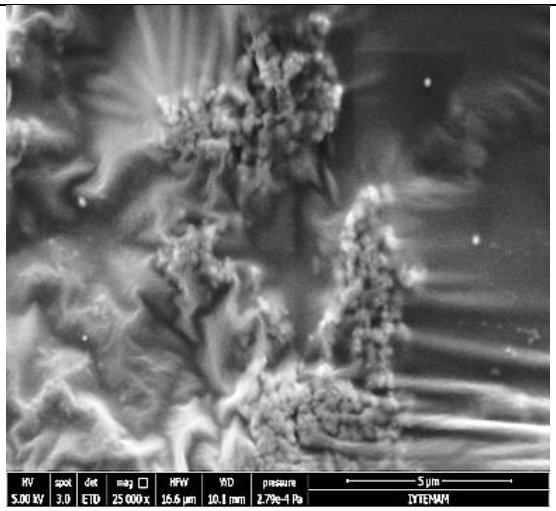

f) With P-123 (10^{-2} M)

Figure 4.16. SEM images of spontaneous emulsion in the presence of different type of surfactants, SDS, CTAB and P-123 at a fixedCS% (2.5 ml).

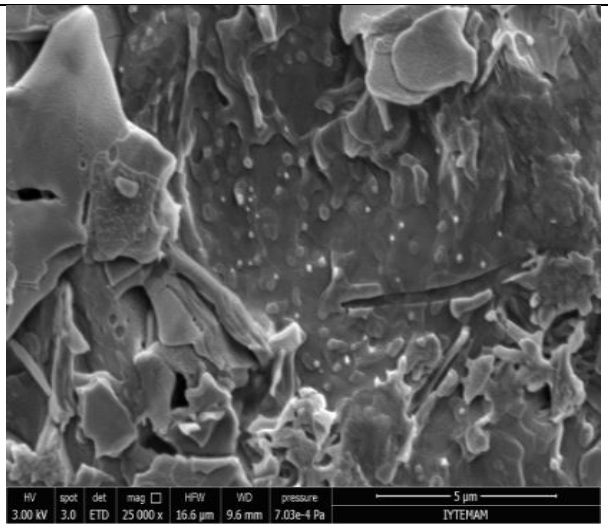

g) Without drug.

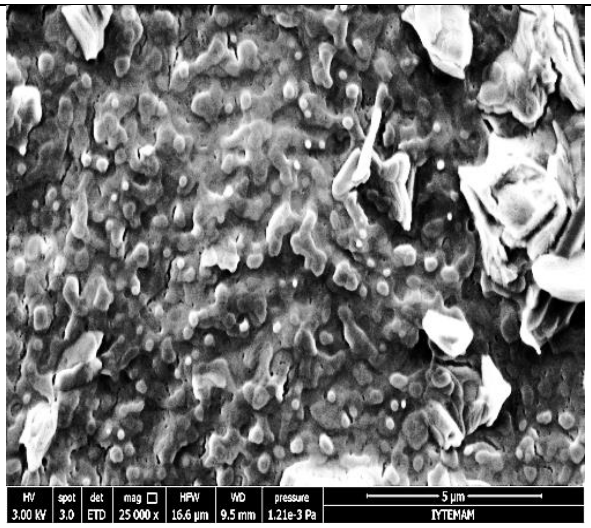

h) With Curcumin (Hydrophobic drug).

Figure 4.17. SEM images of spontaneous emulsion in the presence of SDS and Curcumin at a fixed CS% (2.5 ml).

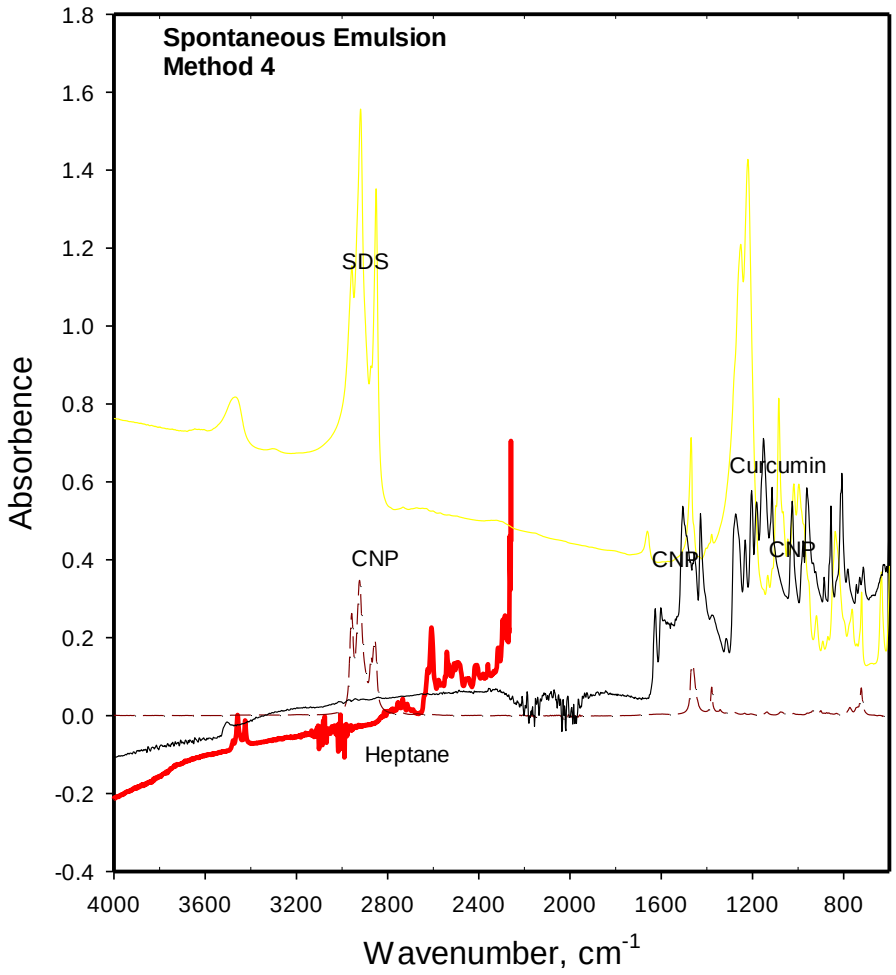

Figure 4.18-a. FTIR spectra of Spontaneous Emulsion Coupled with İonic Gelation Method with drug.

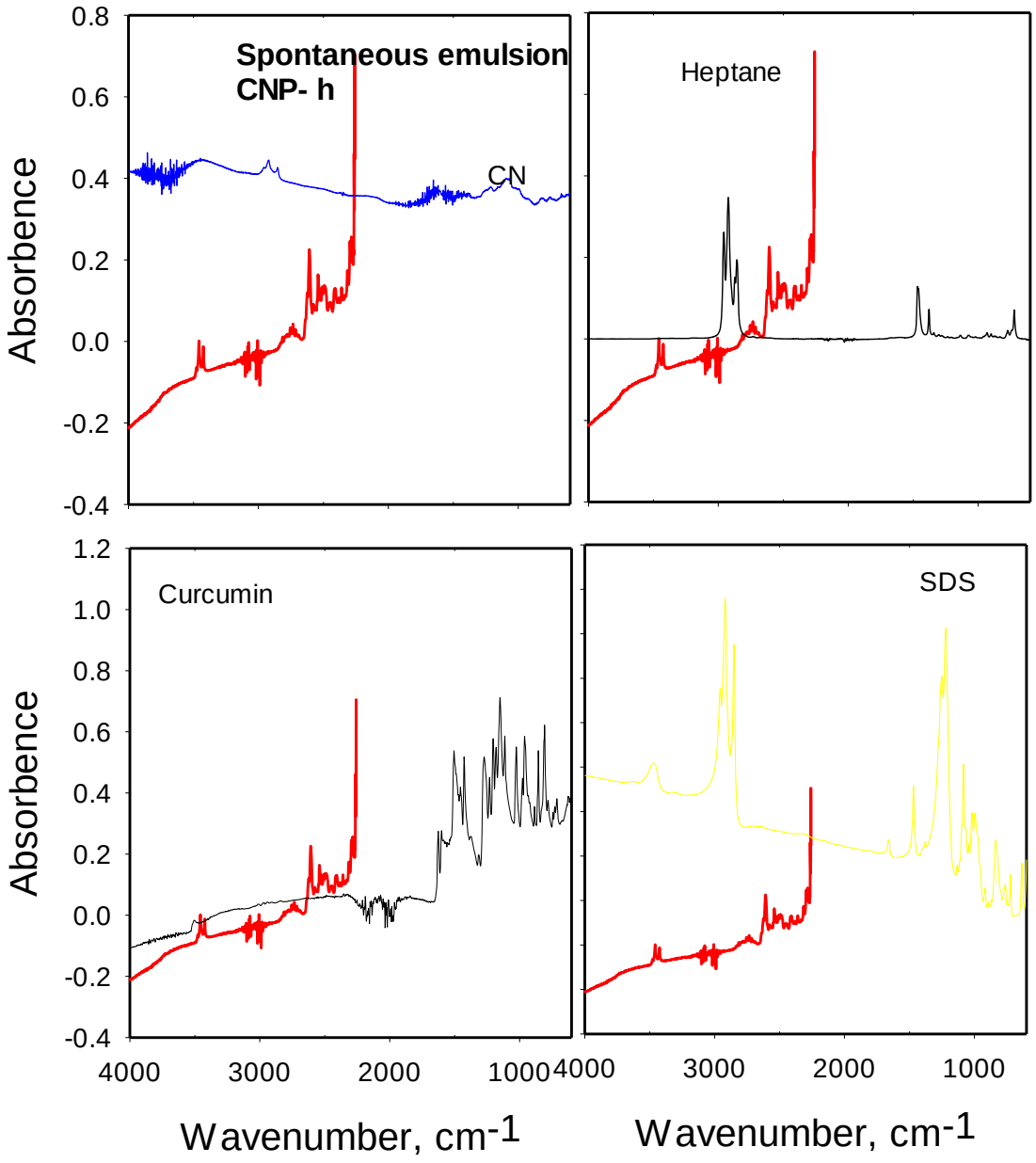

Figure 4.18-b. FTIR spectra of Spantaneous Emulsion Coupled with İonic Gelation Method without drug (flowsheet h).

4.2.5. Thin Film Hydration Coupled with Ionic Gelation Method

In this method, the drug loading to P-123 micelles process was directly coupled with the ionic gelation method to produce micelle embedded chitosan nano particles. The results of this method with and without SDS were given and discussed in the following figures. As it is seen from the Figure 4.19 that the size of P-123 micelles increase in the presence of the drug. Another image of these micelles with a larger

magnification was also given in Figure 4.20. It is seen that the drug loaded P-123 micelles were perfectly spherical and much larger in size (<100nm) compared to the sizes of P-123 micelles without drug (20nm). Then these micelles were covered by a chitosan layer and micelle embedded chitosan nanoparticles were obtained. The results were presented as STEM images in Figure 4.22. As it is seen the sizes of chitosan particles were much larger and there was a broad distribution. The size distribution of these particles, on the other hand, was not able to obtained by DLS. The particles were somehow flocculating and misleading the results. The formation of chitosan layer and the micelles loaded with drug were confirmed by FTIR analysis. These results were also discussed in the following paragraphs (Figure 4.25). The characteristic peaks of chitosan nano particles, P-123 and probucol were all observed (P-123: 2962 cm^{-1} , 1372cm^{-1} , 1438 cm^{-1} , 923 cm^{-1} ; Probucol: 2959 cm^{-1}, 1423 cm^{-1} and 1309 cm^{-1}). In most cases these peaks were overlapped. However, the intensities of the spectrums suggest that the drug loaded micelles are embedded in chitosan structures as planed.

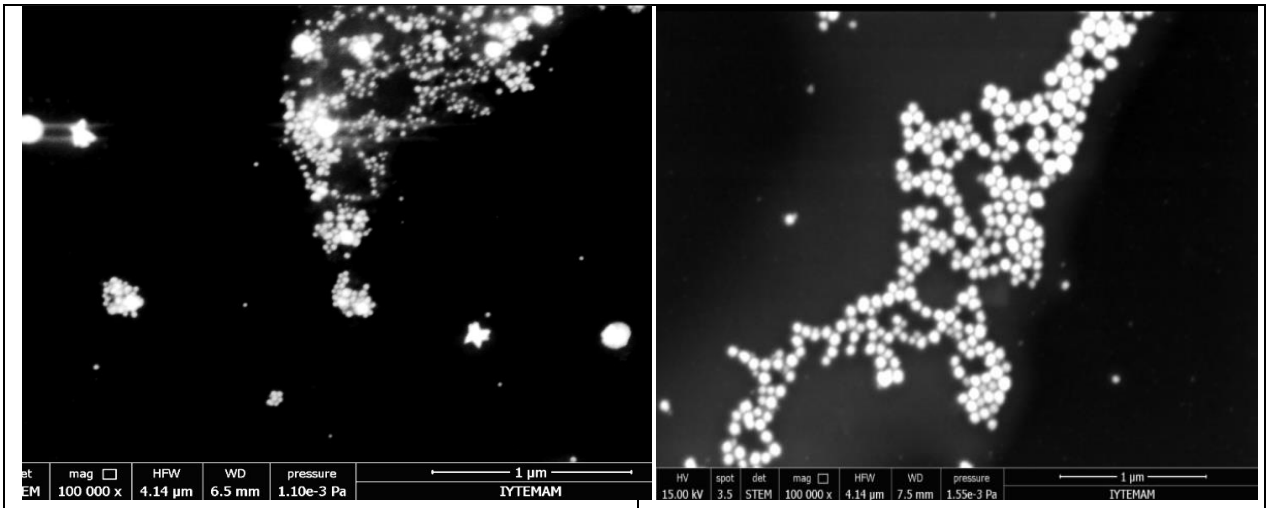

(a) 10^{-3} M P-123 Micelles, without drug

(b) 10^{-3} M P-123 Micelles loaded with Probucol

4.19. STEM images of P-123 micelles in the absence and presence Probucol.

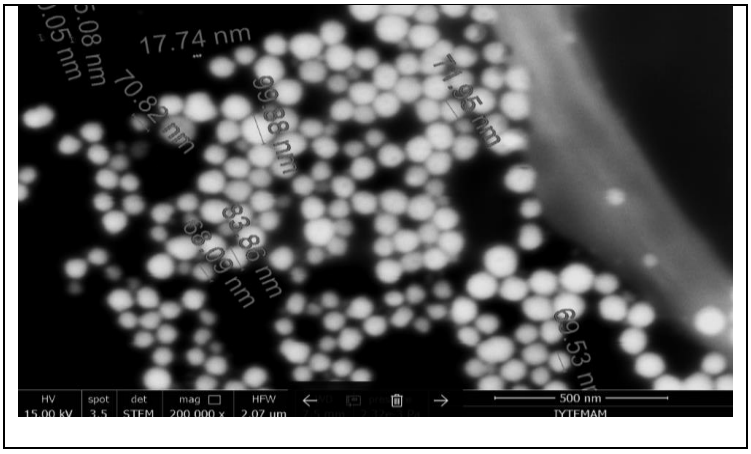

4.20. STEM images of P-123 micelles loaded with drug, Probucol. A closer look.

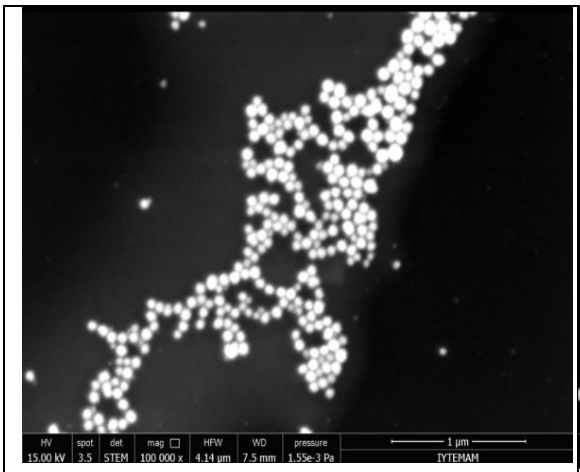

a) P-123 micelles loaded with drug.

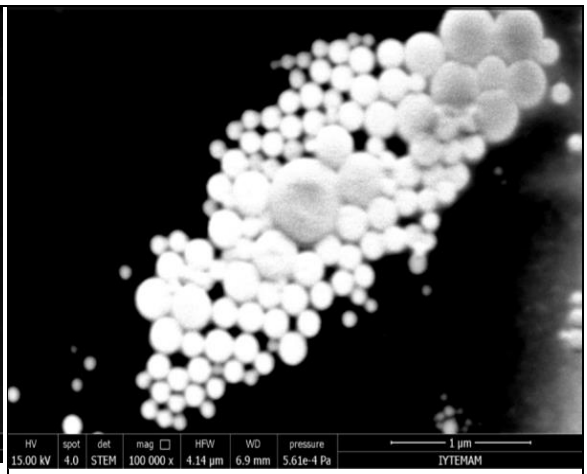

b) Probucol loadded P-123 micelles embeded Chitosan nano particles.

Figure 4.21. STEM images of P-123 micelles loaded with Probucol with and without chitosan coverage.

Similar type of synthesis and characterization studies were also conducted in the presence of SDS where the sizes and the charges of P-123 micelles were modified, and the results are presented in Figure 4.22 together with no SDS case. It is seen that the size of chitosan nano particles that embed micelles are much smaller in the presence of SDS molecules in the structure of micelle. This is because of smaller size of P-123 micelles due to the replacement of some P-123 molecules by the smaller SDS molecules. However, it looks like the system also contain uncovered micelles. Figure 4.23 gives some of these images to show the much smaller particles present in the system at the same time. The presence of these particles might be due to the insufficient amount of CS and TPP in the system. Therefore some of the micelles might be uncovered by chitosan.

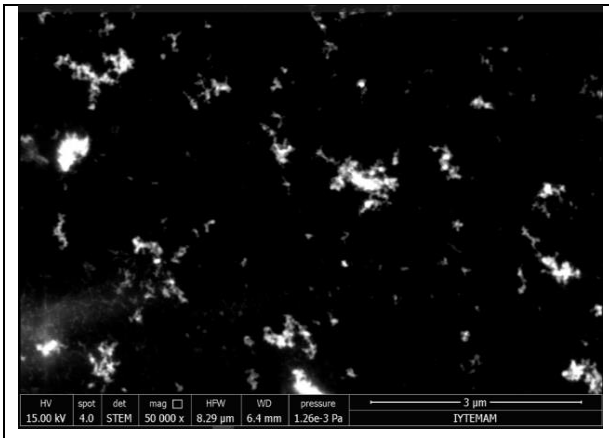

a) P-123+SDS micelles loaded with drug embeded Chitosan nano particles.

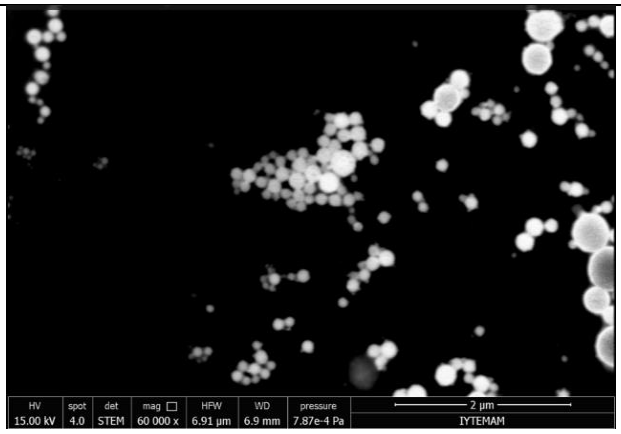

b) P-123 micelles loaded with drug embeded Chitosan nano particles, no SDS.

Figure 4.22. STEM images of drug loaded SDS +P-123 micelles embedded chitosan nano particles produced by Thin Film Hydration Coupled with Ionic Gelation Method.

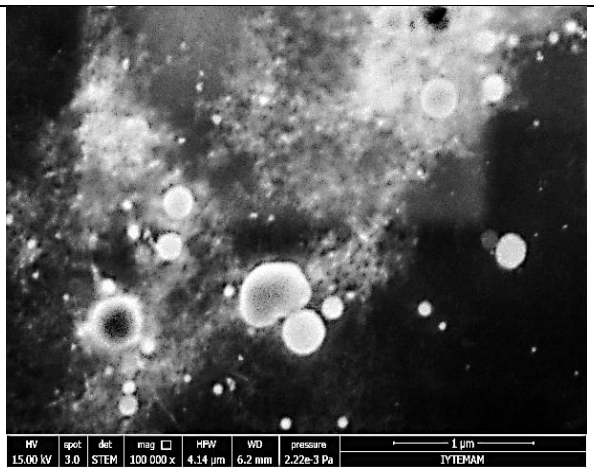

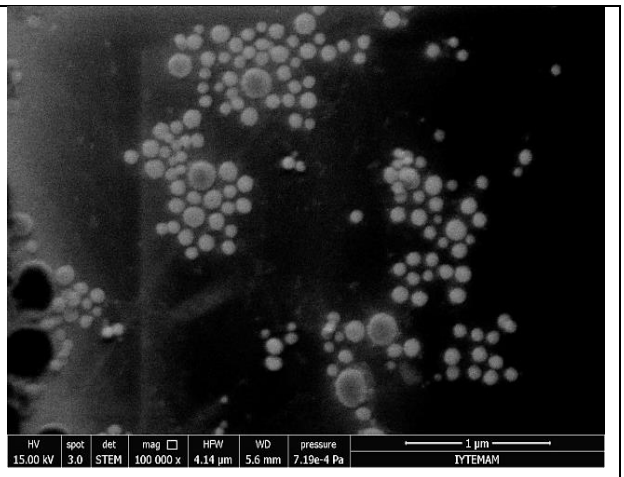

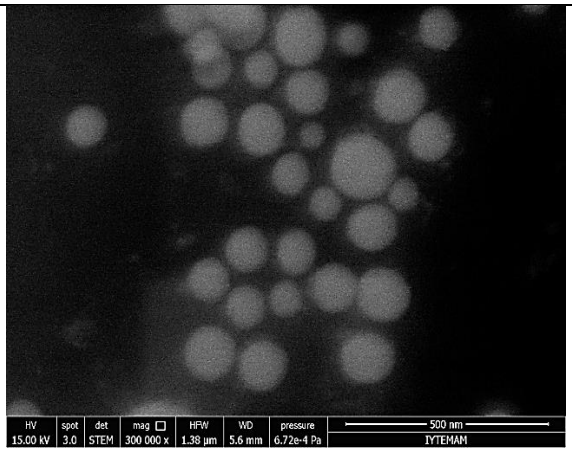

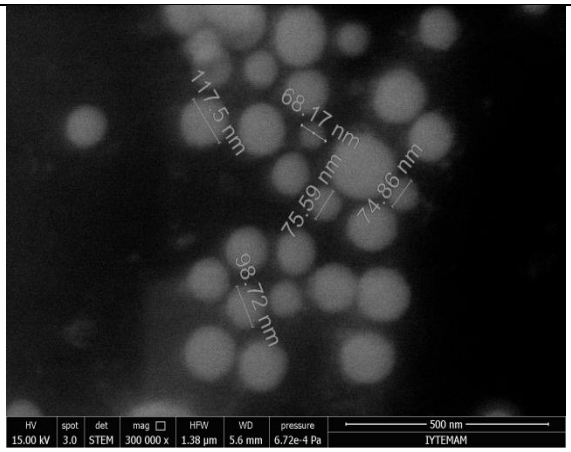

Figure 4.23. Some more STEM images that also show micelle embedded chitosan nanoparticles with and without SDS at different magnifications.

The Figure 4.24 gives the SEM images of these nanoparticles (in the presence of SDS) to show the difficulty of observation of these particles by SEM. Therefore in this part of the study, STEM images were used.

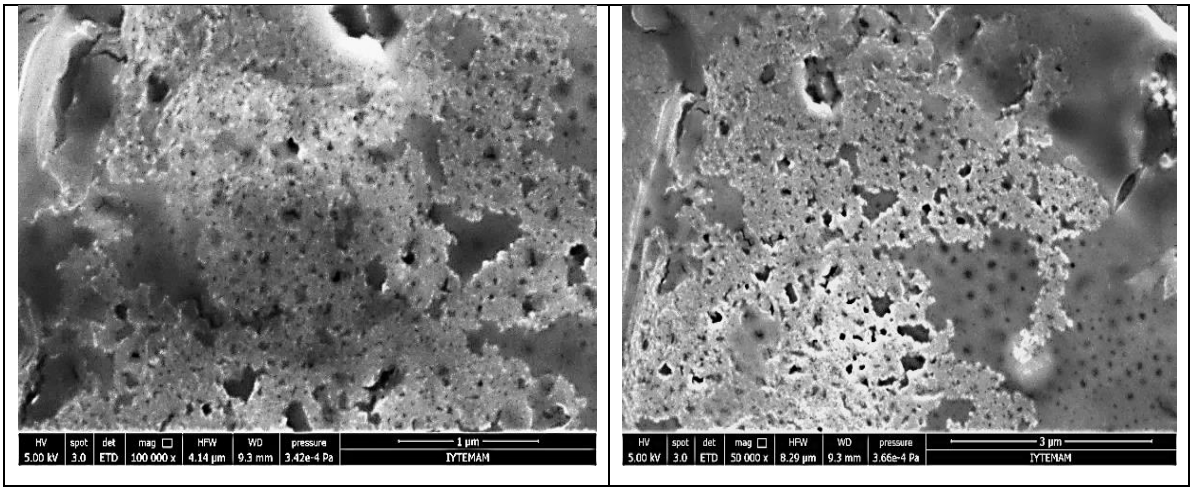

Figure 4.24. SEM images of drug loaded SDS +P-123 micelles embedded chitosan nano particles produced by Thin Film Hydration Coupled with Ionic Gelation Method.

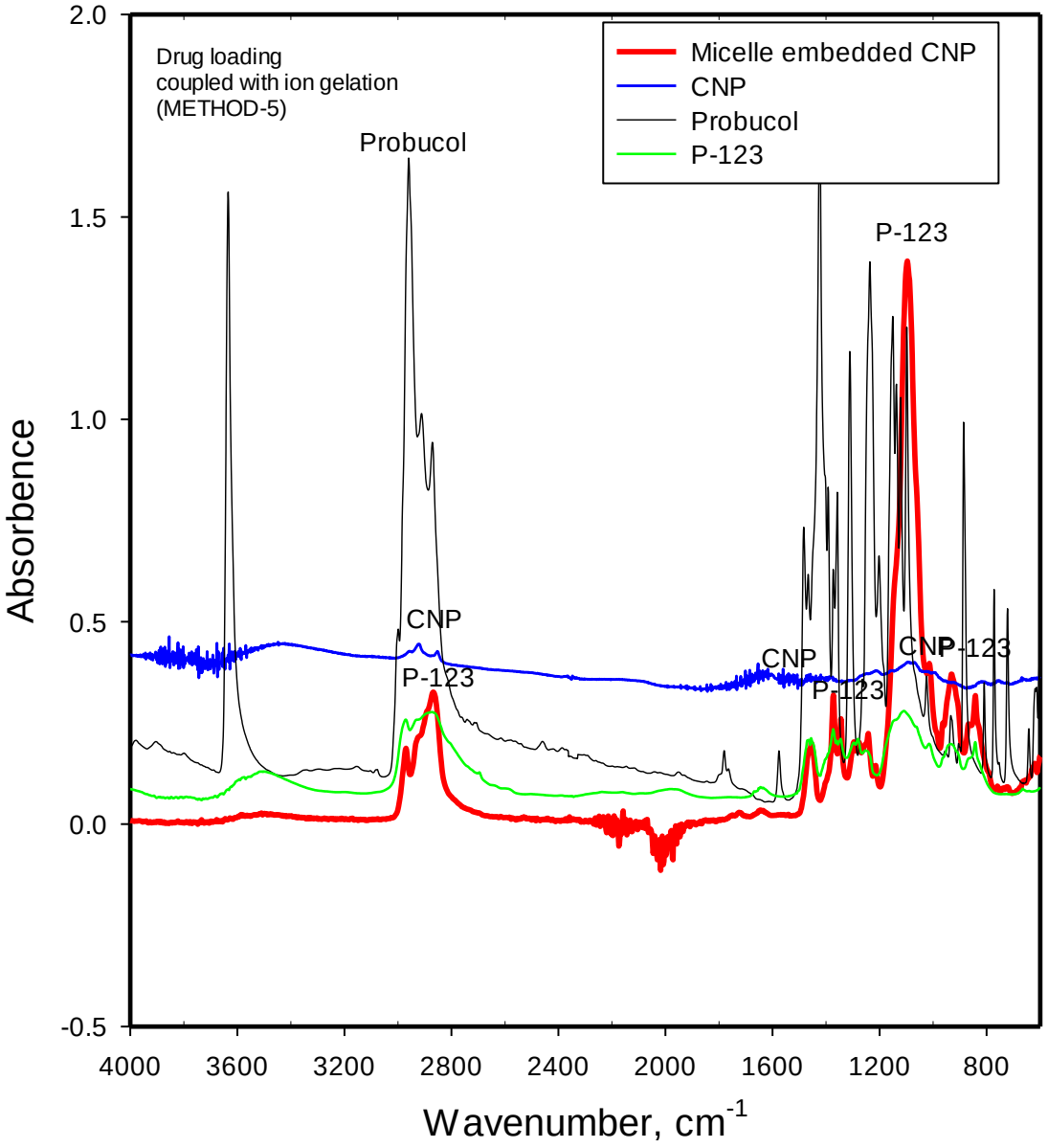

Figure 4.25-a. FTIR spectra of drug loaded SDS +P-123 micelles embedded chitosan nano particles produced by Thin Film Hydration Coupled with Ionic Gelation Method.

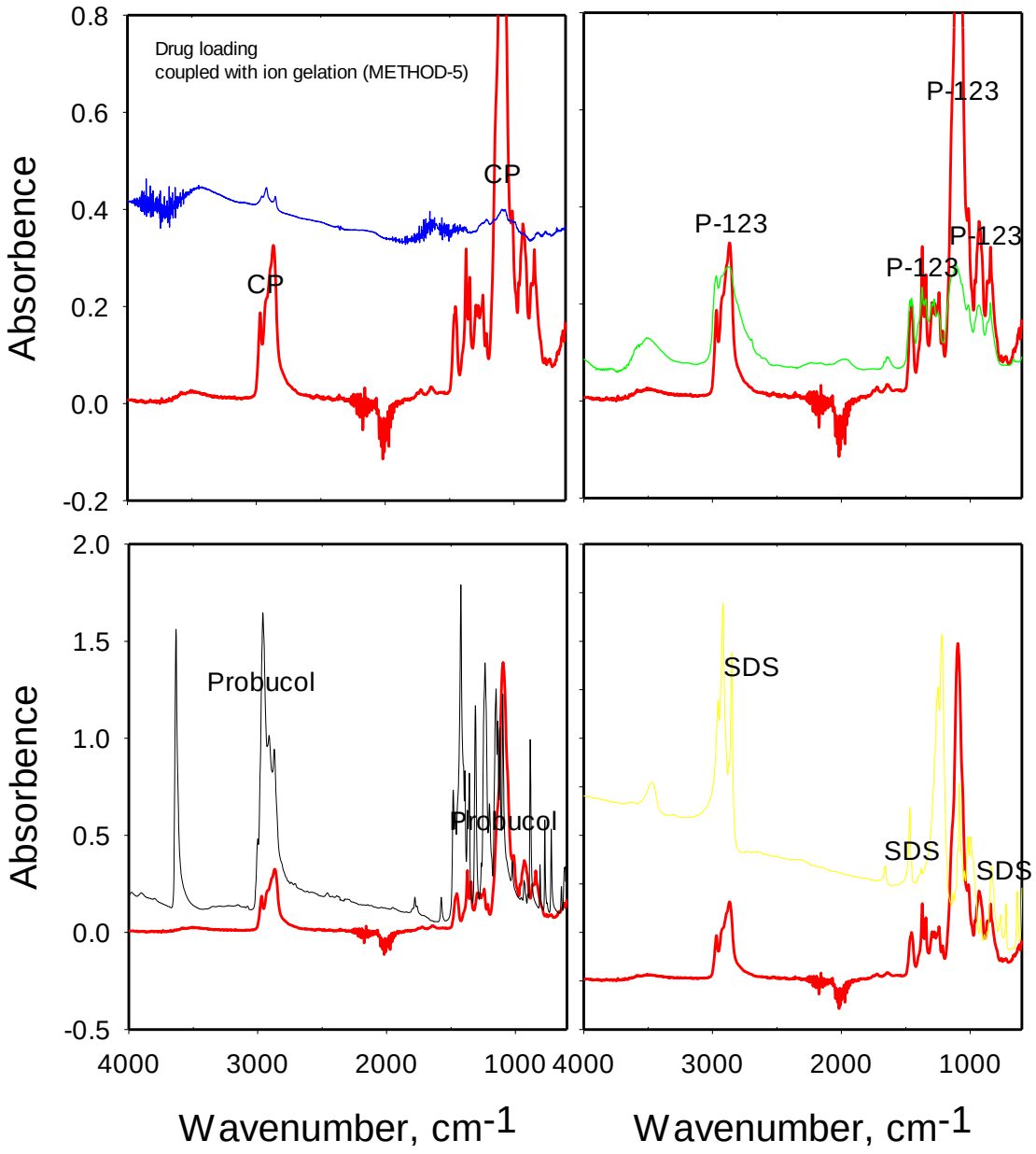

Figure 4.25-b. FTIR spectra of drug loaded SDS +P-123 micelles embedded chitosan nano particles produced by Thin Film Hydration Coupled with Ionic Gelation Method.

4.3. Drug Loading and Release Studies

The drug loading capacity of nanoparticles produced by method 5 that embeds drug loaded P-123 micelles, was determined by the procedure given above (Chapter 3). For this purpose the amount of unloaded drug was determined by UV measurements

and the amount of loaded drug was calculated. The unloaded drug amount was measured as 8.04032 x 10^{-5} M for the initial drug concentration of 7.2556 x 10^{-4} M. Therefore, the loaded drug amount was calculated as 6.451568 x 10^{-4} M. This makes a 88.91% of drug loading capacity.

Similar measurements were also conducted in the presence of SDS with drug loaded P-123+SDS micelle embedded chitosan nano particles. The unloaded drug amount was measured as 9.1757 x 10^{-5} M for the initial drug concentration of 7.2556 x 10^{-4} M. Therefore, the loaded drug amount was calculated as 6.338 x 10^{-4} M which makes 87.35% of drug loading capacity which is expected.

For the same chitosan nanoparticles, the release of drug was tested as a function of time according to the procedure given in Chapter 3. The release results are presented in the following figures for P-123 embedded and for P-123+SDS embedded chitosan nano particles for different pH values . Figure 4.26 for P-123 embedded, Figure 4.27 for P-123+SDS embedded chitosan nano particles for pH 7.4 and temperature 37^{o}C. Similarly Figure 4.28 for P-123 embedded, Figure 4.29 for P-123+SDS embedded chitosan nano particles for pH 6.8 and temperature 37^{o}C.

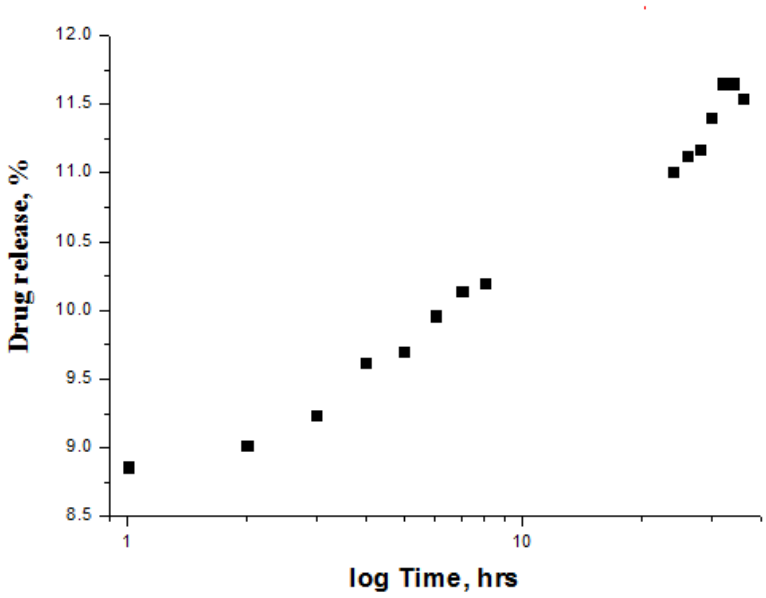

Figure 4.26. Drug concentrations which is released from P-123 micelles embedded chitosan nanoparticles on pH 7.4 and 37℃.

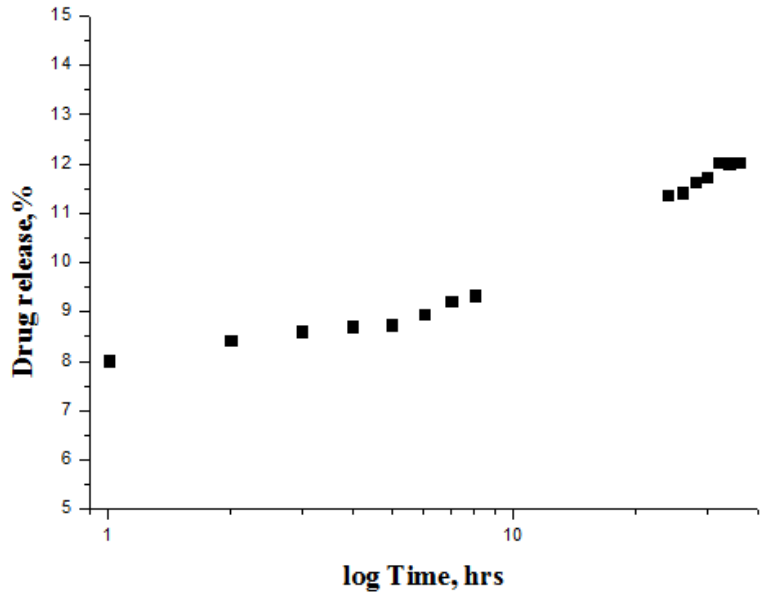

Figure 4.27. Drug concentrations which is released from SDS+P-123 micelles embedded chitosan nanoparticles on pH 7.4 and 37℃.

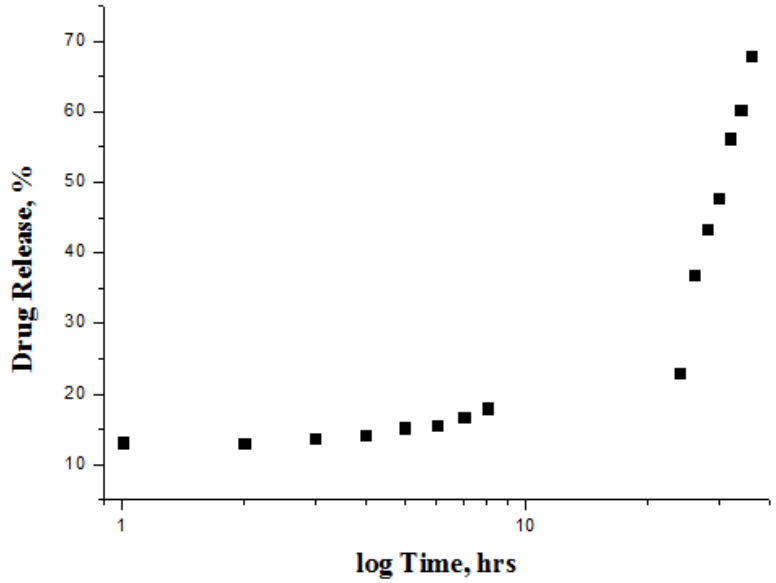

Figure 4.28. Drug concentrations which is released from SDS+P-123 micelles embedded chitosan nanoparticles on pH 6.8 and 37℃.

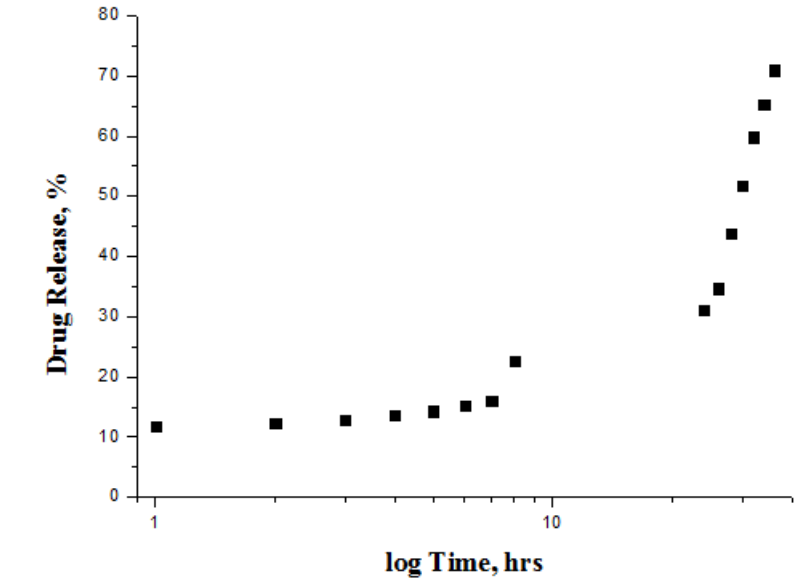

Figure 4.29. Drug concentrations which is released from P-123 micelles embedded chitosan nanoparticles on pH 6.8 and 37℃.

As it is seen from the figures that the release kinetics of drug strongly depends on pH of the medium which is the simulated body fluid in this case. In the case of pH 6.8 almost 80% of drug is released after 24 hrs. However, in the case of pH 7.4, the release of drug is less than 15%. The precence of SDS did not show any significant change and their results were so similar. This is expected since drug is releasing within the micelle to the environment. The effect of chitosan cover (such as its thickness), on the other hand, is expected to be significant in drug release studies.

CHAPTER 5

CONCLUSION

In this study, several different methods were designed and tested to synthesize chitosan nanoparticles that embed a hydrophobic core that are suitable for oil soluble drugs. For this purpose, the micelle of PEO/PPO/PEO type a triblock co-polymer, Pluronic P-123 was used. The size and charge of micelles were adjusted using an anionic surfactant, SDS. Then these micelles were covered by chitosan and characterized using Fourier Transform Infrared Spectroscopy (FTIR), Scanning Electron Microscope (SEM), Scanning Transmission Microscope (STEM), Transmission Electron Microscope (TEM), surface tension and zeta potential measurements. The following specific conclusions were made.

1) The surface tension behavior of P-123 was found to be divided into three concentration regions marked as Regions I, II and III. Region I is believed to consist principally of monomers whereas Region III involves fully developed micelles. The surface tension values were lower in SBF in Region I and same in Region II and III.
2) According to AFM, DLS, STEM results, the average size of P-123 micelles were found to be around 20 nm.
3) According to DLS results, the average size of P-123 micelles decreased down to 5-6 nm and gained negative charge in the presence of SDS.
4. Hydrophobic drug loaded micelle embedded chitosan nano particles were able to manufactured successfully by some of the methods tested.
5. The best method was the coupling of drug loading with simple ionic gelation method among all the others.
6. The sizes of chitosan particles that embed P-123 micelles were larger (<100 nm) than the sizes of P-123 micelles (20 nm) alone.
7. The smaller chitosan nanoparticles (<50 nm) that embed drug loaded P-123 micelles were able obtained when their structure is modified by SDS.

APPENDIX A

FTIR results for each product.

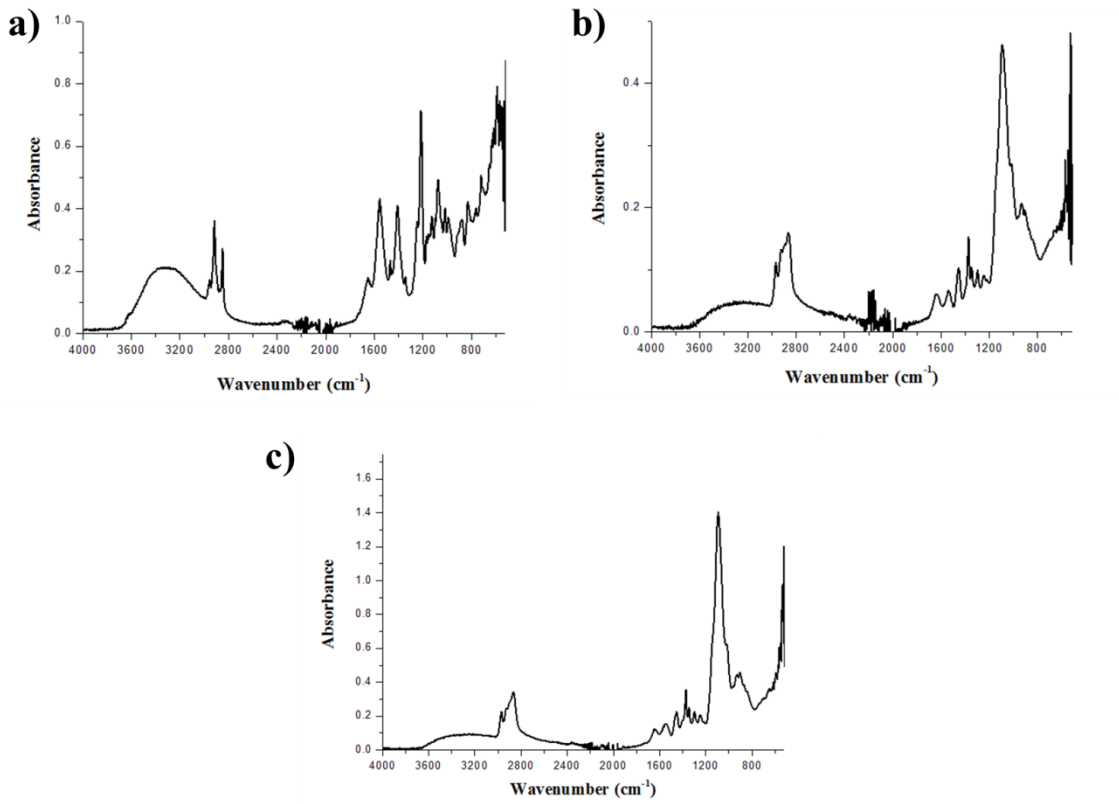

Figure A-1. FTIR spectras of Oil in Water Emulsification Coupled with Ionic Gelation Method

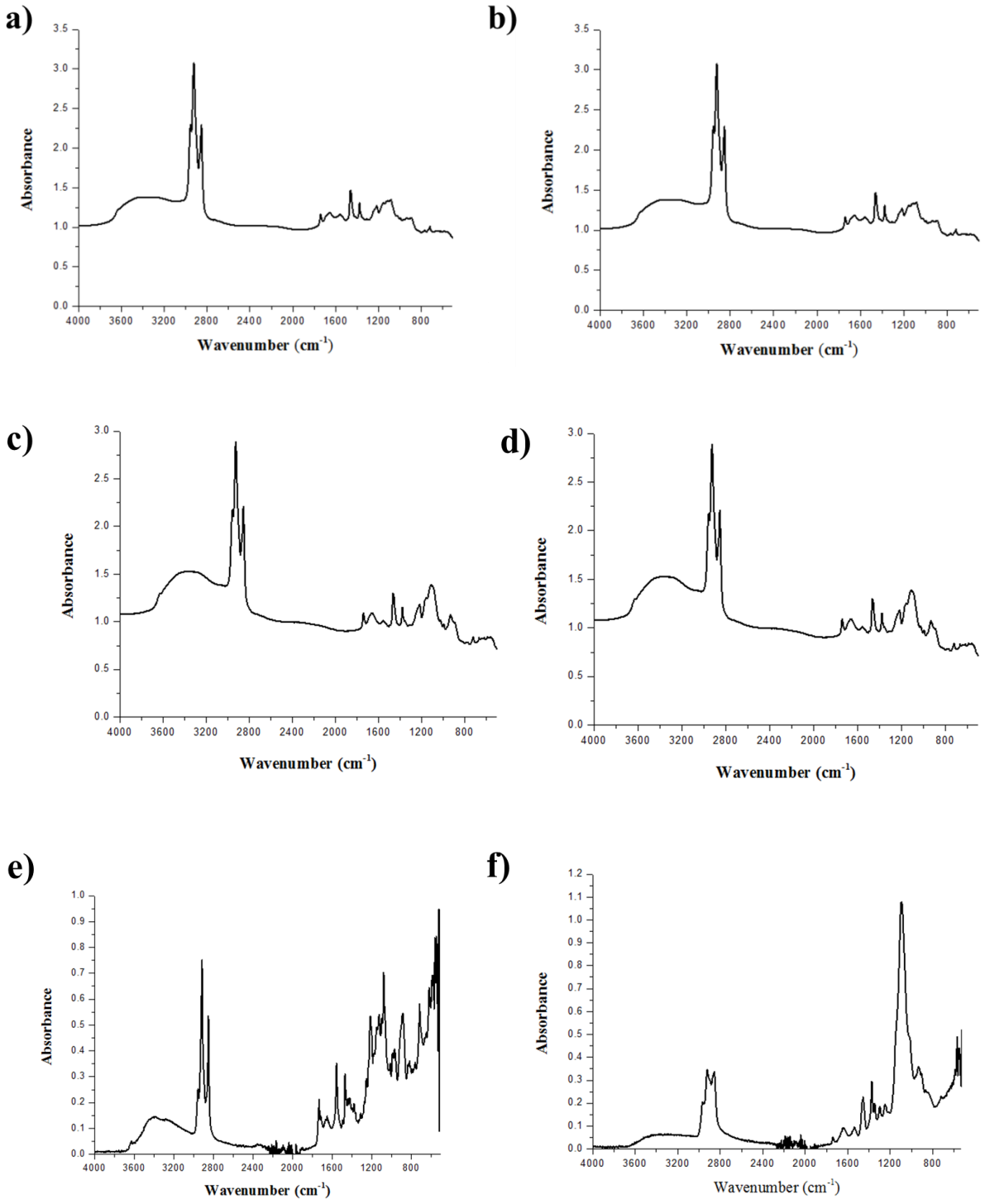

Figure A-2. FTIR spectras of Water in Oil Emulsification Coupled with İonic Gelation Method

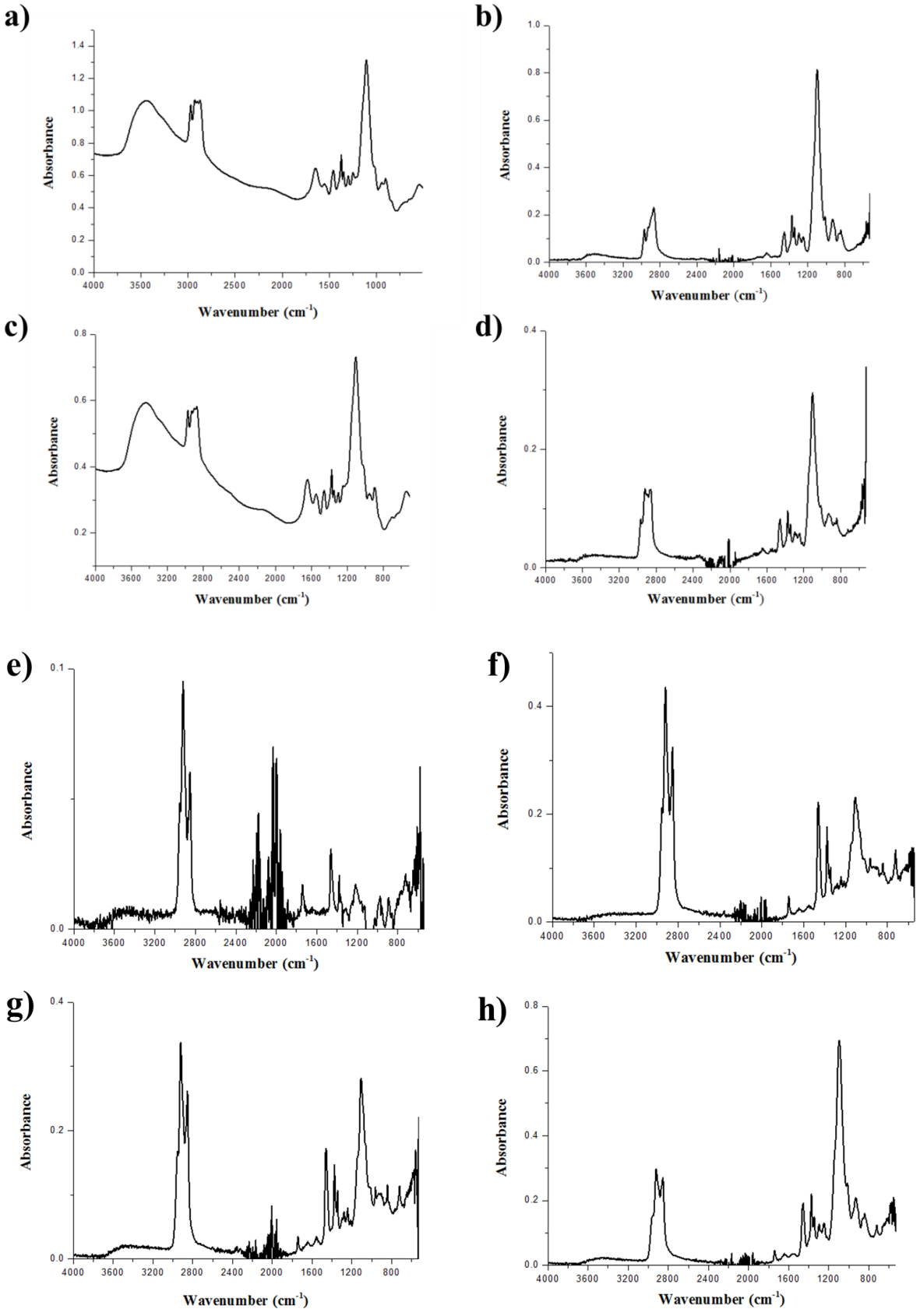
a)
b)
c)
d)
e)
f)
g)
h)
Absorbance
Wavenumber (cm-1)

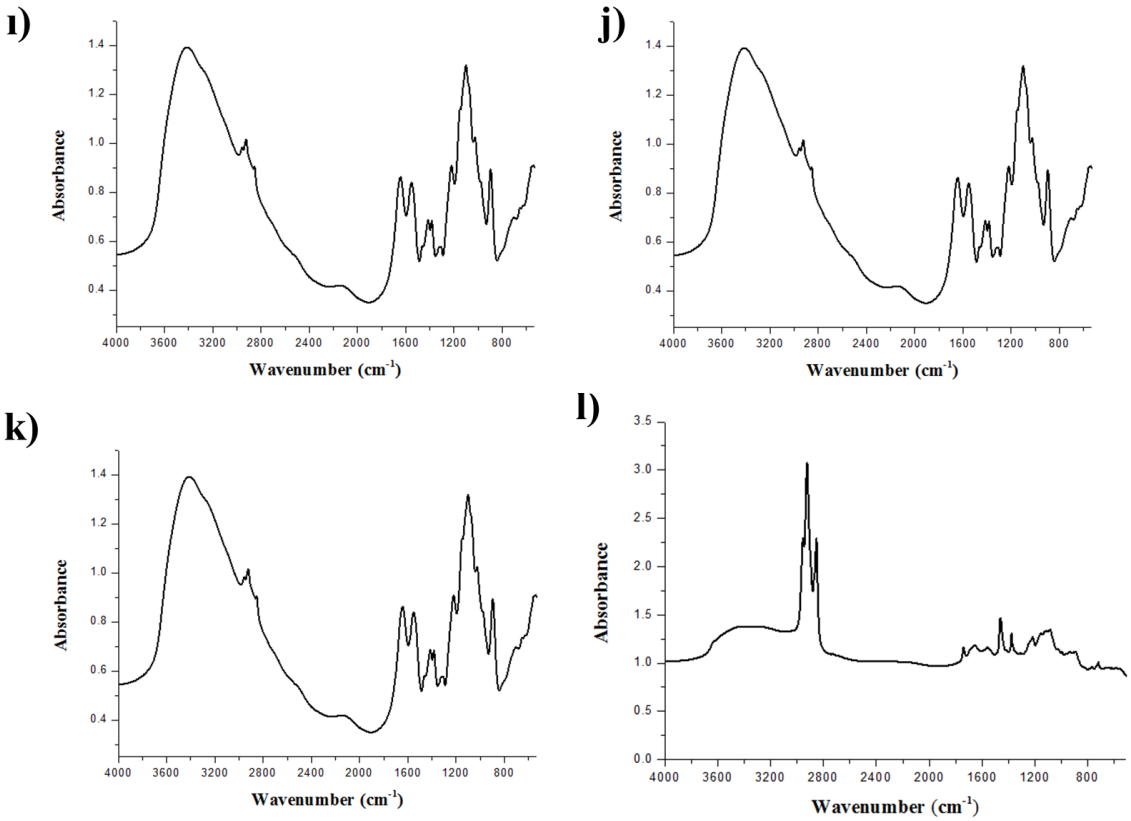

Figure A.3. FTIR spectras of Oil in Water in Oil Emulsification Coupled with İonic Gelation Method

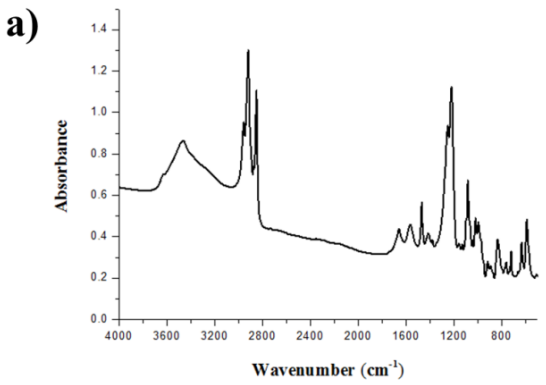
a)
Absorbance
Wavenumber (cm-1)

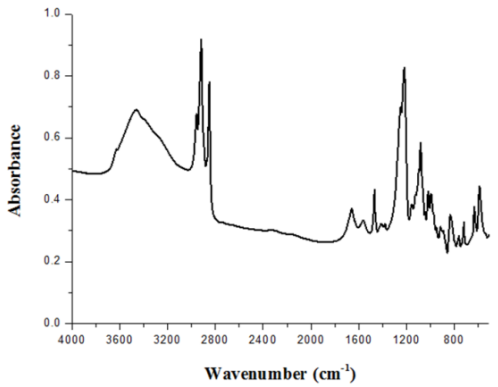
b)
Absorbance
Wavenumber (cm-1)

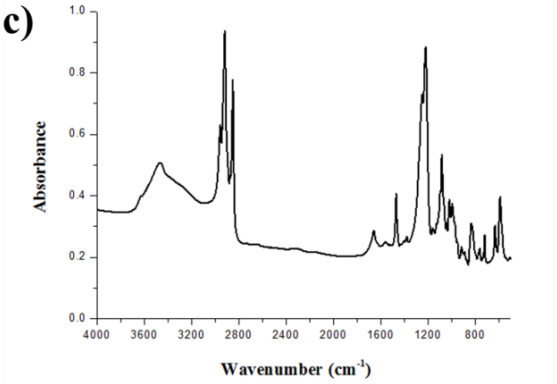
c)
Absorbance
Wavenumber (cm-1)

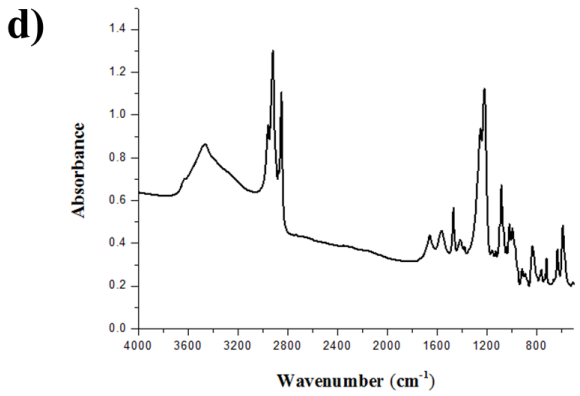
d)
Absorbance
Wavenumber (cm-1)

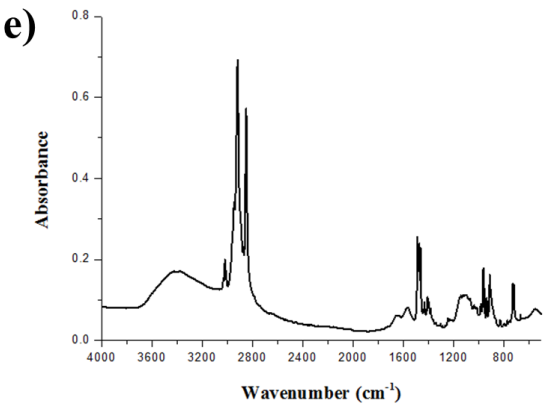
e)
Absorbance
Wavenumber (cm-1)

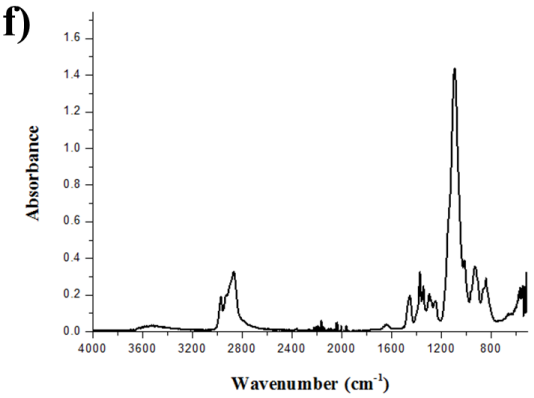
f)
Absorbance
Wavenumber (cm-1)

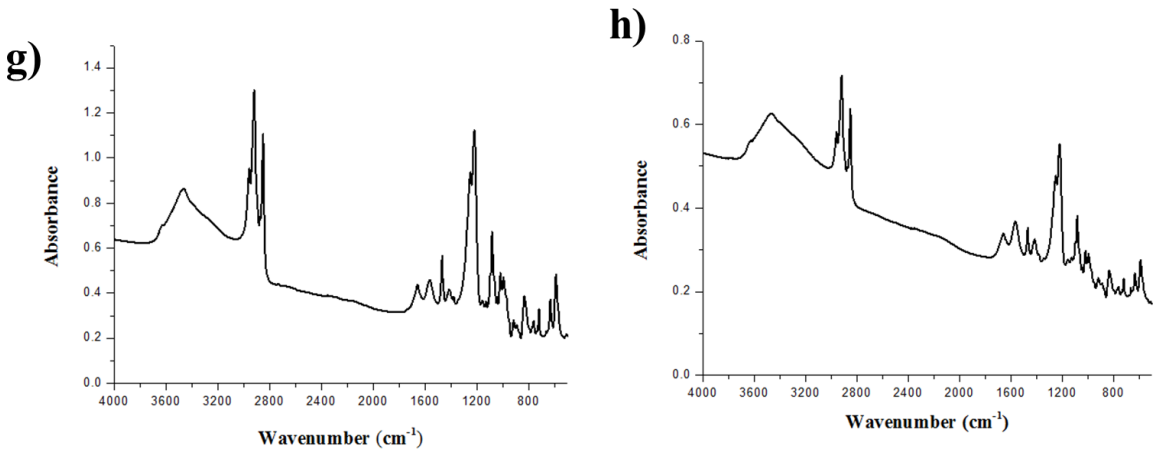

Figure A.4. FTIR spectras of Spantaneous Emulsion Coupled with İonic Gelation Method.

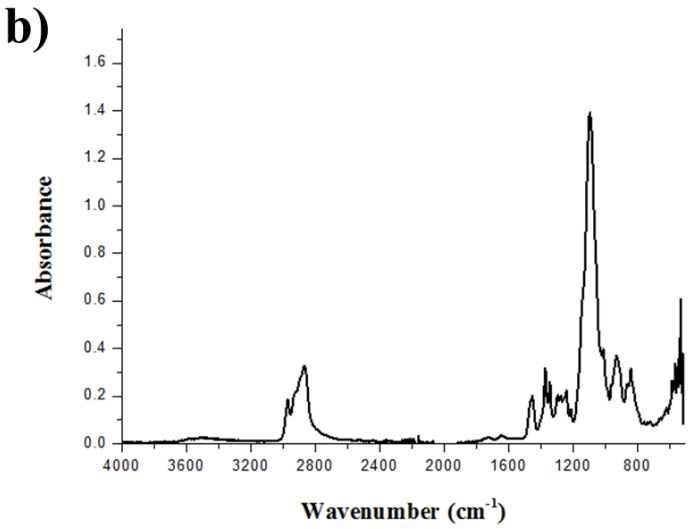

Figure A.5. FTIR spectras of drug loaded SDS +P-123 micelles embedded chitosan nano particles produced by Thin Film Hydration Coupled with Ionic Gelation Method.

REFERENCES

A. Berthold , K. Cremer , j. Kreuter. 1996. "Preparation and characterization of chitosan microspheres as drug carrier for prednisolone sodium phosphate as model for antiinflammatory drugs." *Journal of Controlled Release*:17-25.

Agnihotri, S. A., and T. M. Aminabhavi. 2007. "Chitosan nanoparticles for prolonged delivery of timolol maleate." *Drug Dev Ind Pharm* 33 (11):1254-62. doi: 10.1080/03639040701384942.

Ahmad, N., R. Ahmad, A. A. Naqvi, M. A. Alam, M. Ashafaq, M. Samim, Z. Iqbal, and F. J. Ahmad. 2016. "Rutin-encapsulated chitosan nanoparticles targeted to the brain in the treatment of Cerebral Ischemia." *Int J Biol Macromol* 91:640-55. doi: 10.1016/j.ijbiomac.2016.06.001.

Ajun, Wan, Sun Yan, Gao Li, and Li Huili. 2009. "Preparation of aspirin and probucol in combination loaded chitosan nanoparticles and in vitro release study." *Carbohydrate Polymers* 75 (4):566-574. doi: 10.1016/j.carbpol.2008.08.019.

Avadi, M. R., A. M. Sadeghi, N. Mohammadpour, S. Abedin, F. Atyabi, R. Dinarvand, and M. Rafiee-Tehrani. 2010. "Preparation and characterization of insulin nanoparticles using chitosan and Arabic gum with ionic gelation method." *Nanomedicine* 6 (1):58-63. doi: 10.1016/j.nano.2009.04.007.

Carson, L., C. Kelly-Brown, M. Stewart, A. Oki, G. Regisford, Z. Luo, and V. I. Bakhmutov. 2009. "Synthesis and characterization of chitosan-carbon nanotube composites." *Mater Lett* 63 (6-7):617-620. doi: 10.1016/j.matlet.2008.11.060.

Chang, Ke Liang B. 1997. "Heterogeneous N-deacetylation of chitin in alkaline solution." *Carbohydrate Research*:327-332

Corazzari, Ingrid, Roberto Nisticò, Francesco Turci, Maria Giulia Faga, Flavia Franzoso, Silvia Tabasso, and Giuliana Magnacca. 2015. "Advanced physico-chemical characterization of chitosan by means of TGA coupled on-line with FTIR and GCMS: Thermal degradation and water adsorption capacity." *Polymer Degradation and Stability* 112:1-9. doi: 10.1016/j.polymdegradstab.2014.12.006.

De, Arun Kumar, Shweta Garg, Dinesh Kumar Singhal, Hrudananda Malik, Ayan Mukherjee, Manoj Kumar Jena, Sudarshan Kumar, Jai Kumar Kaushik, Ashok Kumar Mohanty, Bikash Chandra Das, Sadhan Bag, Subrata Kumar Bhanja, and Dhruba Malakar. 2013. "Derivation of goat embryonic stem cell-like cell lines from in vitro produced parthenogenetic blastocysts." *Small Ruminant Research* 113 (1):145-153. doi: 10.1016/j.smallrumres.2013.01.018.

Deng, Z., Z. Zhen, X. Hu, S. Wu, Z. Xu, and P. K. Chu. 2011. "Hollow chitosan-silica nanospheres as pH-sensitive targeted delivery carriers in breast cancer therapy." *Biomaterials* 32 (21):4976-86. doi: 10.1016/j.biomaterials.2011.03.050.

Duarte-Neves, J., L. Pereira de Almeida, and C. Cavadas. 2016. "Neuropeptide Y (NPY) as a therapeutic target for neurodegenerative diseases." *Neurobiol Dis* 95:210-24. doi: 10.1016/j.nbd.2016.07.022.

Duarte, Ana Rita C., João F. Mano, and Rui L. Reis. 2009. "Preparation of chitosan scaffolds loaded with dexamethasone for tissue engineering applications using supercritical fluid technology." *European Polymer Journal* 45 (1):141-148. doi: 10.1016/j.eurpolymj.2008.10.004.

El-Shabouri, M.H. 2002a. "Positively charged nanoparticles for improving the oral bioavailability of cyclosporin-A." *International Journal of Pharmaceutics* 101-108.

El-Shabouri, M.H. 2002b. "Positively charged nanoparticles for improving the oral bioavailability of cyclosporin-A." *International Journal of Pharmaceutics* 249:101-108.

Elgadir, M. Abd, Md Salim Uddin, Sahena Ferdosh, Aishah Adam, Ahmed Jalal Khan Chowdhury, and Md Zaidul Islam Sarker. 2015. "Impact of chitosan composites and chitosan nanoparticle composites on various drug delivery systems: A review." *Journal of Food and Drug Analysis* 23 (4):619-629. doi: 10.1016/j.jfda.2014.10.008.

Fan, Ling, Ronghua Jin, Xueyi Le, Xiaohua Zhou, Shi Chen, Haifeng Liu, and Yahong Xiong. 2011. "Chitosan microspheres for controlled delivery of auxins as agrochemicals." *Microchimica Acta* 176 (3-4):381-387. doi: 10.1007/s00604-011-0732-y.

George, M., and T. E. Abraham. 2006. "Polyionic hydrocolloids for the intestinal delivery of protein drugs: alginate and chitosan--a review." *J Control Release* 114 (1):1-14. doi: 10.1016/j.jconrel.2006.04.017.

Gerweck, Leo E. 1998. "Tumor pH: Implications for Treatment and Novel Drug Design " *Seminars in Radiation Oncology* 8:176-182.

Grenha, A. 2012. "Chitosan nanoparticles: a survey of preparation methods." *J Drug Target* 20 (4):291-300. doi: 10.3109/1061186X.2011.654121.

Hai-Quan Maoa , Krishnendu Roy, Vu L. Troung-Le, Kevin A. Janes,, and Yan Wanga Kevin Y. Lina, J. Thomas Augustb, Kam W. Leong. 2001. "Chitosan-DNA nanoparticles as gene carriers: synthesis, characterization and transfection efficiency."

Hamed, Imen, Fatih Özogul, and Joe M. Regenstein. 2016. "Industrial applications of crustacean by-products (chitin, chitosan, and chitooligosaccharides): A review." *Trends in Food Science & Technology* 48:40-50. doi: 10.1016/j.tifs.2015.11.007.

Hiryuki Tokumitsu, Hideki Ichikawa, Yoshinobu Fukumori. 1999. "Chitosa-Gadopentetic Acid Complex Nanoparticles for Gadolinium Neutron-Capture Therapy of Cancer: Preparation by Novel Emulsion Technique and Characterization." *Pharmaceutical Research* 16.

Hombach, J., and A. Bernkop-Schnurch. 2009. "Chitosan solutions and particles: evaluation of their permeation enhancing potential on MDCK cells used as blood brain barrier model." *Int J Pharm* 376 (1-2):104-9. doi: 10.1016/j.ijpharm.2009.04.027.

Hu, Q., W. Sun, C. Wang, and Z. Gu. 2016. "Recent advances of cocktail chemotherapy by combination drug delivery systems." *Adv Drug Deliv Rev* 98:19-34. doi: 10.1016/j.addr.2015.10.022.

Hu Yong , Xiqun Jianga, Yin Dinga, Haixiong Gea, Yuyan Yuanb, Changzheng Yanga. 2002. "Synthesis and characterization of chitosan–poly(acrylic acid) nanoparticles " *Biomaterials*.

Jindal, N., and S. K. Mehta. 2015. "Nevirapine loaded Poloxamer 407/Pluronic P123 mixed micelles: Optimization of formulation and in vitro evaluation." *Colloids Surf B Biointerfaces* 129:100-6. doi: 10.1016/j.colsurfb.2015.03.030.

Kaihara, S., Y. Suzuki, and K. Fujimoto. 2011. "In situ synthesis of polysaccharide nanoparticles via polyion complex of carboxymethyl cellulose and chitosan." *Colloids Surf B Biointerfaces* 85 (2):343-8. doi: 10.1016/j.colsurfb.2011.03.008.

Kamari, Younes, and Mehran Ghiaci. 2016. "Preparation and characterization of ibuprofen/modified chitosan/TiO2 hybrid composite as a controlled drug-delivery system." *Microporous and Mesoporous Materials* 234:361-369. doi: 10.1016/j.micromeso.2016.07.030.

Krajewska, Barbara. 2004. "Membrane-based processes performed with use of chitin/chitosan materials." *Separation and Purification Technology* 41. doi: 10.1016/j.seppur.2004.03.019.

L. Illum*, I. Jabbal-Gill, M. Hinchcliffe, A.N. Fisher, S.S. Davis. 2001. "Chitosan as a novel nasal delivery system for vaccines." *Advanced Drug Delivery Reviews* 51.

M. Rinaudo, G. Pavlov1, J. Desbrie `res. 1999. "Influence of acetic acid concentration on the solubilization of chitosan." *Polymer 40* 7029-7032.

Mansouri, S., Y. Cuie, F. Winnik, Q. Shi, P. Lavigne, M. Benderdour, E. Beaumont, and J. C. Fernandes. 2006. "Characterization of folate-chitosan-DNA nanoparticles for gene therapy." *Biomaterials* 27 (9):2060-5. doi: 10.1016/j.biomaterials.2005.09.020.

Merzendorfer, H. 2011. "The cellular basis of chitin synthesis in fungi and insects: common principles and differences." *Eur J Cell Biol* 90 (9):759-69. doi: 10.1016/j.ejcb.2011.04.014.

Mohammadi, Ali, Maryam Hashemi, and Seyed Masoud Hosseini. 2016. "Postharvest treatment of nanochitosan-based coating loaded with Zataria multiflora essential oil improves antioxidant activity and extends shelf-life of cucumber." *Innovative Food Science & Emerging Technologies* 33:580-588. doi: 10.1016/j.ifset.2015.10.015.

Ouchi, T., M. Shiratani, H. Kobayashi, T. Takei, and Y. Ohya. 1994. *RELEASE BEHAVIOR OF 5-FLUOROURACIL FROM CHITOSAN-GEL MICROSPHERES MODIFIED CHEMICALLY AND THEIR ANTITUMOR ACTIVITIES*. Edited by C. G. Gebelein and C. E. Carraher, *Biotechnology and Bioactive Polymers*. New York: Plenum Press Div Plenum Publishing Corp.

Pankaj R. Rege, Lawrence H. Block. 1999. "Chitosan processing: influence of process parameters during acidic and alkaline hydrolysis and effect of the processing sequence on the resultant chitosan's properties." *Carbohydrate Research* 321:235-245.

Pilar Calvo, Jose L. 1997. "Chitosan and Chitosan/Ethylene Oxide-Propylene Oxide Block Copolymer Nanoparticles as Novel Carriers for Proteins and Vaccines." *Pharmaceutical Research* 14.

Raghuwanshi, D., V. Mishra, D. Das, K. Kaur, and M. R. Suresh. 2012. "Dendritic cell targeted chitosan nanoparticles for nasal DNA immunization against SARS CoV nucleocapsid protein." *Mol Pharm* 9 (4):946-56. doi: 10.1021/mp200553x.

S. Mitra , U. Gaur , P.C. Ghosh , A.N. Maitra 2001a. "Tumour targeted delivery of encapsulated dextran–doxorubicin conjugate using chitosan nanoparticles as carrier." *Journal of Controlled Release* 317-323.

S. Mitra, U. Gaura, P.C. Ghosh, A.N. Maitra. 2001b. "Tumour targeted delivery of encapsulated dextran–doxorubicin conjugate using chitosan nanoparticles as carrier." *Journal of Controlled Release* 74:317-323.

Saboktakin, M. R., R. M. Tabatabaie, A. Maharramov, and M. A. Ramazanov. 2011. "Synthesis and characterization of pH-dependent glycol chitosan and dextran sulfate nanoparticles for effective brain cancer treatment." *Int J Biol Macromol* 49 (4):747-51. doi: 10.1016/j.ijbiomac.2011.07.006.

Salahuddin, Nehal, and Rehab Abdeen. 2013. "Drug Release Behavior and Antitumor Efficiency of 5-ASA Loaded Chitosan-Layered Silicate Nanocomposites." *Journal of Inorganic and Organometallic Polymers and Materials* 23 (5):1078-1088. doi: 10.1007/s10904-013-9890-1.

Sarma, Runjun, and Dambarudhar Mohanta. 2015. "Luminescence and bio-imaging response of thio-glycolic acid (TGA) and sodium dodecyl sulfate (SDS)-coated fluorescent cadmium selenide quantum dots." *Journal of Luminescence* 161:395-402. doi: 10.1016/j.jlumin.2014.12.060.

Severian Dumitriu , Esteban Chornet. 1998. "Inclusion and release of proteins from polysaccharide-based polyion complexes." *Advanced Drug Delivery Reviews* 223–246.

Singh, R., and J. W. Lillard, Jr. 2009. "Nanoparticle-based targeted drug delivery." *Exp Mol Pathol* 86 (3):215-23. doi: 10.1016/j.yexmp.2008.12.004.

Sionkowska, A., B. Kaczmarek, and R. Gadzala-Kopciuch. 2016. "Gentamicin release from chitosan and collagen composites." *Journal of Drug Delivery Science and Technology* 35:353-359. doi: 10.1016/j.jddst.2016.09.001.

Sivashanmugam, A., R. Arun Kumar, M. Vishnu Priya, Shantikumar V. Nair, and R. Jayakumar. 2015. "An overview of injectable polymeric hydrogels for tissue engineering." *European Polymer Journal* 72:543-565. doi: 10.1016/j.eurpolymj.2015.05.014.

Smitha, K. T., A. Anitha, T. Furuike, H. Tamura, S. V. Nair, and R. Jayakumar. 2013. "In vitro evaluation of paclitaxel loaded amorphous chitin nanoparticles for colon cancer drug delivery."*Colloids Surf B Biointerfaces* 104:245-53. doi: 10.1016/j.colsurfb.2012.11.031.

Syed Othman Syed Mohamad Al-Azi, Yvonne Tze Fung Tan, Tin Wui Wong. 2014. "Transforming large molecular weight pectin and chitosan into oral protein drug nanoparticulate carrier." *Reactive & Functional Polymers*. doi: 10.1016/j.reactfunctpolym.2014.09.005.

Tian, L., and Y. H. Bae. 2012. "Cancer nanomedicines targeting tumor extracellular pH." *Colloids Surf B Biointerfaces* 99:116-26. doi: 10.1016/j.colsurfb.2011.10.039.

Tikhonov, Vladimir E., Evgeniya A. Stepnova, Valery G. Babak, Igor A. Yamskov, Javier Palma-Guerrero, Hans-Börje Jansson, Luis V. Lopez-Llorca, Jesus Salinas, Denis V. Gerasimenko, Inna D. Avdienko, and Valery P. Varlamov. 2006. "Bactericidal and antifungal activities of a low molecular weight chitosan and its N-/2(3)-(dodec-2-enyl)succinoyl/-derivatives." *Carbohydrate Polymers* 64 (1):66-72. doi: 10.1016/j.carbpol.2005.10.021.

Tokumitsu H., Hideki Ichikawa, Yoshinobu Fukumori. 1999. "Chitosan-Gadopentetic Acid Complex Nanoparticles for Gadolinium Neutron-Capture Therapy of Cancer: Preperation by Novel Emulsion Droplet Coalesence Technique and Characterization." *Pharmaceutical Research* 16.

Trapani, A., E. De Giglio, D. Cafagna, N. Denora, G. Agrimi, T. Cassano, S. Gaetani, V. Cuomo, and G. Trapani. 2011. "Characterization and evaluation of chitosan nanoparticles for dopamine brain delivery." *Int J Pharm* 419 (1-2):296-307. doi: 10.1016/j.ijpharm.2011.07.036.

Walke, S., G. Srivastava, M. Nikalje, J. Doshi, R. Kumar, S. Ravetkar, and P. Doshi. 2015. "Fabrication of chitosan microspheres using vanillin/TPP dual crosslinkers for protein antigens encapsulation." *Carbohydr Polym* 128:188-98. doi: 10.1016/j.carbpol.2015.04.020.

Wang, Dong-sheng, Jian-guo Li, He-ping Li, and Fa-qing Tang. 2009. "Preparation and drug releasing property of magnetic chitosan-5-fluorouracil nano-particles." *Transactions of Nonferrous Metals Society of China* 19 (5):1232-1236. doi: 10.1016/s1003-6326(08)60434-3.

Warnken, Zachary N., Hugh D. C. Smyth, Alan B. Watts, Steve Weitman, John G. Kuhn, and Robert O. Williams. 2016. "Formulation and device design to increase nose to brain drug delivery." *Journal of Drug Delivery Science and Technology* 35:213-222. doi: 10.1016/j.jddst.2016.05.003.

Wilczewska, Agnieszka Z., Katarzyna Niemirowicz, Karolina H. Markiewicz, and Halina Car. 2012. "Nanoparticles as drug delivery systems." *Pharmacological Reports* 64 (5):1020-1037. doi: 10.1016/s1734-1140(12)70901-5.

Xu, Yurui, Sajid Asghar, Liu Yang, Hongying Li, Zhilin Wang, Qineng Ping, and Yanyu Xiao. 2016. "Lactoferrin-coated polysaccharide nanoparticles based on chitosan hydrochloride/hyaluronic acid/PEG for treating brain glioma." *Carbohydrate Polymers*. doi: 10.1016/j.carbpol.2016.09.085.

Yong Hu, Xiqun Jiang, Yin Ding,Haixiong Ge,Yuyan Yuan,Changzheng Yang. 2002. "Synthesis and characterization of chitosan–poly(acrylic acid) nanoparticles." *Biomaterials*.

Yu, C. Y., B. C. Yin, W. Zhang, S. X. Cheng, X. Z. Zhang, and R. X. Zhuo. 2009. "Composite microparticle drug delivery systems based on chitosan, alginate and pectin with improved pH-sensitive drug release property." *Colloids Surf B Biointerfaces* 68 (2):245-9. doi: 10.1016/j.colsurfb.2008.10.013.

Yuan, Y., J. Tan, Y. Wang, C. Qian, and M. Zhang. 2009. "Chitosan nanoparticles as non-viral gene delivery vehicles based on atomic force microscopy study." *Acta Biochimica et Biophysica Sinica* 41 (6):515-526. doi: 10.1093/abbs/gmp038.

Zhang, C. Y., Q. Chen, W. S. Wu, X. D. Guo, C. Z. Cai, and L. J. Zhang. 2016. "Synthesis and evaluation of cholesterol-grafted PEGylated peptides with pH-triggered property as novel drug carriers for cancer chemotherapy." *Colloids Surf B Biointerfaces* 142:55-64. doi: 10.1016/j.colsurfb.2016.02.025.

Zhang, C., L. Yu, Y. Zhou, Q. Zhao, and S. Q. Liu. 2016. "Chitosan oligosaccharides inhibit IL-1beta-induced chondrocyte apoptosis via the P38 MAPK signaling pathway." *Glycoconj J* 33 (5):735-44. doi: 10.1007/s10719-016-9667-1.

Zhang, X., X. Yang, J. Ji, A. Liu, and G. Zhai. 2016. "Tumor targeting strategies for chitosan-based nanoparticles." *Colloids Surf B Biointerfaces* 148:460-473. doi: 10.1016/j.colsurfb.2016.09.020.

Zhou, F., S. Wu, Y. Yuan, W. R. Chen, and D. Xing. 2012. "Mitochondria-targeting photoacoustic therapy using single-walled carbon nanotubes." *Small* 8 (10):1543-50. doi: 10.1002/smll.201101892.

Zhuang Liu, Xiaoming Sun, Nozomi Nakayama-Ratchford, and Hongjie Dai. 2007. "SupramolecularChemistryonWaterSolubleCarbonNanotubesforDrug LoadingandDelivery." American Chemical Society:50.